

Loss of preload in pretensioned bolts



Minor Thesis by

Martin Paul Nijgh

Delft University of Technology, October 2016



Abstract

Preload loss in pretensioned bolts is an inevitable phenomenon. This thesis focuses on the different causes for bolt relaxation and their relation to joint design. Investigating bolt relaxation is relevant because there is a direct relation between the bolt preload and the resistance of the connection. In order to assess the loss of preload in pretensioned bolts, test results of extended creep tests (cf. EN 1090-2) have been used. It was found that bolt relaxation is mainly a function of coating thickness of the joint members. The larger the coating thickness, the more bolt relaxation occurs. The influence of bolt relaxation due to flattening of surface roughness could not be quantified due to the governing influence of coating thickness, but the surface roughness is of large importance for the slip resistance. External static loading has an influence on short-term bolt relaxation which can be modelled using an equation derived in this thesis. Proper joint design is key to achieving a high strength friction grip connection with a high preload level and thus a high slip resistance over the entire service lifetime. Higher ratios of clamping length over bolt diameter lead to less bolt relaxation. The results of this thesis can be used to gain insight in the behaviour of preloaded connections, as well as to have an indication on how to achieve a preloaded connection with relatively small preload losses.

Table of Contents

List of Tables	i
List of Figures	ii
Introduction	v
1 History	1
2 State of the Art	2
2.1 Current Regulation and Calculation Methods	2
2.1.1 Dimensions	3
2.1.2 Mechanical Properties of Bolts	6
2.1.3 Assembly	8
2.1.4 Mechanical Properties of Bolted Assemblies	15
2.1.5 Fatigue	22
2.2 Bolt Relaxation	24
2.2.1 Embedment	25
2.2.2 Gasket Creep	28
2.2.3 Elastic Interaction	28
2.2.4 Contraction of the clamping package	29
2.2.5 Vibration loosening	29
2.2.6 Bolt Bending	32
2.2.7 Thermal Effects	32
2.2.8 Stress Relaxation	33
2.3 Failure Mechanisms	34
2.4 Surface Treatments	36
2.4.1 Hot dip galvanizing	36
2.4.2 Thermally Sprayed Metal Coatings	37
2.4.3 High Performance Paint Coatings	38
2.4.4 Blasting of Surfaces	39
2.5 Actual Pretension Measurement	40
2.5.1 Strain-gauged fasteners	40
2.5.2 Ultrasonic	40
3 Test Results	42
3.1 Test Set-up	42
3.2 Test Matrix	45
3.3 Test Procedure	46
3.4 Relaxation directly after tightening	47
3.5 Relaxation directly after re-tightening	50
3.6 Relaxation during the application of an external load	52
3.7 Long-term relaxation under static external loading	53

4	Discussion & Modelling	59
4.1	Relaxation directly after tightening.....	59
4.1.1	Analytical Model based on experimental results	59
4.2	Bolt relaxation due to load application	63
4.2.1	Derivation of Analytical Model.....	63
4.2.2	Comparison between model and experimental results	66
5	Successful Strategies	68
	Conclusion.....	73
	References	74
	Appendix A: Surface Treatment per Specimen.....	78

List of Tables

Table 1 - General dimensional properties of bolts	3
Table 2 - General dimensions per metric bolt size.....	4
Table 3 - Preload level [kN] for different bolt sizes and property classes	10
Table 4 - Reliability of tightening processes of preloaded bolt assemblies (Berenbak, 2012)	12
Table 5 - Categories of bolted connections in EN 1993-1-8	15
Table 6 - Text Matrix.....	45
Table 7 - Predicted average loss of pretension [%] depending on the no. of coated surfaces (Heistermann, 2011)	54
Table 8 - Average joint deformation after 24 hours.....	70

List of Figures

Figure 1-1 - Archimedes' screw (3 rd century BC) (Chambers, 1875)	1
Figure 2-1 - Requirements for HSFG bolts for the HR bolt system (EN 14399) (European Committee for Standardization, 2015)	2
Figure 2-2 - General dimensions of bolts, nuts and washers (Andrews Fasteners Ltd).....	3
Figure 2-3 - Pitch, minor and major diameter (Pencom).....	4
Figure 2-4 - Thread length of HR vs HV bolt system for an M20 bolt	5
Figure 2-5 – Indentation of identification mark XYZ, bolt system HV and property class 10.9 on bolt (left) and nut (right) (European Committee for Standardization, 2015)	5
Figure 2-6 - Bolt Properties Classes according to ISO 898-1 (rows 10-18 not included) (International Organization for Standardization, 2009)	6
Figure 2-7 - Stress-Strain diagram for bolt property classes 4.8, 8.8, 10.9 and 12.9 (Blendulf, 2009)	7
Figure 2-8 - Minimum grip length according to EN 14399 (European Committee for Standardization, 2015)	8
Figure 2-9 - Definition of the grip and clamp length by EN 14399 (European Committee for Standardization, 2015)	9
Figure 2-10 - Precautions regarding the assembly of the clamped members (European Committee for Standardization, 2011)	9
Figure 2-11 - Additional rotation as the second step in the Combined Method (European Committee for Standardization, 2011)	10
Figure 2-12 - HRC Tightening Method (Bickford, 2008)	11
Figure 2-13 - Undeformed Direct Tension Indicator (AppliedBolting)	11
Figure 2-14 - DTI (no. 1) installed under the bolt head (European Committee for Standardization, 2011)	11
Figure 2-15 - Hydraulic Torque Wrench (WindTechTv.org).....	12
Figure 2-16 - Torsion stresses in the bolt resulting from torqueing (SKF, 2001).....	13
Figure 2-17 - Equivalent (Von Mises) stress resulting from bolt tension and torsion (SKF, 2001)	13
Figure 2-18 - Hydraulic bolt tensioner (SKF, 2001)	14
Figure 2-19 - Load transfer in HSFG (cat B/C) connections (ESDEP).....	15
Figure 2-20 - Factor k_s used to determine the design slip resistance (EN 1993-1-8) (European Committee for Standardization, 2011)	16
Figure 2-21 - Slip factor μ for surface treatment classes A-D (EN 1090-2) (European Committee for Standardization, 2011)	16
Figure 2-22 - Force transfer in Category E connections (ESDEP).....	17
Figure 2-23 - Plate and bolt stiffness determine the external load distribution (Culpepper, 2009)	17
Figure 2-24 - Stress spreading under the head and nut (Culpepper, 2009)	18
Figure 2-25 - Discrete bolt parts (shank and threaded part) (Culpepper, 2009)	18
Figure 2-26 – External tensile force taken up by bolt force increase and clamp force decrease (BoltScience)	19
Figure 2-27 - Clamp force has reduced to zero, initiating a gap between the members (BoltScience)	19
Figure 2-28 - Bolt force vs. externally applied tensile load (Kulak, 2005)	20
Figure 2-29 - Reduction of bolt force and increase of clamping force under external compressive loading (BoltScience).....	20
Figure 2-30 - Preload reduction F_z of a bolt due to joint contraction f_z (VDI, 2003).....	21
Figure 2-31 - Fatigue category classification for bolts according to EN 1993-1-9.....	22
Figure 2-32 - Fatigue category classification in case of shear connections according to EN 1993-1-9. Top: conventional, bottom: preloaded assembly	22
Figure 2-33 - Guide values for amounts of embedding (VDI 2230-1, Table 5.4/1) (VDI, 2003)	25
Figure 2-34 - Guide values for embedding (Jha, 2015)	25

Figure 2-35 – Bolt head-plate embedment due to surface imperfections (Eccles, 2011).....	26
Figure 2-36 - Loss of bolt stress vs. coating thickness (1 mil = 0.0254 mm) (Yang & DeWolf, 2000)	26
Figure 2-37 - Pressure reduction due to load spread (Culpepper, 2009).....	27
Figure 2-38 - Flattening of rough surface of thread and nut causes relaxation of bolt force (Bickford & Nassar, 1998).....	27
Figure 2-39 - Embedment due to undersized and oversized holes, edited after Bickford & Nassar (1998)	28
Figure 2-40 - Poisson effect with no lateral constraints (Wikimedia Commons, 2010)	29
Figure 2-41 - Nut rotation due to differential turning of bolt head and nut (Shoji & Sawa, 2005) ..	30
Figure 2-42 - Junker Test device to determine self-loosening of bolts under cyclic loading (Maryland Metrics).....	30
Figure 2-43 - Huckbolt ® Installation Sequence (Alcoa Fastening Systems & Rings)	31
Figure 2-44 - Nord-Lock SC-washers (Nord-Lock Bolt Securing Systems)	31
Figure 2-45 - Thread with inclined and step parts in order to reduce vibration loosening.....	32
Figure 2-46 - Relative preload after 1000 hours at a constant temperature, drawn after Davet (2007)	33
Figure 2-47 – Mechanical behaviour of slip-resistant connections under increasing shear load, drawn after Taha & Daidié (2012).....	34
Figure 2-48 - Force-displacement diagram showing the mechanical behaviour of slip resistant connections under increasing shear load, drawn after Taha & Daidié (2012)	35
Figure 2-49 - Hot dip galvanizing process (American Galvanizers Association).....	36
Figure 2-50 - Cross section of hot dip galvanized member (MetalPlate Galvanizing L.P.)	37
Figure 2-51 – Thermally Sprayed Metal Coating process, using a wire-source and a hand sprayer (Avant Guards Coatings)	37
Figure 2-52 - Cross section of a thermally metal sprayed coating (Lindsley, 2016).....	38
Figure 2-53 - Cross section of an alkaline zinc silicate coating (Lindsley, 2016)	38
Figure 2-54 - Application of alkali zinc silicate coating (Ashok Paint Agencies).....	39
Figure 2-55 - Grit (left) and shot (right) particles used for abrasive blast cleaning (Mogilev Metallurgical Works)	39
Figure 2-56 - Strain-gauged bolt (Techno Test Instruments)	40
Figure 2-57 - Ultrasonic determination of bolt elongation (Boltight)	41
Figure 3-1 - Extended Creep Test Set-up using M20 bolts according to EN 1090-2 (European Committee for Standardization, 2011)	42
Figure 3-2 - Set-up used to obtain test results, fulfilling EN 1090-2 demands (Vries, P.A. de, 2016)	43
Figure 3-3 - Shank lengths for HR8.8 and HR10.9 bolts (courtesy of P.A. de Vries).....	44
Figure 3-4 - Test Procedure of the SIROCO test programme at TU Delft containing relevant steps for determination of preload loss	46
Figure 3-5 - Relative preload loss directly after tightening the bolts for the first time	47
Figure 3-6 - Relative preload loss after 30 minutes versus the total coating thickness of the specimen	48
Figure 3-7 - Relative preload loss after 30 minutes versus the total surface roughness of the specimen	49
Figure 3-8 – Possible effect of load cell on the introduction of the preload into the underlying plate (not to scale).....	49
Figure 3-9 - Relative preload loss directly after re-tightening of the bolts	50
Figure 3-10 - Relative preload loss after re-tightening compared to relative preload loss after first tightening instance (at equal time intervals from (re)tightening)	51
Figure 3-11 - Preload loss due to (static) external load	52
Figure 3-12 – Extrapolated average relative preload in bolt versus log(time).....	53
Figure 3-13 Extrapolated average losses of pretension (Heistermann, 2011).....	54

Figure 3-14 – Extrapolated relative preload loss vs time for ASiZn-43 and results from Heistermann (2011).....	55
Figure 3-15 - Extrapolated relative preload loss since (re)-tightening vs time	56
Figure 3-16 - Relative preload loss after 10000 minutes vs external load	56
Figure 3-17 - Long-term preload loss, while sustaining external force F1	58
Figure 4-1 - Joint deformation 30 minutes after preloading versus total coating thickness for clamping length of 48 mm.....	59
Figure 4-2 - Joint deformation 21 days after preloading versus total coating thickness for results of TU Delft and Yang & DeWolf (2000).....	60
Figure 4-3 - Joint deformation versus time	61
Figure 4-4 - Percentage overshoot per SM specimen	62
Figure 4-5 - y-z axis convention.....	63
Figure 4-6 - Restrained lateral contraction in y-direction (only 1 cover plate shown) (not to scale)	64
Figure 4-7 – Washer of an M20 bolt on cover plate. Load spreading under 45° angle (only a small part of the cover plate is shown).....	65
Figure 4-8 - Modelled preload loss versus observed preload loss.....	66
Figure 4-9 - Preload loss in bolt 1 over preload loss in bolt 2 vs. external shear load	67
Figure 5-1 - Set-up of test study	68
Figure 5-2 - Basic Dimensions of HR Assemblies (European Committee for Standardization, 2015)	68
Figure 5-3 - Percentage of preload loss per 10 micron of joint deformation as a function of l/d ...	69
Figure 5-4 - Absolute preload loss per 10 micron of joint deformation as a function of l/d.....	69
Figure 5-5 - Percentage preload loss 24 hours after re-tightening as a function of l/d.....	70
Figure 5-6 - C_b and $1-C_b$ as a function of the stiffness ratio k_m/k_b	71
Figure 5-7 - Bolt with reduced shank area	71

Introduction

Already in 1934 the first experiments have been carried out with preloaded bolts to see if preloading of bolts had any advantage. Today, preloaded bolts are often used in connections, mainly if the connection is subject to load reversal, high stress ranges or if slip of the members should be prevented. The behaviour of such connections depends on the magnitude of the preload in the bolts. However, directly after applying a preload, the preload decreases rapidly and it slowly continues to do so until the end of time. The main issue related to (significant) bolt relaxation is that the connection behaviour changes, for example: the bolts may slip into bearing or experience major fatigue issues. As a consequence, the connection cannot continue to function in the intended way.

Bolt relaxation has been studied numerous times in literature. Most of the literature is about bolt relaxation due to cyclic loading (vibration loosening), since this is the field in which preloaded connections can create the largest benefits. There is a general consensus in literature that the connection behaviour and the magnitude of bolt relaxation is mostly related to the coating thickness and surface roughness of the clamped plates, as well as to the length of the bolt.

For this thesis, on-going research of TU Delft has been used, which originates from an international research programme on the slip resistance of preloaded connections (SIROCO). This test data is used to distinguish between the different causes for bolt relaxation, and to provide an overview of the influences which govern its magnitude. The test data is obtained using an extended creep test (cf. EN 1090-2) and thus the results of this thesis mainly hold for statically loaded connections.

The main goal (and research question) of this thesis is to describe the behaviour of preloaded connections, and to give insight in the cause-and-effect of bolt relaxation based on literature and experimental data. Before going in-depth on the field of bolt relaxation, this thesis first discusses the individual components in bolted assemblies and the current legislation involved. Hereafter, literature research is carried out and work of other authors is presented. Finally, the test results of the TU Delft research are presented and processed, allowing for experimental conclusions and an overview of what connection detailing leads to low preload losses after 24 hours.

1 History

The concept of bolting objects together dates from the Roman times. The Romans developed the first unthreaded bolt which was secured by inserting a wedge on the location where in present time the nut would be screwed on (Graves, 1984). Also, the Romans developed the first structural screw, but did not extend their concept to a counterpart with an internal thread. The idea of a non-structural screw dates back further: there is a consensus that the concept of threading was conceived by the Greek philosopher Archytas of Tarentum, who used screws for the extraction of oil and juice from olives and grapes. One of the most famous applications of a non-structural screw is Archimedes' water screw as shown in Figure 1-1.

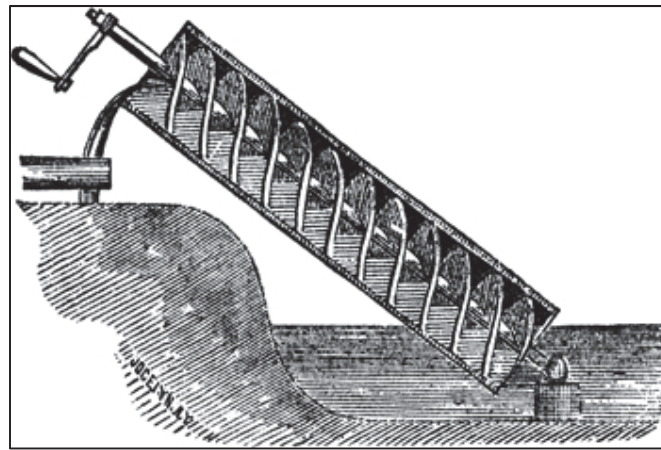


Figure 1-1 - Archimedes' screw (3rd century BC)
(Chambers, 1875)

The modern way of bolting dates from the 16th century (Graves, 1984). In 1568 the first bolt factory opened in France, however the threads had to be hand-made which reduced the factory output (Wilbur, 1905). In order to meet the market demand, a factory process for the mass production of threaded fasteners was developed in Britain in 1760. Since it was now rather easy to create bolts and screws in all sizes and varieties, many different versions appeared. In order to reduce the amount of different fasteners on the market, a standardization campaign was initiated in 1841. It was not before 1684 that the current design of the bolt was made, which had a 60 degree flank angle (see Figure 2-3) rather than the 55 degree angle suggested in 1841.

The idea of pre-tensioning bolts in order to achieve slip-resistant connections dates from 1934, when the Steel Structures Committee of Scientific and Industrial Research of Great Britain published a report stating that bolts with a yield strength of more than 372 MPa (the modern day equivalent is a property class 5.8 bolt with a yield strength of 400 MPa) would be able to be pretensioned to such an extent that slip of the joined members can be prevented (Fisher & Beedle, 1964). In 1938, Wilson carried out tests to compare the fatigue resistance of pretensioned bolts to the fatigue resistance of rivets, and concluded that their fatigue resistance was equal. As of 1947, the development of pretensioned connections rapidly increased due to the founding of the Research Council on Riveted and Bolted Structural Joints which sponsored research on pretensioned connections. Also, the American Railway Engineering Association invested money in research of slip-resistant connections in order to overcome problems related to fatigue in railway bridges. Already in 1948 the first bridge was installed using pretensioned bolts in order to investigate the performance under loading. In 1949 the first material specification for high-strength bolts was published in the United States of America, followed by the first (German) Code of Practice in 1956 (Fisher & Beedle, 1964).

2 State of the Art

2.1 Current Regulation and Calculation Methods

The goal of this chapter is to take account of the most important bolt types, dimensions and properties, such that a good basis for the understanding of preloaded bolted assemblies is obtained.

The general requirements for pretension bolts are prescribed in EN 14399, as indicated in Figure 2-1. A similar figure exists for nuts and washers used in pretensioned assemblies. As can be seen from Figure 2-1, EN 14399 refers to many other norms. It is beyond the scope of this thesis to go into detail of all these norms and regulations, however, the most important aspects will be discussed.

This chapter first discusses the current regulation on the dimensions individual components present in an bolted assembly. Secondly, the mechanical properties of high strength friction grip (HSFG) bolts are discussed. Thirdly, the rules regarding the complete bolted assembly and the tightening of it are presented. Finally, the mechanical properties of the bolted assembly are considered, including existing calculation models.

Material		Steel
General requirements		EN 14399-1 ^a
Thread	Tolerance	6g ^b
	International Standards	ISO 261, ISO 965-2
Mechanical properties	Property class	8.8 or 10.9
	European Standard	EN ISO 898-1
Impact strength	Value	K _{V,min} = 27 J at -20 °C
	Test specimen ^c	ISO 148-1
	Test	EN 10045-1
Tolerances	Product grade	C except: dimension r. Tolerance for lengths ≥ 160 mm ± 4,0 mm
	International Standard	EN ISO 4759-1
Surface finish ^d	Normal	as processed ^e
	hot dip galvanized	EN ISO 10684
	Others	to be agreed ^f
Surface discontinuities		Limits for surface discontinuities are covered in EN 26157-1.
Acceptability		For acceptance procedure, see EN ISO 3269.
^a For the time being EN 14399-1 refers only to EN 14399-3 and EN 14399-4 as far as dimensions and mechanical characteristics of the components and functional characteristics of the assemblies are concerned. Such references shall also apply to EN 14399-7. ^b The tolerance class specified applies without surface finish. Hot-dip galvanized bolts are intended for assembly with oversize tapped nuts. ^c The preparation of the test specimens with V-notch in the fastener shall be as specified in EN ISO 898-1. ^d Attention is drawn to the need to consider the risk of hydrogen embrittlement in the case of bolts of property class 10.9, when selecting an appropriate surface treatment process (e.g. cleaning and coating), see the relevant coating standards. ^e "As processed" means the normal finish resulting from manufacture with a light coating of oil. ^f Other coatings may be negotiated between the purchaser and the manufacturer provided they do not impair the mechanical properties or the functional characteristics. Coatings of cadmium or cadmium alloy are not permitted.		

Figure 2-1 - Requirements for HSFG bolts for the HR bolt system (EN 14399) (European Committee for Standardization, 2015)

2.1.1 Dimensions

The most important dimensional properties that can be distinguished for bolts, nuts and washers are shown in Figure 2-2. All dimensional properties, except the length, are generally constant for each metric bolt size. Bolt sizes are denoted as the letter M followed by two digits showing the nominal major diameter (in mm) of the bolt. For example, M20 is a bolt with a nominal major diameter of 20 mm with a length that may still be determined.

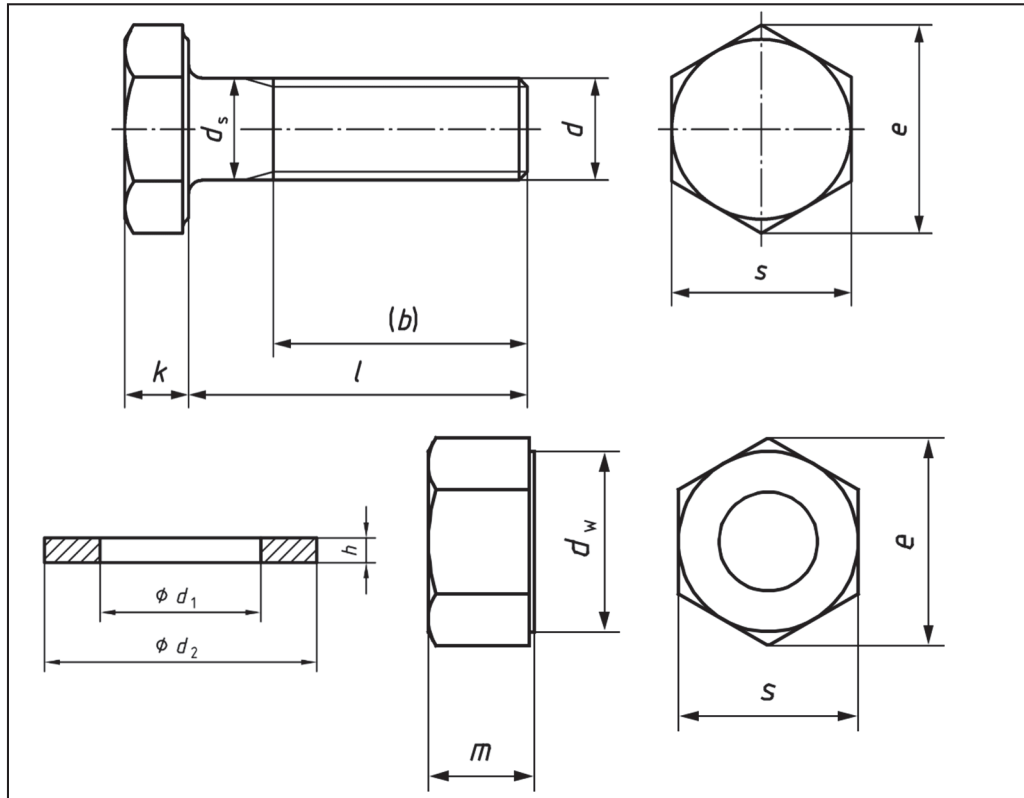


Figure 2-2 - General dimensions of bolts, nuts and washers (Andrews Fasteners Ltd)

The symbols shown in Figure 2-2 are explained in Table 1.

Table 1 - General dimensional properties of bolts

Symbol	Dimension
b	Thread length
d	Major diameter thread
d_s	Shank diameter
d_w	Bearing surface diameter
d_1	Inner diameter washer
d_2	Outer diameter washer
h	Thickness washer
l	Bolt length
e	Width across corners
k	Height of head
m	Height of nut
s	Width across flats

An important dimension not shown in Figure 2-2 is the pitch p . The pitch is the distance between two subsequent crests. Figure 2-3 illustrates the notion of pitch and simultaneously introduces the notions of minor diameter d_3 and pitch diameter d_2 .

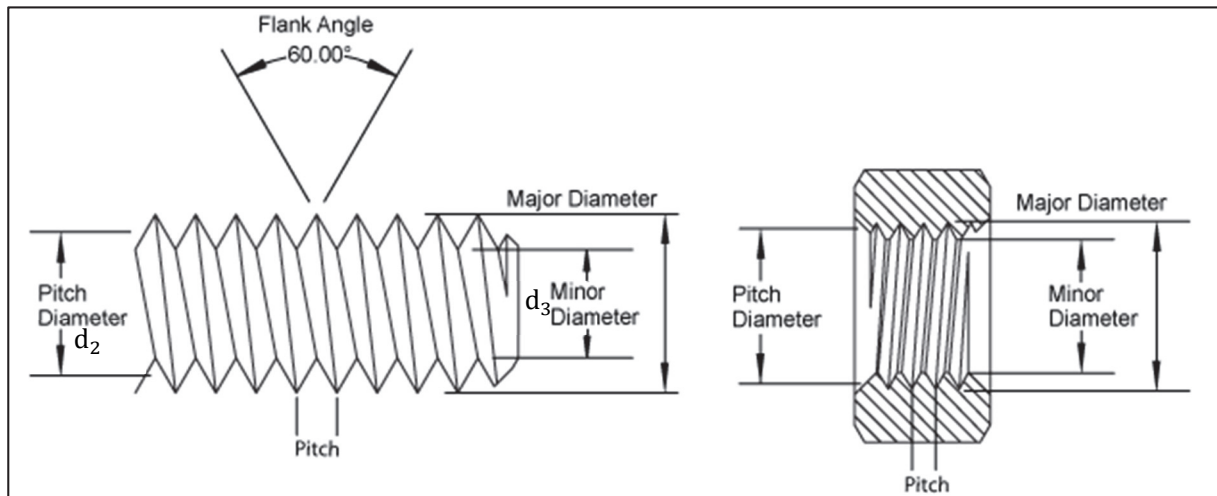


Figure 2-3 - Pitch, minor and major diameter (Pencom)

Table 2 shows the magnitude for each metric bolt size for some of the dimensional properties discussed above. The height of the nuts and length of the thread have not been included since these differ between HR and HV bolt systems. It should be noted that for all metric bolt sizes, bolts are available with the normal (coarse) pitch p and a fine pitch. Fine-pitched bolts generally offer a more precise way of tightening at lower torque (Park Tool, 2015).

Table 2 - General dimensions per metric bolt size

Bolt Size	M12	M16	M20	M22	M24	M27	M30	M36
d (mm)	12	16	20	22	24	27	30	36
d_s (mm)	$\approx d$							
s (mm)	22	27	32	36	41	46	50	60
p (mm)	1.75	2	2.5	2.5	3.0	3.0	3.5	4.0
d_2 (mm)	24	30	37	39	44	50	56	66
h (mm)	3	4	4	4	4	5	5	6

HV and HR bolt systems

Within EN 14399 a distinction is made between HR and HV bolt systems. The HR and HV bolt systems differ in the magnitude of the dimensional properties that have been discussed before. The HR bolt system has a British/French history. The HR bolt system has a longer thread length and a thick nut which allows for ductility by plastic elongation of the bolt threads. The HR bolt system is relatively insensitive to overtightening during preloading. If the maximum preload is exceeded significantly, the bolt will break and the bolt failure is well-detectable (Steel Industry Guidance Notes, 2008). The HV bolt system originates from Germany. It has a shorter thread length and thinner nuts: it relies on the plastic deformation of the threads within the nut to reach the required ductility. The HV bolt system is more sensitive to overtightening but its failure mechanism is not well detectable. However, the HV bolt system can still transmit shear forces like a non-preloaded assembly. (Steel Industry Guidance Notes, 2008)

In Figure 2-4 an overview of the thread lengths of the HR and HV bolt systems is plotted against the total bolt length for an M20 bolt.

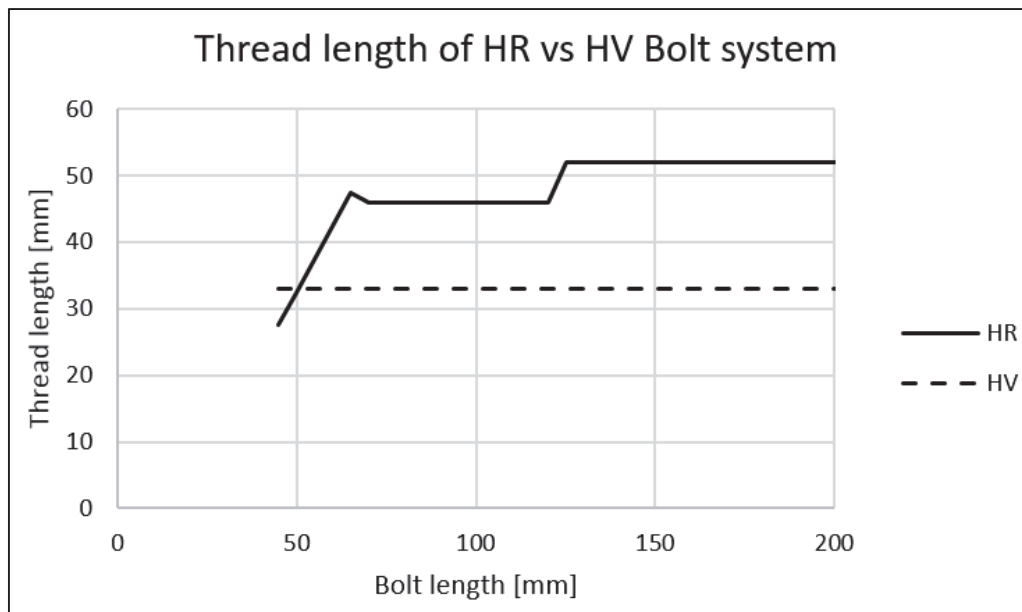


Figure 2-4 - Thread length of HR vs HV bolt system for an M20 bolt

The strength of HR and HV assemblies is equal. However, care should be taken not to mix an HR bolt with an HV nut (or vice versa). For this purpose, both bolt systems are clearly separated in parts 3 and 4 of EN 13499. EN 13499 requires that the bolt, nut and washer are supplied by one manufacturer since preloaded bolted assemblies are very sensitive to differences in manufacture and lubrication. The manufacturer of the assembly is responsible for its functioning.

Fastener Identification

It is a prerequisite for a manufacturer to identify his identification mark together with the bolt system and property class into the respective components, as shown in Figure 2-5. Thus, it can be checked easily whether only parts of the same bolt system and of the same manufacturer are used. Also, it is generally encouraged to choose for only the HR or HV system within a single project. This greatly reduces the chance of a failure on the construction site due to a mix up of components.

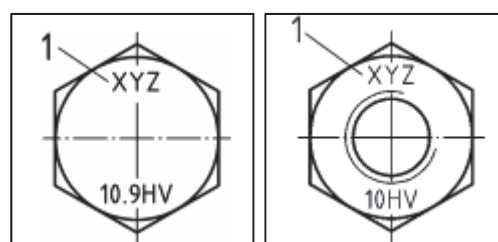


Figure 2-5 – Indentation of identification mark XYZ, bolt system HV and property class 10.9 on bolt (left) and nut (right) (European Committee for Standardization, 2015)

2.1.2 Mechanical Properties of Bolts

The mechanical properties of bolts are dependent on the bolt property class. The different bolt property classes are laid down in ISO 898-1, as shown in Figure 2-6. The first number of the bolt property class indicates the tensile strength in MPa when multiplying this number by 100. The second value (after the dot) divided by 10 indicates the relative stress [MPa] at 0,2% plastic strain with respect to the tensile strength. For example, a bolt of property class 8.8 has a tensile strength of 800 MPa and a (fictitious) yield strength of 640 MPa.

No.	Mechanical or physical property		Property class									
			4.6	4.8	5.6	5.8	6.8	8.8		9.8	10.9	12.9/ 12.9
								$d \leq 16$ mm ^a	$d > 16$ mm ^b	$d \leq 16$ mm		
1	Tensile strength, R_m , MPa	nom. ^c	400		500		600	800		900	1000	1200
		min.	400	420	500	520	600	800	830	900	1040	1220
2	Lower yield strength, R_{eL} ^d , MPa	nom. ^c	240	—	300	—	—	—	—	—	—	—
		min.	240	—	300	—	—	—	—	—	—	—
3	Stress at 0,2 % non-proportional elongation, $R_{p0,2}$, MPa	nom. ^c	—	—	—	—	—	640	640	720	900	1080
		min.	—	—	—	—	—	640	660	720	940	1100
4	Stress at 0,0048 δ non-proportional elongation for full-size fasteners, R_{pf} , MPa	nom. ^c	—	320	—	400	480	—	—	—	—	—
		min.	—	340 ^e	—	420 ^e	480 ^e	—	—	—	—	—
5	Stress under proof load, S_p ^f , MPa	nom.	225	310	280	380	440	580	600	650	830	970
	Proof strength ratio $S_{p,nom}/R_{eL \text{ min}}$ or $S_{p,nom}/R_{p0,2 \text{ min}}$ or $S_{p,nom}/R_{pf \text{ min}}$		0,94	0,91	0,93	0,90	0,92	0,91	0,91	0,90	0,88	0,88
6	Percentage elongation after fracture for machined test pieces, A , %	min.	22	—	20	—	—	12	12	10	9	8
7	Percentage reduction of area after fracture for machined test pieces, Z , %	min.	—					52		48	48	44
8	Elongation after fracture for full-size fasteners, A_f (see also Annex C)	min.	—	0,24	—	0,22	0,20	—	—	—	—	—
9	Head soundness		No fracture									

Figure 2-6 - Bolt Properties Classes according to ISO 898-1 (rows 10-18 not included) (International Organization for Standardization, 2009)

EN 1993-1-8 has taken over the property classes of ISO 898-1 (Figure 2-6), however it only allows for pretensioning of bolts of property classes 8.8 and 10.9. Bolts of other property classes may not be pretensioned.

Based on ISO 898-1, the stress strain diagram for bolts can be drawn. The stress-strain diagram for bolt property classes 4.8, 8.8, 10.9 and 12.9 is shown in Figure 2-7. The Young's Modulus of bolts is constant for all property classes and can be taken equal to the Young's Modulus of mild steels, $E = 210$ GPa. From Figure 2-7 it can be seen that a bolt with a higher property class has a higher strength (favourable) but a lower ductility (unfavourable) than the same bolt of a lower property class.

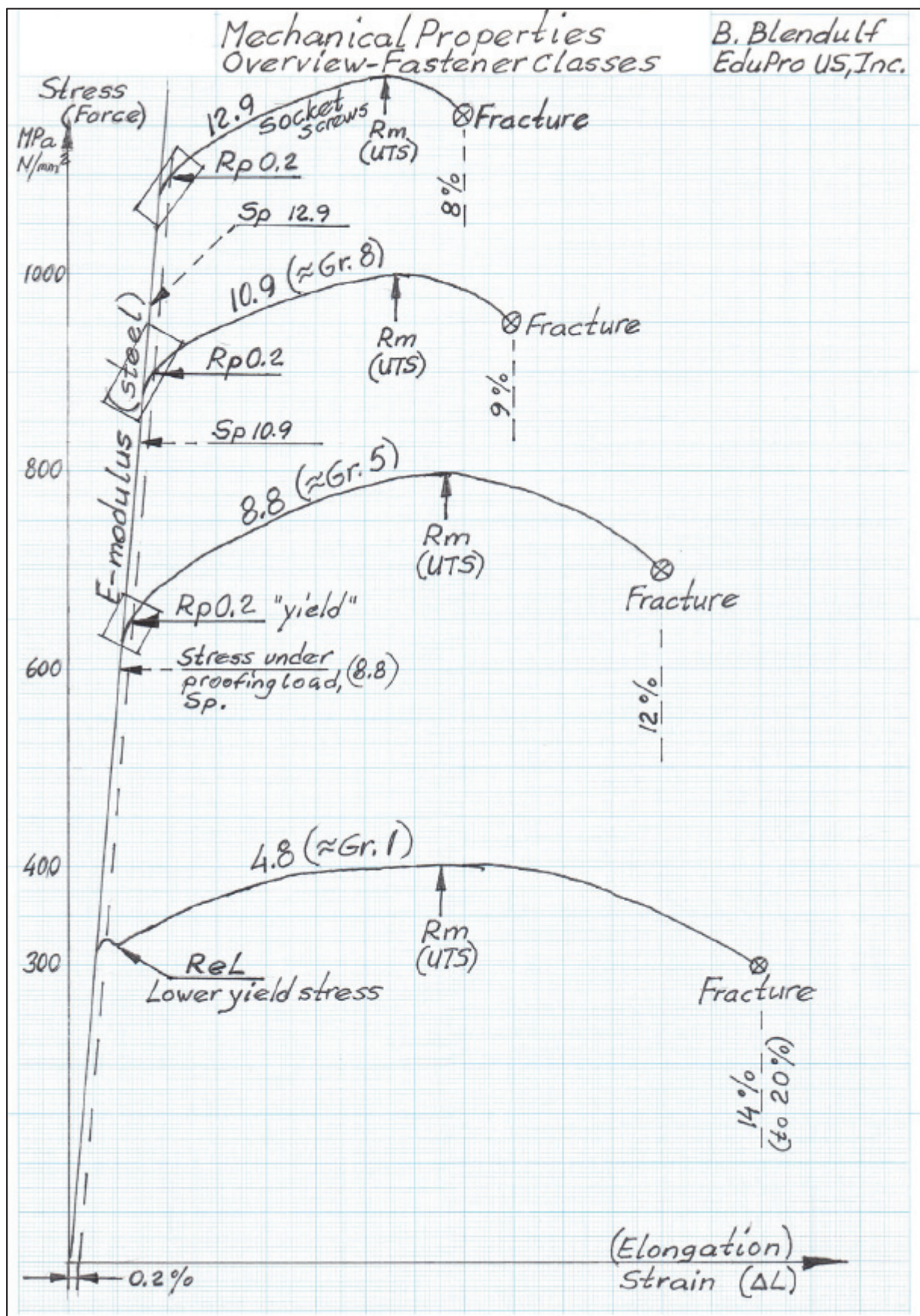


Figure 2-7 - Stress-Strain diagram for bolt property classes 4.8, 8.8, 10.9 and 12.9 (Blendulf, 2009)

2.1.3 Assembly

In order to achieve a well-functioning pretensioned connection, regulations have been put in place regarding the complete bolted assembly. The term 'assembly' indicates both the sum of all joined/clamped parts, but also the tightening process of the pretension bolts joining these parts.

Clamped Parts

Bolts

As mentioned in Section 2.1.2, only bolts of property classes 8.8 and 10.9 may be pretensioned. The use of all other property classes is forbidden by EN 1993-1-8. It is also prescribed that, in case of pretensioned bolts, a minimum of four threads above and one thread under the nut surface should be present. In addition, EN 1090-2 dictates that the minimum bolt size for use in structural applications is M12. The hole diameter is generally 1-2 mm larger than the bolt diameter. The bolts should be stored and used in such a way that the lubricant on the threads remains as applied in the bolt factory, so that the frictional properties of the bolt are unaffected.

Nuts

When placing the nut on the bolt, it should be checked that the nut can turn freely on the bolt. EN 1090-2 suggests that this can be done by hand-tightening the bolt. In case the nut cannot move freely on the bolt, both the bolt and the nut should be disposed of. Locking of the nuts to the bolt is forbidden. A possible explanation is that bolt-locking (e.g. by adhesives) can still lead to high preload losses (up to 40%) under cyclic loading (Jiang, Zhang, & Lee, 2003) and may provide a false feeling of safety. Also, it is not allowed to weld any attachments to the nut (and the bolt), since it affects the material properties significantly by counteracting the heat treatment the bolt and nut have undergone.

Washer

In case of class 8.8 bolts, EN 1090-2 prescribes the use of a washer under either the head or the nut of the bolt – dependent on which of the two is tightened (preferably the nut). In case of class 10.9 bolts, a washer should be present under both the head and the nut. The goal of inserting a washer is to reduce the damage to the surface of the clamped members due to tightening of the bolt and to introduce the load over a larger area in the underlying member. Washers can also be used to increase the clamp length $\sum t$, however only 3 additional washers may be used up to a maximum additional thickness of 12 mm. In case of tightening by the Torque or HRC method, only 1 additional washer may be used which must be installed on the side that is tightened. In all other cases, the additional washers may be installed on either side of the plates.

In case the bolt axis is not parallel to the hole and the mutual angle is more than 2°, bevelled washers must be used in such a way that the bolt head becomes perpendicular to the hole.

Clamped Plates

The plates that are clamped together by the pretensioned bolts should have a minimum total thickness (grip length) t_{s2} to ensure a proper functioning of the preloaded joint, as dictated in EN 14399. This criterion, shown in Figure 2-8, should be fulfilled.

For proper function of the preloaded bolted joint, the following condition for the grip length t_{s2} shall be fulfilled:
 $(l_{g,max} + 2P - 2h_{min}) < t_{s2} < (l_{min} - P - m_{max} - 2h_{max})$, where P is the pitch of thread, m_{max} is the maximum nut height and h_{min} is the minimum washers thickness.

Figure 2-8 - Minimum grip length according to EN 14399 (European Committee for Standardization, 2015)

The graphical definition of the grip length t_{s2} and the clamp length $\sum t$ (which includes the washers) is shown in Figure 2-9.

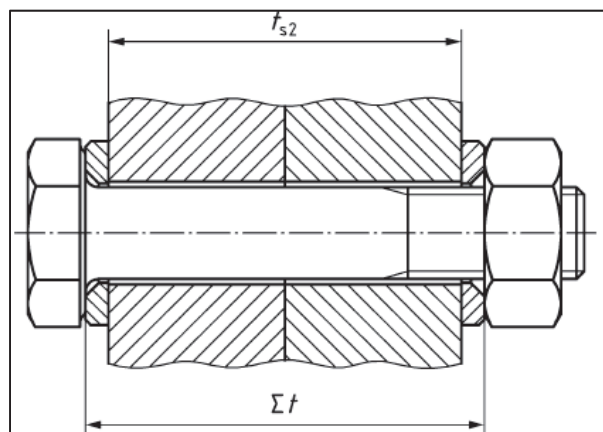


Figure 2-9 - Definition of the grip and clamp length by EN 14399 (European Committee for Standardization, 2015)

Individual plates that form an individual layer, for example in a double lap joint, may not differ in thickness more than 1 mm according to EN 1090-2. If steel plates are used to bridge a gap of more than 1 mm, the minimum filler plate thickness is 2 mm. The mechanical properties of filler plates must be similar to that of the other plates in the connection.

The plates must comply to the preventive prescriptions shown in Figure 2-10, which originate from EN 1090-2.

The following precautions shall be taken prior to assembly:

- a) the contact surfaces shall be free from all contaminants, such as oil, dirt or paint. Burrs that would prevent solid seating of the connecting parts shall be removed;
- b) uncoated surfaces shall be freed from all films of rust and other loose material. Care shall be taken not to damage or smooth the roughened surface. Untreated areas around the perimeter of the tightened connection shall be left untreated until any inspection of the connection has been completed.

Figure 2-10 - Precautions regarding the assembly of the clamped members (European Committee for Standardization, 2011)

Before starting the tightening of the pretension bolts, the clamped members must be fitted together, the bolts must be snug-tightened and there may not be a gap between the members larger than 2 mm. EN 1090-2 defines snug-tight as *“achievable by the effort of one man using a normal sized spanner without an extension arm, and can be set as the point at which a percussion wrench starts hammering”*.

Tightening

Preload level

The tightening of pretension bolts should be done according to EN 1090-2, which results in the pretension level of (2.1).

$$F_{p,C} = 0,7f_{ub}A_s \quad (2.1)$$

In (2.1), f_{ub} is the nominal tensile strength of the bolt and A_s is the cross-sectional area of the bolt in the threaded region. Table 3 shows the target preload level in kN for bolts pretensioned according to (2.1).

Table 3 - Preload level [kN] for different bolt sizes and property classes

Property Class	M12	M16	M20	M22	M24	M27	M30	M36
8.8	47	88	137	170	198	257	314	458
10.9	59	110	172	212	247	321	393	572

According to EN 1090-2, the preload in the bolts should be introduced first in the stiffest and last in the least stiffest part of the connection. Since the tightening of one bolt may loosen another due to elastic interaction, multiple steps of retightening may be necessary to obtain an equal preload level in all bolts.

Tightening Methods

The preload may be obtained using the following methods mentioned in EN 1090-2:

- Torque Method

The torque method introduces the preload by applying a certain torque proportional to the diameter of the bolt, the preload level and a factor k_m declared by the fastener manufacturer to the nut or head of the bolt. The torque is applied in two steps – first the bolt is tightened using 75% of the target torque, in the second step this is increased to 110% of the target torque.

- Combined Method

The combined method introduces the preload by first applying the first step of the torque method. The second step of the combined method is to rotate the head of the bolt or the nut over an additional angle, dependent on the clamping length $\sum t$ and the bolt diameter, as indicated in Figure 2-11.

Total nominal thickness "t" of parts to be connected (including all packs and washers) d = bolt diameter	Further rotation to be applied, during the second step of tightening	
	Degrees	Part turn
$t < 2d$	60	1/6
$2d \leq t < 6d$	90	1/4
$6d \leq t \leq 10d$	120	1/3
NOTE Where the surface under the bolt head or nut (allowing for taper washers, if used) is not perpendicular to the bolt axis, the required angle of rotation should be determined by testing		

Figure 2-11 - Additional rotation as the second step in the Combined Method (European Committee for Standardization, 2011)

- HRC Tightening Method

The HRC tightening method works with a special bolt with a spline end at the end of the threaded region. The preload is introduced using a shear wrench with two independent sockets. These sockets turn in opposite direction and introduce the torque. After reaching the target torque, the spline end will break off. The principle is shown in Figure 2-12.

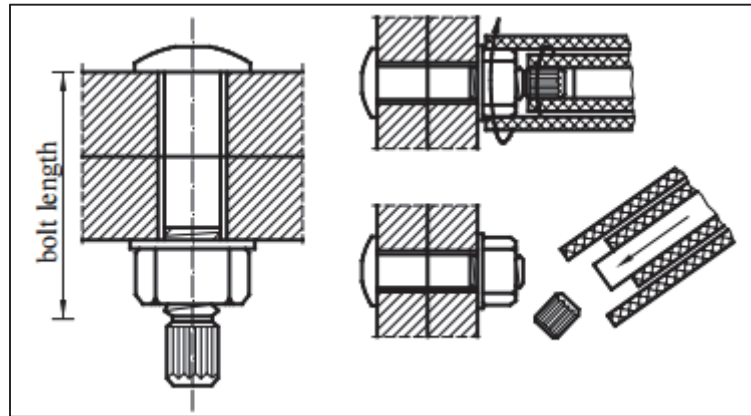


Figure 2-12 - HRC Tightening Method (Bickford, 2008)

- DTI (Direct Tensioning Indicator) Method

Direction Tensioning Indicators are small disks with protuberances that will compress under a certain (predetermined) axial load, thereby proving that the necessary pretension force has been reached within the bolt. An undeformed DTI is shown in Figure 2-13. An advantage of DTIs is they are insensitive to friction in the threads and under the head and nut. An example of a correctly installed DTI assembly is shown in Figure 2-14. It should be noted that the DTI does not function as a washer, which must be installed separately.

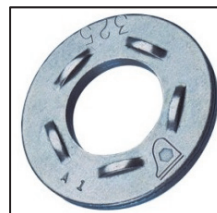


Figure 2-13 - Undeformed Direct Tension Indicator (AppliedBolting)

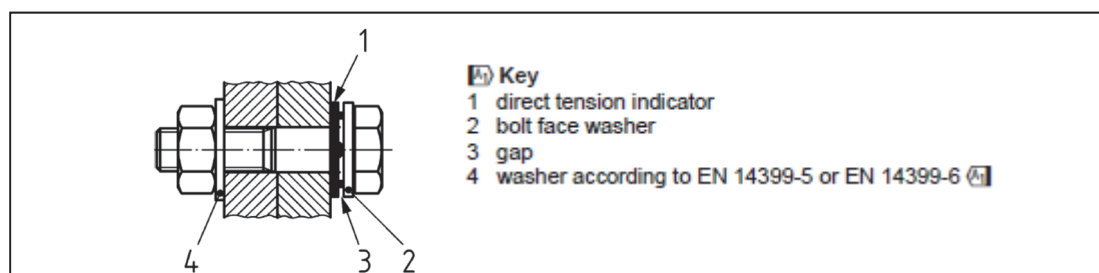


Figure 2-14 - DTI (no. 1) installed under the bolt head (European Committee for Standardization, 2011)

The use of different tightening methods is allowed by EN 1090-2, on the condition that the tightening apparatus is calibrated using the manufacturer's recommendations. One of the tightening methods not discussed in EN 1090-2 is axial preloading, which will be discussed later in this section.

EN 1090-2 prescribes that the preload should generally be obtained by turning the nut rather than the bolt head. In case the nut is not reachable for tightening, the head of the bolt may be used. However, special precautions may need to be taken in this case. Although time-dependent loss of preloading force have been taken into account in the prescriptions of the different tightening methods mentioned in EN 1090-2, it may be necessary to re-tighten the bolts after some days, especially in the case of the Torque Method. It is never allowed to loosen the bolt and re-tighten it if the preload has reached or exceeded $F_{p,C}$.

The reliability of the abovementioned tightening processes has been assessed in the report "Evaluation Tightening Preloaded Bolt Assemblies According to EN 1090-2" and is shown in Table 4.

Table 4 - Reliability of tightening processes of preloaded bolt assemblies (Berenbak, 2012)

Tightening Process	Reliability
Torque Method	79,4%
Combined Method	100%
HRC Method	81%
DTI Method	>95%

The Torque Method and the (first step of the) Combined Method can be carried out using an hydraulic bolt wrench (Figure 2-15). Hydraulic torque wrenches apply a predetermined amount of torque on the nut using oil pressure. The main issue with torque wrenches is the low correlation between exerted torque and the final preload, due to uncertainty of the friction in the threads of the nut and the bolt and under the nut. Hence, even after calibration of the torque wrench, differences in preload exist between different bolts. Another issue that arises when using a torque wrench, is the introduction of torsion stresses in the bolt, as indicated in Figure 2-16.



Figure 2-15 - Hydraulic Torque Wrench (WindTechTv.org)

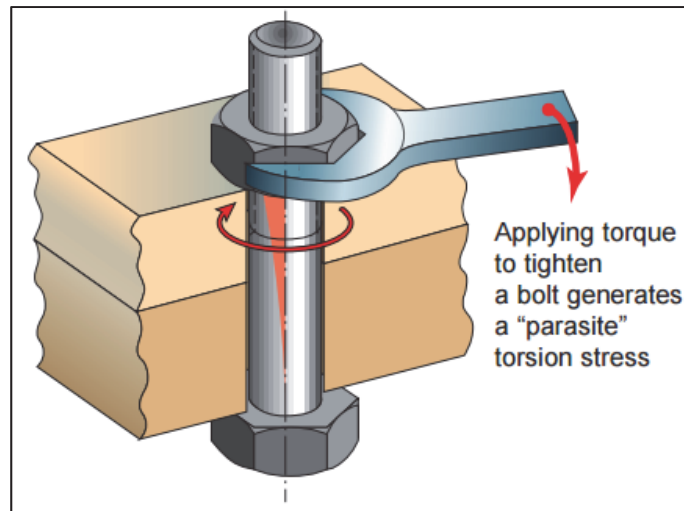


Figure 2-16 - Torsion stresses in the bolt resulting from torquing (SKF, 2001)

The additional torsion stress can be more than 30% of the tension stress (SKF, 2001). As a result of the torsion stresses, yielding may occur based on the Von Mises or Tresca yield criterion when the actual bolt tension does not exceed the yield stress (Figure 2-17). When the torsional stresses relax, the bolt tension may increase 1-2% due to the nut screwing itself further onto the bolt thread. (Bickford & Nassar, 1998)

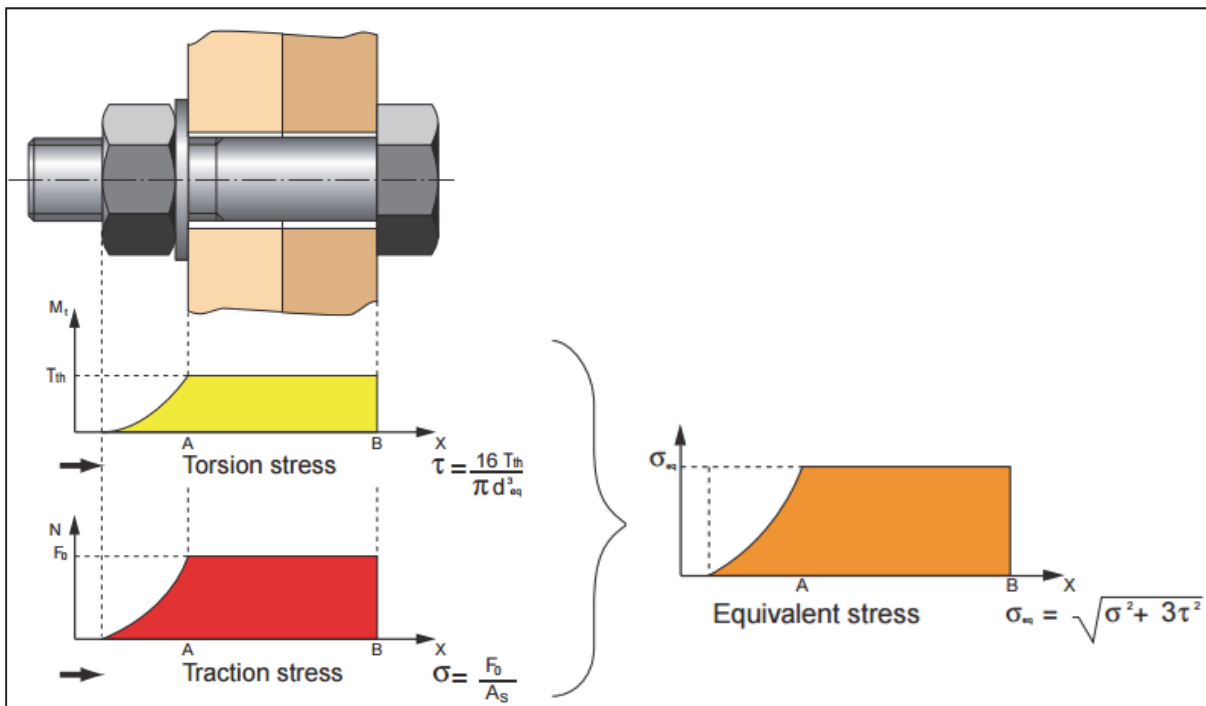


Figure 2-17 - Equivalent (Von Mises) stress resulting from bolt tension and torsion (SKF, 2001)

It is a prerequisite that the torque is exerted smoothly and continuously (EN 1090-2). The reason behind this is that the static coefficient of friction μ_s in the bolt thread-nut interface is generally higher than the kinematic coefficient of friction μ_k (Culpepper, 2009).

As mentioned before, one of the tightening methods not mentioned in EN 1090-2 is axial preloading. This process can be carried using an hydraulic bolt tensioner (Figure 2-18). Hydraulic bolt tensioners do not cause torsional stresses in the bolt, since the preload is not obtained by

torqueing but directly by tensioning. The tension is introduced through the threads under the nut by an auxiliary threaded cylinder, which is jacked up using oil pressure, as can be seen from Figure 2-18 (red). As a result, the nut loses contact with the joint and can be re-tightened manually. After finishing this step, the oil pressure is relieved and the joint remains under compression.

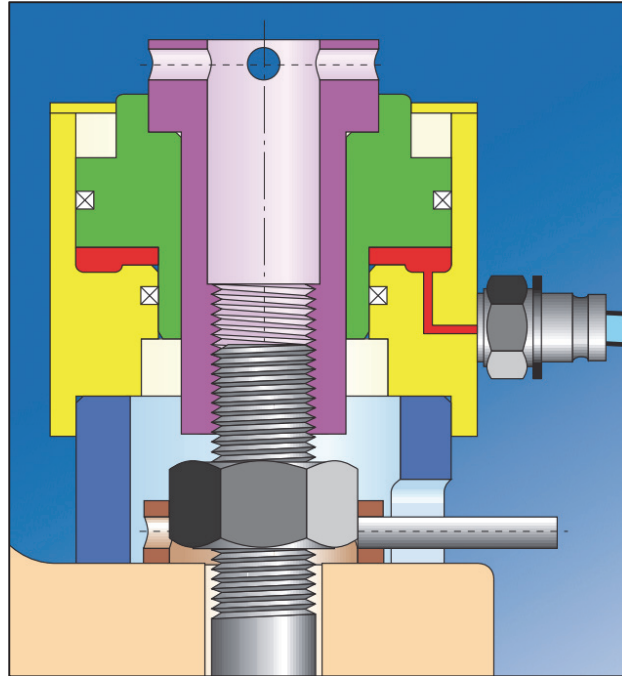


Figure 2-18 - Hydraulic bolt tensioner (SKF, 2001)

The preload is obtained more accurately by hydraulic bolt tensioning than by torque wrenching, since no frictional resistance is encountered during the tightening process. A minor loss of preload is observed when releasing the hydraulic pressure, because the nut has no full contact with the load transferring side of the bolt (Bickford & Nassar, 1998). This is in contrast to torqueing wrenching, since in this case the nut is always fully pressed against the bolt thread. Therefore, it is recommended to carry out bolt tensioning twice: the first time to compress the surface roughness and the second time to obtain the required preload in the bolt (SKF, 2001). In order to use bolt tensioning, additional thread length is necessary. Bolt tensioning equipment is expensive (up 30 times as expensive as torque wrench equipment) and is often only suitable for one bolt size (Raynor-Keck, 2013).

2.1.4 Mechanical Properties of Bolted Assemblies

The mechanical properties of bolted assemblies are grouped in 5 categories, shown in Table 5.

Table 5 - Categories of bolted connections in EN 1993-1-8

Category	External Loading	Pretensioned	Load Transfer	Remark
A	Shear	No	Bolt bearing	
B	Shear	Yes	Friction	Slip-resistant in SLS
C	Shear	Yes	Friction	Slip-resistant in ULS
D	Tension	No	Bolt tension	
E	Tension	Yes	Bolt tension and clamp force reduction	Less bolt force increase than cat. D.

The shear load transfer by friction of categories B and C is illustrated in Figure 2-19. The preload prevents the plates from sliding relative to each other, thus transferring the load by friction. The term 'slip-resistant' means that the connection slips only marginally, and fails when the slip is equal to 0,15 mm or if the external force at slipping is lower than the maximum external force reached prior to 0,15 mm of slip. Failure by slip means that the displacement is so large that the connection becomes more of bearing type.

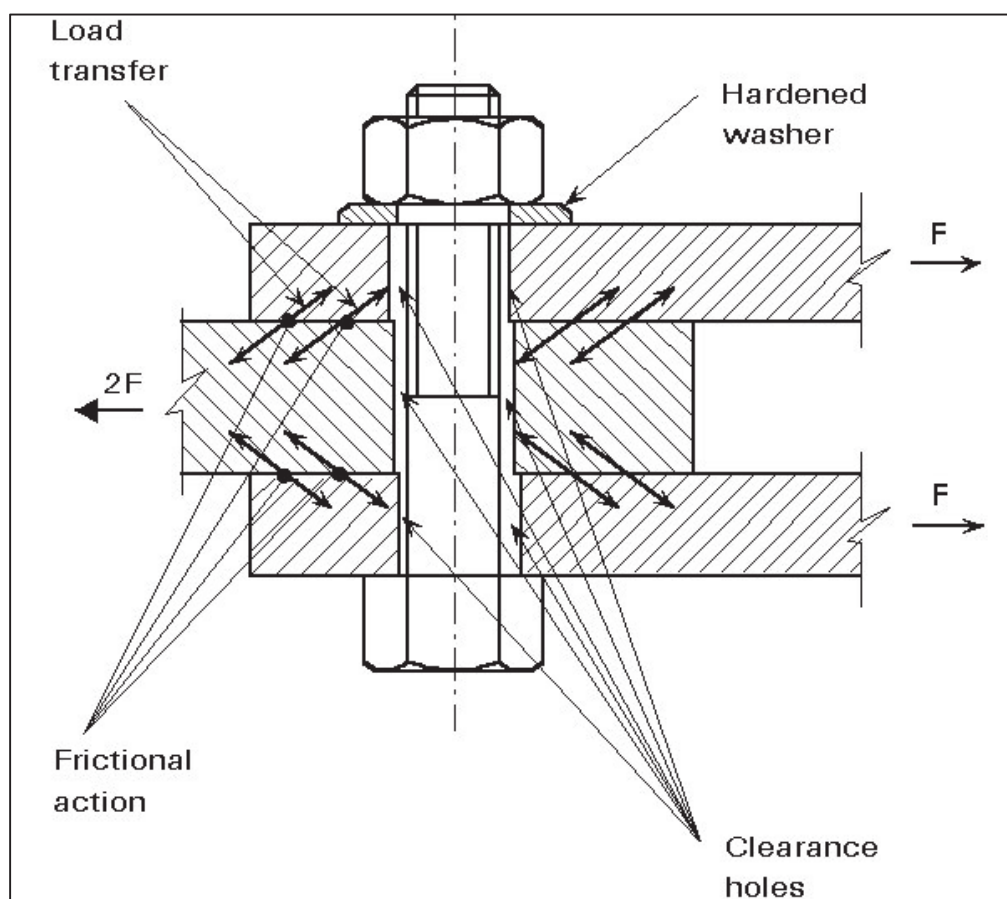


Figure 2-19 - Load transfer in HSFG (cat B/C) connections (ESDEP)

For pretensioned bolts the same rules for the end distance, edge distance and spacing apply as for non-pretensioned bolts. Consequently, failed preloaded bolts have the same design resistance (shear and bearing) as normal non-pretensioned bolts. Thus, after failing the slip criteria, actual failure (collapse) of the connection does not necessarily occur, but the function of the bolt (resisting slip) is no longer fulfilled. The design slip resistance of a preloaded bolt is defined as (2.2) in EN 1993-1-8.

$$F_{s,Rd} = \frac{k_s n \mu}{\gamma_{M3}} F_{p,C} \quad (2.2)$$

In (2.2) the parameter n indicates the amount of friction surfaces, μ is the applicable slip factor and k_s takes into account the type of hole for the bolt (Figure 2-20).

Description	k_s
Bolts in normal holes.	1,0
Bolts in either oversized holes or short slotted holes with the axis of the slot perpendicular to the direction of load transfer.	0,85
Bolts in long slotted holes with the axis of the slot perpendicular to the direction of load transfer.	0,7
Bolts in short slotted holes with the axis of the slot parallel to the direction of load transfer.	0,76
Bolts in long slotted holes with the axis of the slot parallel to the direction of load transfer.	0,63

Figure 2-20 - Factor k_s used to determine the design slip resistance (EN 1993-1-8) (European Committee for Standardization, 2011)

The factor μ is dependent on the surface treatment of the clamped members. Figure 2-21 shows the values for μ depending on the surface classes A-D as defined in EN 1090-2 as referred to by EN 1993-1-8.

Surface treatment	Class	Slip factor μ
Surfaces blasted with shot or grit with loose rust removed, not pitted.	A	0,50
Surfaces blasted with shot or grit:	B	0,40
a) spray-metallized with a aluminium or zinc based product;		
b) with alkali-zinc silicate paint with a thickness of 50 μm to 80 μm		
Surfaces cleaned by wire-brushing or flame cleaning, with loose rust removed	C	0,30
Surfaces as rolled	D	0,20

Figure 2-21 - Slip factor μ for surface treatment classes A-D (EN 1090-2) (European Committee for Standardization, 2011)

In case of painted surfaces, EN 1090-2 dictates that the surface condition has to fulfil EN ISO 12944-4, EN ISO 8503-2 and the manufacturer's recommendations on the use of the product. Also, the painting must be carried out according to EN ISO 12944-7. Furthermore, if two or more coating are applied, each coating must be distinguishable by colour. The surface of the members must be dry before use in an assembly or bundling for transport. Metal spraying must be done in accordance with EN ISO 2063 according to EN 1090-2. Metal spraying may be done using zinc, aluminium or zinc/aluminium 85/15 alloy.

The slip factor may be determined experimentally following Annex G of EN 1090-2 by means of a double lap shear test with two bolts (2 shear planes per bolt). In this case μ can be calculated using (2.3), in which F_{Si} is the slip load for the i -th specimen.

$$\mu_i = \frac{F_{Si}}{4F_{p,C}} \quad (2.3)$$

Category E connections have a more transparent force transfer than category B and C connections since they do not rely on surface roughness for force transfer. The preload in the bolt causes a clamping force in the plates as shown in Figure 2-22. In order to separate the plates from each other with an external tension force, the preload force must first be overcome. Since the plates are generally much stiffer than the bolts, any external load will mostly be taken up by a reduction in clamping force. This is beneficial for the fatigue performance of the joint, since the critical element (the bolt) is stressed to a smaller extent.

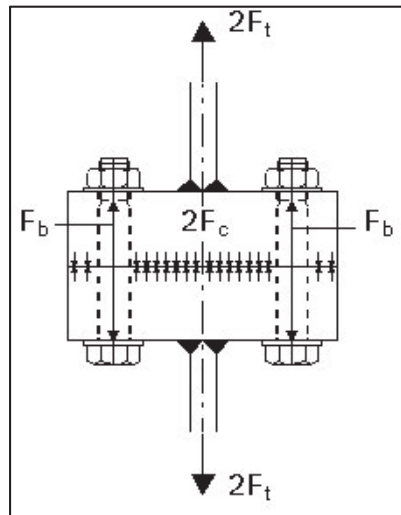


Figure 2-22 - Force transfer in Category E connections (ESDEP)

The ratio of bolt force increase and clamp force decrease due to external tensile loading is depending on the stiffness of both components, which can be schematized as a set of springs as indicated in Figure 2-23.

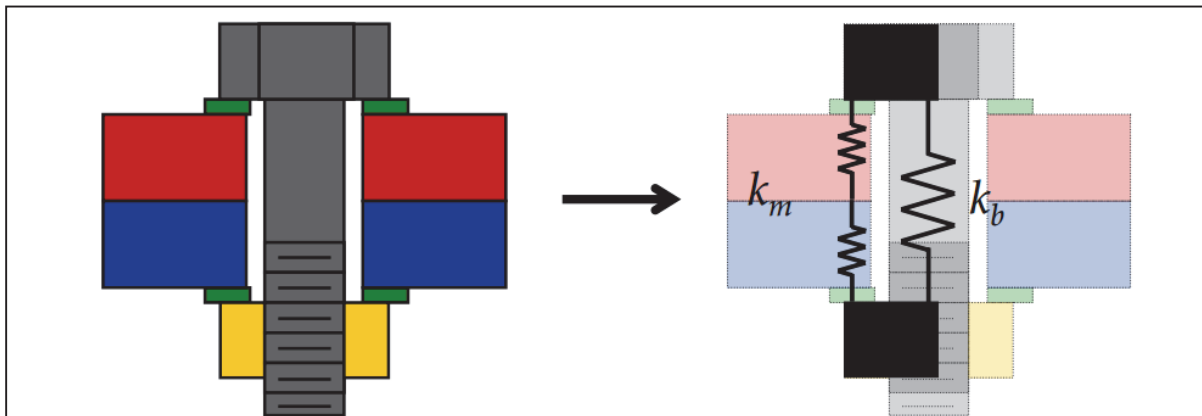


Figure 2-23 - Plate and bolt stiffness determine the external load distribution (Culpepper, 2009)

The deformation of the plates can be calculated using Hooke's Law (2.4). The stressed area is dependent on the distance from the plate surface due to stress spreading, as indicated in Figure 2-24. The stressed area can be calculated using (2.5). Often the half-apex angel α is taken as 30° .

$$\Delta l = \frac{P}{EA(z)} dz \quad (2.4)$$

$$A(z) = \pi \left[\left(z \tan(\alpha) + \frac{d_w}{2} \right)^2 - \frac{d_h^2}{2} \right] \quad (2.5)$$

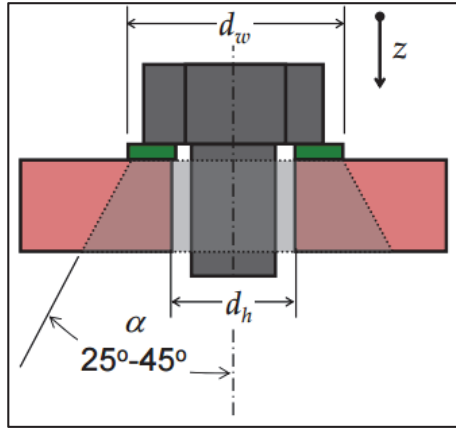


Figure 2-24 - Stress spreading under the head and nut (Culpepper, 2009)

When integrating (2.4) through the plate thickness, the stiffness of the member (2.6) can be derived.

$$k_{m,1} = \frac{\pi E d \tan(\alpha)}{\ln \left[\frac{(d_w - d_h + 2t \tan(\alpha))(d_w + d_h)}{(d_w + d_h + 2t \tan(\alpha))(d_w - d_h)} \right]} \quad (2.6)$$

Assuming that only materials with equal Young's Moduli are joined, the result shown in (2.6) is valid for half the thickness of the plates, thus $t = 0.5t_{s2}$. Inserting this into (2.6) and applying the theory of serial springs yields (2.7), which is the spring stiffness of the entire homogeneous plate package.

$$k_m = \frac{\pi E d \tan(\alpha)}{2 \ln \left[\frac{(d_w - d_h + t_{s2} \tan(\alpha))(d_w + d_h)}{(d_w + d_h + t_{s2} \tan(\alpha))(d_w - d_h)} \right]} \quad (2.7)$$

If a collar is present around the bolt shank in order to increase the clamping length, the collar may be schematized as a member that is completely under compression. The total package stiffness must then be taken including the stiffness of the collar, which is serial to the plates.

The bolt stiffness can be computed using Hooke's Law. In this case there are two discrete parts with a different cross sectional area, namely the bolt shank and the threaded part (Figure 2-25).

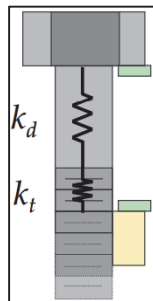


Figure 2-25 - Discrete bolt parts (shank and threaded part) (Culpepper, 2009)

Since the springs with stiffnesses k_d and k_t shown in Figure 2-25 are serial, the net stiffness can be calculated using (2.8) and (2.9).

$$k_b = \left(\frac{1}{k_t} + \frac{1}{k_d} \right)^{-1} = \frac{k_t k_d}{k_t + k_d} \quad (2.8)$$

$$k_t = \frac{E_b A_t}{l_t} ; k_d = \frac{E_b A_d}{l_d} \quad (2.9)$$

The total stiffness of the parallel spring system consisting of the plates and the bolt can be calculated using (2.10). The fraction of the external tensile load taken by the bolt can be expressed by (2.11).

$$k = k_b + k_m \quad (2.10)$$

$$C_b = \frac{k_b}{k} = \frac{k_b}{k_b + k_m} \quad (2.11)$$

Typically $C_b \approx 0.2$, which indicates that 20% of the external load is taken up by additional tension in the bolt. The other 80% of the external load is taken by the reduction of the clamping force. This is illustrated in Figure 2-26.

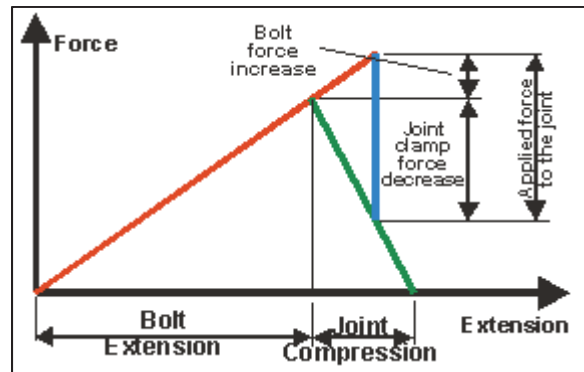


Figure 2-26 – External tensile force taken up by bolt force increase and clamp force decrease (BoltScience)

As soon as the clamp force has decreased with the magnitude of the initial bolt preload force, separation of the plates (a gap) occurs and force transfer only occurs by bolt tensioning, as shown in Figure 2-27 and Figure 2-28

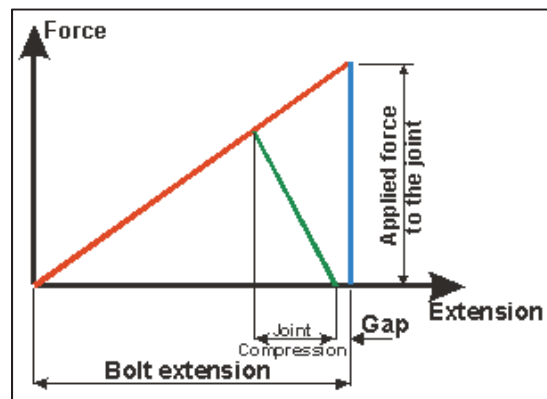


Figure 2-27 - Clamp force has reduced to zero, initiating a gap between the members (BoltScience)

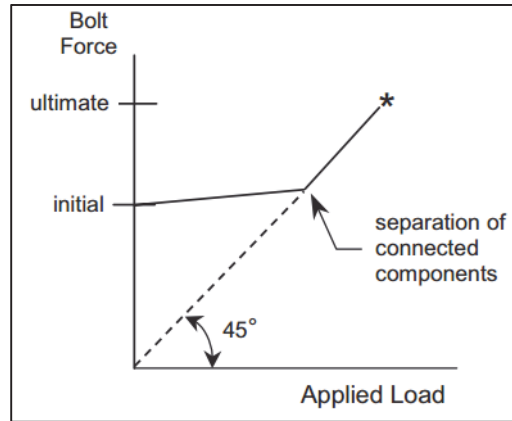


Figure 2-28 - Bolt force vs. externally applied tensile load (Kulak, 2005)

In case of external compressive loading, a similar story as mentioned above applies. However, in this case the line of the clamping package (green) is extended rather than the bolt line (red), since the compression induces contraction rather than extension.

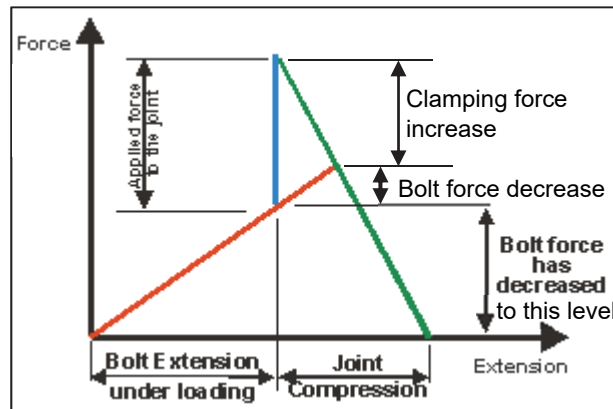


Figure 2-29 - Reduction of bolt force and increase of clamping force under external compressive loading (BoltScience)

Embedment and contraction of plate material due to shear loading are factors that may cause a negative imposed deformation (contraction) of the joint. Figure 2-30 shows the imposed joint contraction f_z and the resulting preload reduction F_z . The preload reduction can be calculated using (2.12).

$$F_z = \frac{f_z}{(\delta_s + \delta_p)} = f_z \cdot k_b \cdot \left[\frac{k_m}{k_b + k_m} \right] \quad (2.12)$$

In (2.12), δ_s and δ_p are the elastic resiliencies of respectively the bolt and the plate package (inverses of stiffness) and respectively denoted as δ_b and δ_m in the notation system introduced in this section.

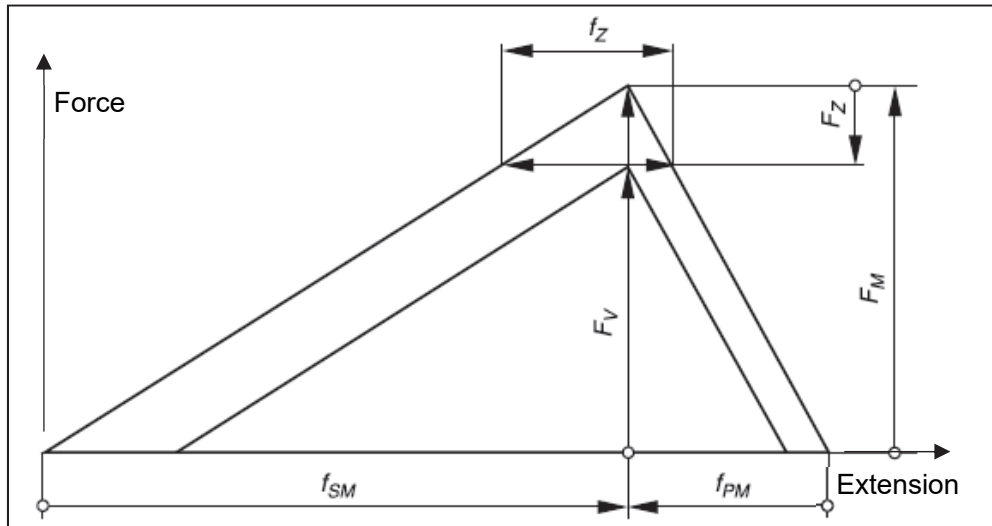


Figure 2-30 - Preload reduction F_Z of a bolt due to joint contraction f_Z (VDI, 2003)

Figure 2-30 and equation (2.12) can be understood as follows:

1. Due to joint contraction of magnitude f_Z the bolt, behaving as a spring, shortens and thus gets closer to its equilibrium length. As a result, the preload in the bolt decreases.
2. The plate package shortens as well, but gets further from its equilibrium thickness and thus offers additional resistance against this deformation. However, since the bolt preload has reduced, the plates have a net expansion in thickness direction and hereby compensate for some of the preload loss.

Thus, the thickening of the plates counteracts the shortening of the bolt and thereby reduces the preload loss. If the plates were to be infinitely rigid and thus not expand, the preload loss would amount to $F_Z = f_Z \cdot k_b$. Since the plates are not infinitely rigid, the preload loss reduces a little due to multiplication with the factor $k_m / (k_b + k_m)$ in (2.12), which is the equivalent of $1 - C_b$.

2.1.5 Fatigue

Pretensioned bolts have the same fatigue classification as conventional bolts according to EN 1993-1-9 when loaded in tension, namely category 50 (see Figure 2-31). Preloaded bolts offer an advantage with respect to conventional bolts since the reduction in stress range in the bolt may be taken into account. Thus, the service lifetime of a pretensioned bolt is higher than of a conventional bolt if all other parameters (e.g. external stress range) are equal. For bolts with diameter larger than 30 mm the size effect factor k_s must be applied.

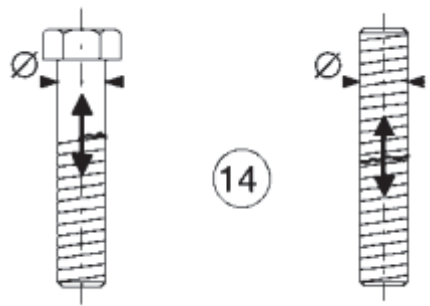
50	<p>size effect for $t > 30\text{mm}$:</p> $k_s = (30/t)^{0,25}$	
----	---	--

Figure 2-31 - Fatigue category classification for bolts according to EN 1993-1-9

In case of shear loading, different rules apply for the fatigue of the joined members and fasteners. For conventional bolts, the bolt is governing the fatigue life and has fatigue category 100 (Figure 2-32, top) provided that the threads are not in any of the shear planes and no load reversal occurs. In case of load reversal, it is not allowed to use non-pretensioned bolts according to EN 1993-1-8. In preloaded shear connections the fatigue life is governed by the plates rather than the bolts (Figure 2-32, bottom). In this case, the stress range in the plate must be computed using the gross cross-sectional area. Also, all requirements regarding edge and pitch distances mentioned in EN 1993-1-8 must be met.

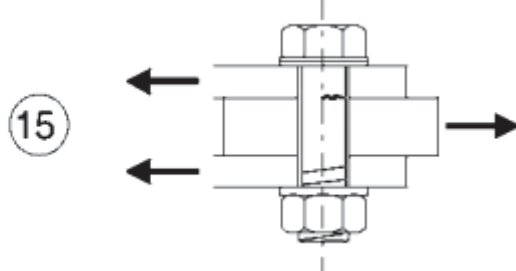
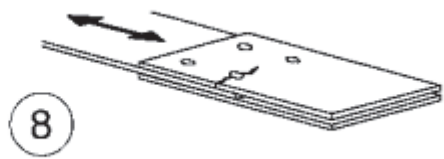
100 $m=5$	
112	

Figure 2-32 - Fatigue category classification in case of shear connections according to EN 1993-1-9. Top: conventional, bottom: preloaded assembly

Bolt relaxation may reduce the fatigue lifetime of the connection significantly due to the reduction in clamp load. Research indicates that in case of shear connections, the plate(s) will fail earlier than expected (Chakherlou, Oskouei, & Vogwell, 2008).

2.2 Bolt Relaxation

Much research has been carried out in the field of pretension bolts, especially on bolt relaxation. It is generally acknowledged that the pretension in the bolt is not constant, and thus the preload level is not a constant but a function of time as indicated by (2.13).

$$F_{p,c} = F_{p,c}(t) \quad (2.13)$$

The loss of pretension is important because according to (2.2), the slip load F_s reduces due to a reduction in $F_{p,c}$ and thus the connection may fail earlier than expected based on a fixed preload level. A reduction in $F_{p,c}$ is commonly referred to as bolt relaxation. Bolt relaxation is theoretically an eternal process as has also been confirmed in a practical sense (Heistermann, 2011). On the contrary, it is suggested that the preload level is already nearly stable after a period of 12 days (Yang & DeWolf, 2000), and also a 7 day stabilisation period is mentioned in literature (Reuther, Baker, Yetka, Cleary, & Riddell, 2014).

As suggested by Shoji & Sawa (2005), the only method to solve problems related to pretension loss is to re-tighten the bolts periodically during the service lifetime of the structure. It is acknowledged that this countermeasure leads to high maintenance cost and is thus not very economical. Thus, it is better to prevent (or minimize) pretension losses rather than solve them after they have occurred (Shoji & Sawa, 2005).

The notions of short term relaxation and long term relaxation are used in order to distinguish between two inherently different causes for relaxation (Abid, Khalil, & Wajid, 2015). Short term relaxation is defined as relaxation that *“occurs shortly, after the joint has been assembled or at least soon after it has been put into service, due to the number of reasons, such as bolt bending, soft parts (gasket), improper tooling and torqueing, bolt quality, non-parallelism of flange joint surfaces, geometric variance and so on (p. 44)”*. On the contrary, long term relaxation is *“generally due to the stress relaxation and vibration loosening. Stress relaxation can be related to the creep, as this is substantial under high temperature applications (p. 44)”*.

More generally, the main relaxation mechanisms are rotational and non-rotational relaxation (Eccles, 2011). Rotational relaxation occurs due to the relative turning between the inner and outer threads and is commonly referred to as self-loosening. In case of non-rotational relaxation, no relative rotation between the bolt and the nut occurs.

Assuming that all connections are fabricated according to EN 1090-2, the following causes for bolt relaxation exist (Abid et al., 2015) (Messler, 2004):

- Embedment
- Gasket creep
- Elastic interactions
- Contraction of clamping package
- Vibration loosening
- Bolt Bending
- Thermal effects
- Stress relaxation

The causes for relaxation only partially determine the magnitude of the pretension loss. The design of the joint also plays a large role: the ratio of the bolt stiffness and the plate package stiffness has a significant influence on the magnitude of preload loss (see 2.1.4). The effect of joint design on the magnitude of the pretension loss is also acknowledged in literature (Heistermann, 2011) (Bickford & Nassar, 1998).

2.2.1 Embedment

Embedment is defined as the plastic deformation of surfaces (Eccles, 2011). Generally embedment occurs at any discontinuity over the thickness of the clamped package, such as in the:

- Bolt head-plate interface
- Plate-plate interface
- Plate-nut interface
- Nut-thread interface
- Due to other influences

In VDI 2230-1 (2003, Table 5.4/1) and in the work of Jha (2015) guide values are included so that abovementioned embedment causes can be quantified to a certain extent depending on the surface roughness R_z . These guide values are shown in Figure 2-33 and Figure 2-34.

Average roughness height R_z according to DIN 4768	Loading	Guide values for amounts of embedding in μm		
		in the thread	per head or nut bearing area	per inner interface
< 10 μm	tension/compression	3	2,5	1,5
	shear	3	3	2
10 μm up to < 40 μm	tension/compression	3	3	2
	shear	3	4,5	2,5
40 μm up to < 160 μm	tension/compression	3	4	3
	shear	3	6,5	3,5

Figure 2-33 - Guide values for amounts of embedding (VDI 2230-1, Table 5.4/1) (VDI, 2003)

Type of Surface	Machined Thread	Formed Thread	Machined Surface	Ground Surface
Amount of embedding at each interface (mm)	0.005	0.003	0.004	0.002

Figure 2-34 - Guide values for embedding (Jha, 2015)

Embedment relaxation starts directly after tightening and theoretically will not end before a perfect fit-up between all subsequent members in the joint is obtained. The amount of preload loss due to embedment is estimated to be in between 10% (Mahmoud, Lopez, & Riveros, 2016) and 18.4%, the latter in case of thick coating layers of 508 μm (Yang & DeWolf, 1999) after 21 days. Ten percent of embedment loss is a minimum estimate according to bolt equipment manufacturers: a minimum load transfer factor of 1.1 must be taken in order to account for embedment losses (Tentec, 2006). Abid et al. (2015) suggest to tighten and loosen bolts several times in order to reduce embedment relaxation during the service lifetime of the structure. However, care should be taken not to tighten the bolt above $0,7f_{ub}A_s$ when planning to loosen the bolt, since EN 1090-2 prohibits to re-use bolts in this case.

Bolt head-plate embedment

Embedment in the interface between the bolt head and the underlying plate is caused by plastic deformation of imperfections and coating layers that prohibit direct steel-to-steel contact. The plastic deformation of the steel itself is caused by peak stresses arising from the fact that surfaces are never perfectly flat. The rougher the surface, the less contact exists between two components. The cause of bolt head-plate embedment is illustrated using Figure 2-35.

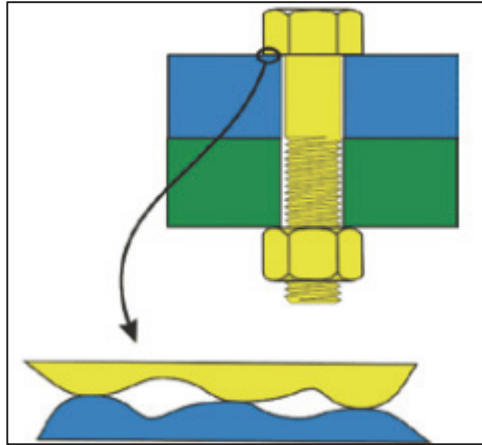


Figure 2-35 – Bolt head-plate embedment due to surface imperfections (Eccles, 2011)

Coatings and paint also give rise to embedment of the surfaces, which can be attributed to the lower axial stiffness (Young's Modulus) of the used materials. The thicker the coating thickness, the higher the embedment relaxation is (Yang & DeWolf, 2000). This is illustrated by Figure 2-36.

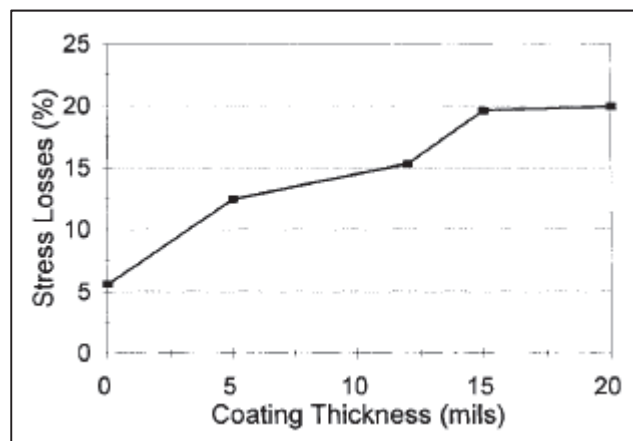


Figure 2-36 - Loss of bolt stress vs. coating thickness (1 mil = 0.0254 mm) (Yang & DeWolf, 2000)

Plate-plate embedment

The embedment process between the clamped plates is similar to the bolt head-plate embedment. However, the average stress at the plate-plate interface is lower due to the effect of load spreading, as shown in Figure 2-37. This results in a relatively lower embedment at the plate-plate interface.

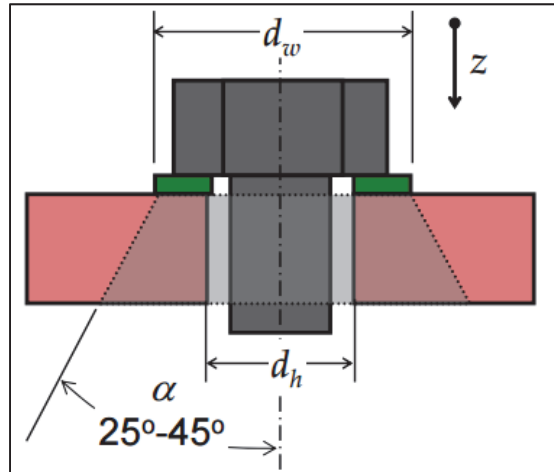


Figure 2-37 - Pressure reduction due to load spread (Culpepper, 2009)

Plate-nut embedment

The embedment process between the plate and nut is similar to the bolt head-plate embedment.

Thread-nut embedment

Embedment in the thread-nut region occurs due to the peak stresses caused by the transmission of the bolt force to the nut. Flattening of rough thread surfaces is the cause for bolt shortening and thus bolt relaxation. The phenomenon is shown in Figure 2-38.

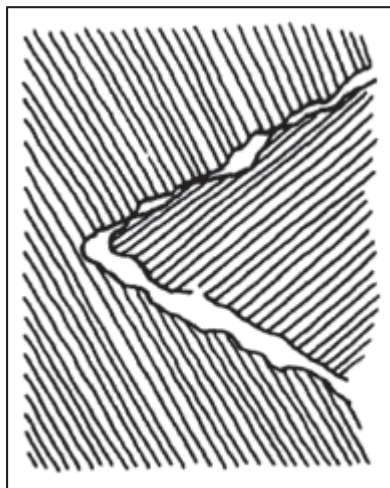


Figure 2-38 - Flattening of rough surface of thread and nut causes relaxation of bolt force (Bickford & Nassar, 1998)

Other causes for embedment

Apart from the causes for embedment generally acknowledged in literature, Bickford & Nassar (1998) list causes for embedment if certain execution aspects are ignored:

- Undersized holes (Figure 2-39, left)
- Oversized holes (Figure 2-39, right)
- Poor thread engagement e.g. due to different sized nut and bolt (plastic deformation due to reduced thread contact area)
- Too short thread engagement length (plastic deformation due to reduced thread contact area)

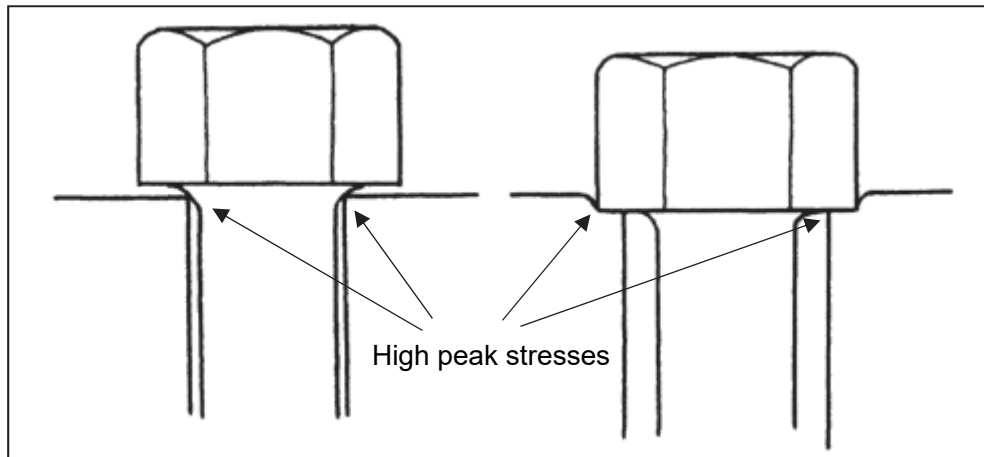


Figure 2-39 - Embedment due to undersized and oversized holes, edited after Bickford & Nassar (1998)

2.2.2 Gasket Creep

Gaskets are often installed in bolted joints in order to obtain a leak-free joint. Gaskets provide containment by deforming, hereby blocking all potential 'exits' or leaks for a given substance. In to close off all leaks, the gasket must be rather soft in order to deform easily and provide a complete seal. Potential materials for gaskets include cork, rubber, plastics and soft metals (Messler, 2004). The softness of the material is the reason for gasket creep: the soft material flows out due to the introduction of the bolt preload force. As a result, the clamping package reduces in thickness which, in turn, causes bolt relaxation. Gasket creep is proportional to the thickness of the gasket, thus it is advised to use a gasket that is "as thick as it needs to be but as thin as possible" (Bickford, 1990). Relaxation due to gasket creep is inherently unavoidable, but can be compensated for by overloading or retightening of the bolts (Davet, 2007). A well-designed gasket may cause a preload reduction of up to 5% (Blake, 1985).

2.2.3 Elastic Interaction

Bolt relaxation due to elastic interaction occurs during the tightening of the bolts. Since it is generally not possible to tighten all adjoining bolts simultaneously, the bolts are pretensioned one after the other. Preloading the bolt causes the clamped members in the vicinity of the bolt to contract. When a second bolt is present within the area of influence of the bolt that has been tightened first, the contraction of the plate material due to preloading bolt 2 causes bolt relaxation in bolt 1. The same holds for joints with more bolts. Davet (2007) mentions preload losses up to 60% due to elastic interaction are not uncommon, and that the magnitude of the preload loss is dependent on for example the size of the joint, the distance between the bolts and the stiffness of the joint members.

2.2.4 Contraction of the clamping package

Loading a connection with HSFG bolts in shear (mostly) means that a tensile axial force is introduced in the clamped members. The introduction of an axial load leads to a positive strain (elongation) in the direction of loading. Poisson's theory states that an elongation in one direction means that the object wants to contract in the two perpendicular directions (the width and thickness directions). Due to the reduction in thickness of the clamping package, the bolt reduces in length, causing bolt relaxation. The Poisson effect (Figure 2-40) is often mentioned in literature as a reason for the reduction in preload force in the bolt (Heistermann, 2011) (Oskouei & Chakherlou, 2009). Oskouei & Chakherlou (2009) do not only mention the existence of the preload reduction due to static external loading, but has also carried out numerical research and concluded that higher Poisson's ratios will lead to larger preload losses. Other research shows that there are two mechanisms for preload loss due to an external shear load: the axial stresses cause recoverable transversal strains, whereas the smoothing of the surface roughness due to the shear load transfer causes non-recoverable transversal strains (Husson, 2008). Both lead to preload loss.

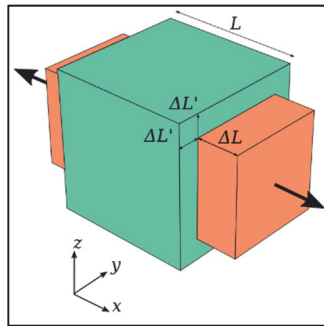


Figure 2-40 - Poisson effect with no lateral constraints (Wikimedia Commons, 2010)

2.2.5 Vibration loosening

Preload loss due to vibration loosening – caused by cyclic external loading - has been investigated more often than preload loss due to contraction of the clamped members under static external loading. A possible explanation is that slip-resistant connections are mostly used for cyclically loaded structures, and thus their behaviour under such cyclic loads is more important than their static behaviour. Preload loss due to cyclic external loading is often referred to as self-loosening. Self-loosening can cause complete loosening of the connection (100% preload reduction), especially in case of short (stiff) bolts (Friede & Lange, 2009)

The mechanism of self-loosening is described by Blume & Illgner (1988). The moment needed to unfasten a bolt (M_L) is given by (2.14) (Blume & Illgner, 1988).

$$M_L = -M_{T,P} + M_{T,F} + M_{H,F} \quad (2.14)$$

In (2.14), $M_{T,P}$ is the moment originating from the thread pitch and helps to loosen the bolt. The moments $M_{T,F}$ and $M_{H,F}$ originate from the friction in respectively the thread and under the head of the bolt. Self-loosening occurs in case of (2.15).

$$M_{T,P} > M_{T,F} + M_{H,F} \quad (2.15)$$

A displacement under the head of the bolt occurs if the motion between the centre line of the bolt and the centre line of the nut exceeds the marginal slip a (2.16) (valid in case of a single lap joint) (Blume, 1969).

$$a = \frac{F_v \mu l_k^3}{12 EI} \quad (2.16)$$

In (2.16), F_v is the preload force, μ is the slip factor, l_k is the clamping length ($\sum t$) and EI is the bending stiffness of the bolt.

If both the marginal slip and friction force (moment) are exceeded due to an external load, then the bolt and nut threads will turn with respect to each other (Shoji & Sawa, 2005). If this turn is not recovered in the same loading cycle, the bolt force reduces. Per cycle the loss is rather small, but the total preload loss accumulates quickly due to the repetitive character of the loading (Shoji & Sawa, 2005). The force that is responsible for turning the nut is shown in Figure 2-41.

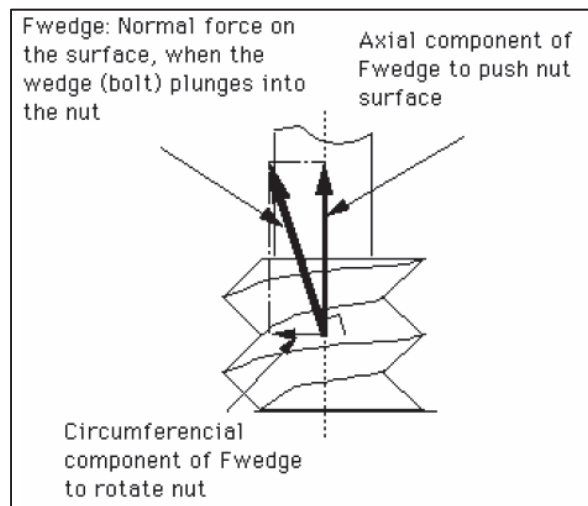


Figure 2-41 - Nut rotation due to differential turning of bolt head and nut (Shoji & Sawa, 2005)

The friction force in the threads is harder to overcome in case of higher preloads and a higher slip factor of the threads (Shoji & Sawa, 2005). Also, fine-pitched threads have less vibration loosening due to the reduced circumferential force component caused by the increased number of revolutions per unit of length along the bolt (Ramey & Jenkins, 1995). DIN 65151/25201-4 describes a vibration test (Junker test) in order to determine the cyclic self-loosening of bolts, as shown in Figure 2-42.

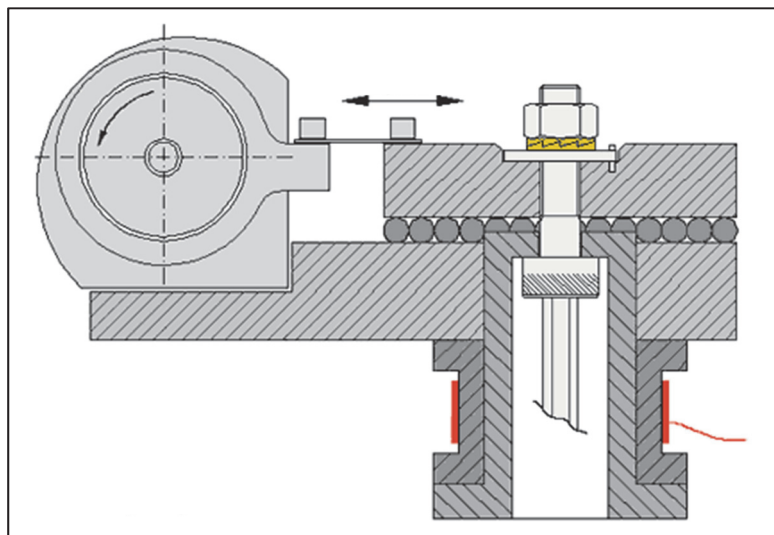


Figure 2-42 - Junker Test device to determine self-loosening of bolts under cyclic loading (Maryland Metrics)

In order to overcome the issue of preload loss due to vibration loosening, several systems are on the market that prevent the relative motion of the nut and the bolt. An example is the Huck-bolt (Figure 2-43). The Huck-bolt is put in the hole and a collar is loosely fitted over the bolt (1). The second step is to tighten the bolt using an axial tensioner tool which grips in the threads of the upper threads (2). During the force introduction, the tool moves downward and deforms the loosely fitted collar plastically: the collar material is pressed into the threads of the Huck-bolt (3). Finally, the bolt breaks off at the narrowing just above the top of the collar (4). Due to the fact that the collar material is pressed into the threads of the Huck-bolt, filling up all gaps, no self-loosening can occur. According to the Huck-bolt manufacturer (Alcoa Fastening Systems & Rings), the fatigue life of the connection can increase with 400% compared to conventional pretensioned bolts.

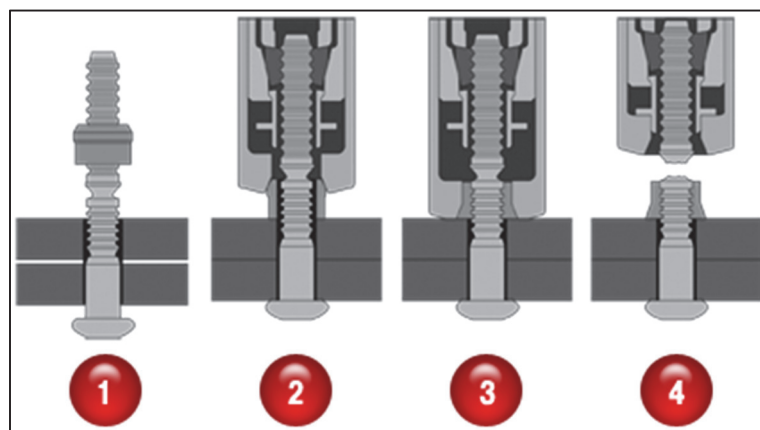


Figure 2-43 - Huckbolt® Installation Sequence (Alcoa Fastening Systems & Rings)

As an alternative to special bolts such as the Huck-bolt, Nord-Lock has invented a washer that is resistant to vibration loosening. An assembly containing Nord-Lock SC-washers is shown in Figure 2-44. The cam angle α is larger than the pitch angle β , which ensures that the bolt cannot self-loosen since this is restrained by the wedge effect of the cams.

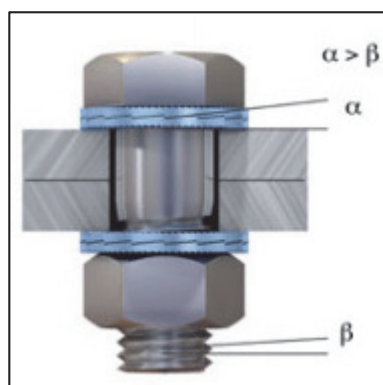


Figure 2-44 - Nord-Lock SC-washers (Nord-Lock Bolt Securing Systems)

A final alternative is mentioned in the work of Sase & Fujii (2001), which consists of a special bolt and nut with steps and inclined parts on the threads (Figure 2-45). Since the clamping force in the bolt presses against the step part, it is harder to turn the nut due to the wedge effect of the step. However, producing threads in this shape is rather difficult and prevents its common use (Sase & Fujii, 2001).

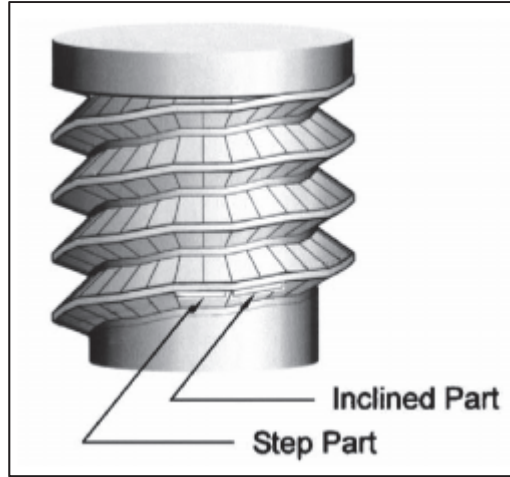


Figure 2-45 - Thread with inclined and step parts in order to reduce vibration loosening

2.2.6 Bolt Bending

Bolt bending is also named as a cause for preload loss (Patil, Shilwant, & Kadam, 2006). The underlying mechanism is that bending of the bolt causes a force in the friction surface between the nut and the threads. If this force is large enough, bolt loosening may occur in a similar way as discussed in Section 2.2.5. However, bolt bending will only occur after a significant amount of slip (Taha & Daidié, 2012), as discussed in Section 2.3. The mechanism of bolt bending is very similar to that of vibration loosening, however, in bolt bending larger rotations may occur all at once.

2.2.7 Thermal Effects

Research shows that in case of difference in temperatures between the bolt and the clamped members may lead to loss of preload (Patil, Shilwant, & Kadam, 2006). The effect may be worse for materials with a different coefficient of thermal expansion. Davet (2007) indicates that temperature differential between joint components may cause the preload to increase, in case the clamped members expand in thickness direction. Due to the increase in preload, additional embedment and deformation of the gasket occurs, which is non-recoverable and causes a net preload loss after the member temperatures have become equal. The VDI 2230 design guide for bolted connections includes a calculation method (2.17) to determine the preload loss due to thermal effects.

$$\Delta F'_{vth} = \frac{l_k(\alpha_s \Delta T_s - \alpha_p \Delta T_p)}{\delta_s \frac{E_{SRT}}{E_{ST}} + \delta_p \frac{E_{PRT}}{E_{PT}}} \quad (2.17)$$

In (2.17), the subscript “s” denotes “schraub” (bolt) and the subscript “p” denotes plates. The elastic resilience (inverse of stiffness) is denoted with δ and “RT” stands for room temperature.

2.2.8 Stress Relaxation

Stress relaxation is defined as a decrease in stress under constant strain. Under increased temperatures, the stiffness of the bolt reduces. Because the material still behaves linear elastically and thus follows Hooke's Law, the consequence is that the stress in the bolt drops, causing a loss of preload. The percentage of preload left in the bolt after 1000 hours is plotted against the temperature in Figure 2-46.

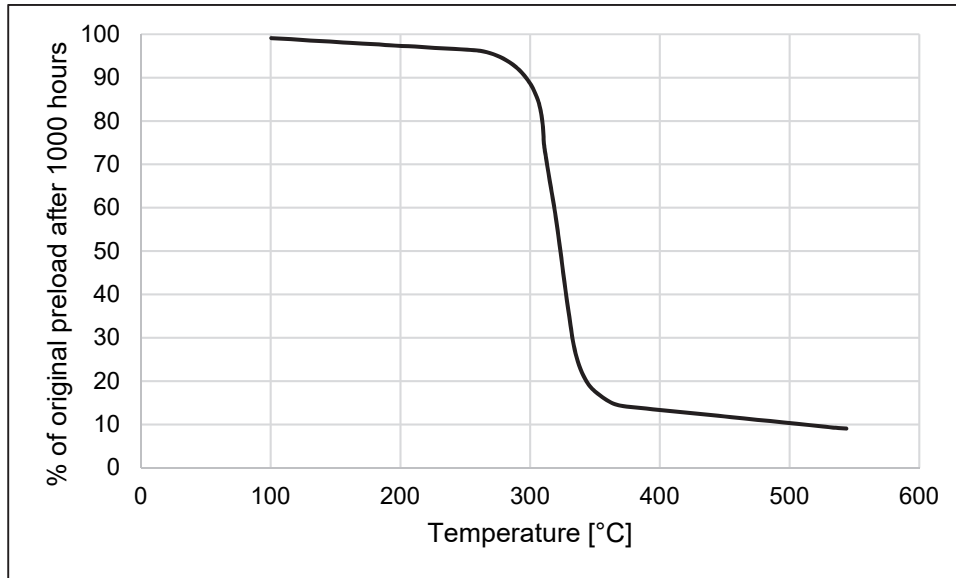


Figure 2-46 - Relative preload after 1000 hours at a constant temperature, drawn after Davet (2007)

As can be seen from Figure 2-46, stress relaxation can be neglected at normal temperatures for building structures. However, in permanently hot (industrial) environments, preload loss due to stress relaxation may be significant. It should be noted also during a fire the pretensioned bolts will relax, which means that the connection must be assessed after the fire has been put out.

2.3 Failure Mechanisms

In the research of Taha & Daidié (2012), the mechanical behaviour of double lap slip-resistant connections loaded in shear is investigated. Under an increasing shear load, the following stages in mechanical behaviour can be distinguished:

- I. Adhesion between the plates for small external loads ($F < 2 \cdot \mu F_{p,c}$) (Figure 2-48, 1)
- II. Dynamic friction (slipping) for higher loads than mentioned under 1 (Figure 2-47 & Figure 2-48, 2)
 - a. First elastic deformation (Figure 2-48, 3)
 - b. Secondly plastic deformation (Figure 2-47 & Figure 2-48, 4)
- III. Failure due to bolt bending (caused by excessive slip) (Figure 2-47 & Figure 2-48, 5)

The force-displacement curve showing the abovementioned stages is shown in Figure 2-48.

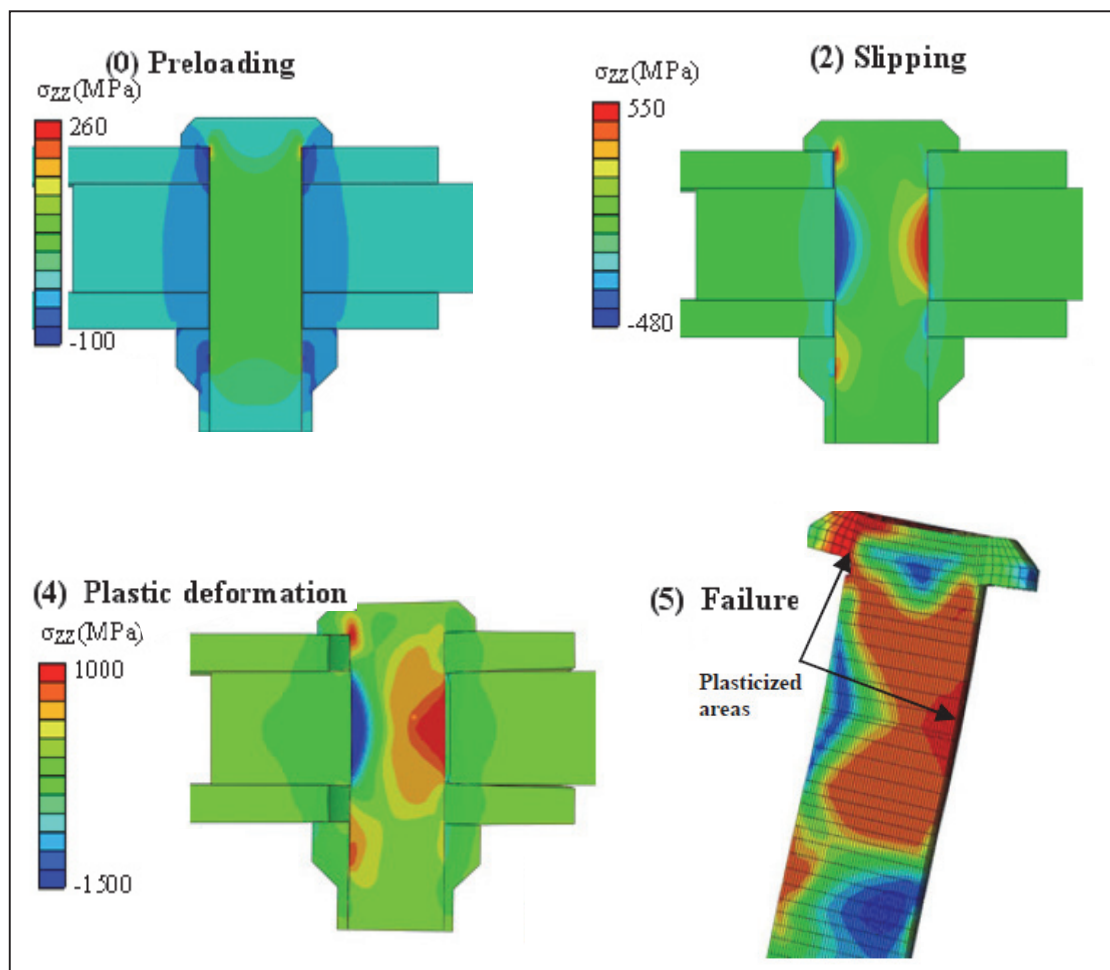


Figure 2-47 – Mechanical behaviour of slip-resistant connections under increasing shear load, drawn after Taha & Daidié (2012)

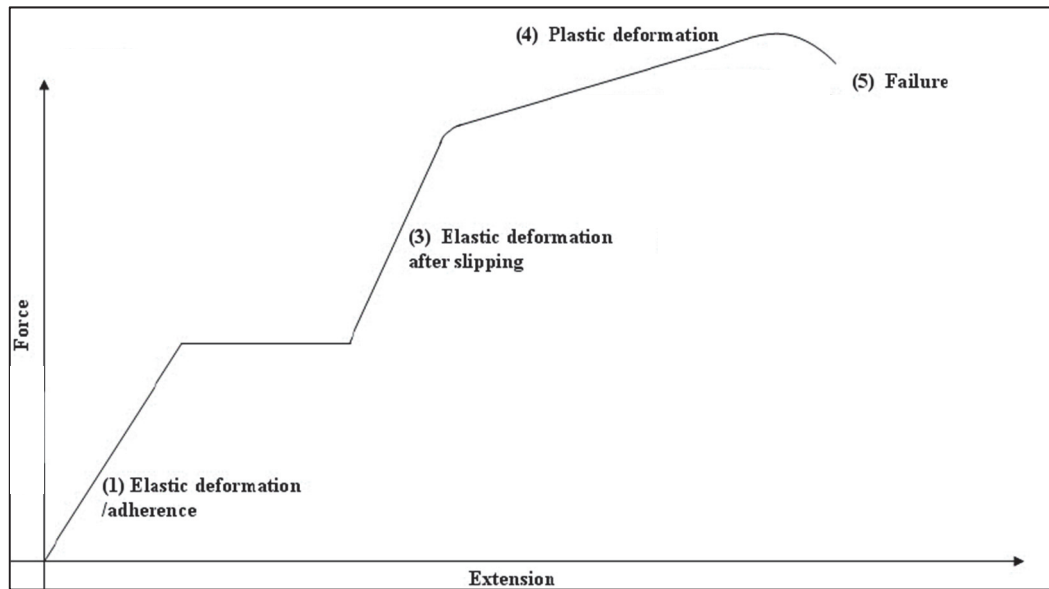


Figure 2-48 - Force-displacement diagram showing the mechanical behaviour of slip resistant connections under increasing shear load, drawn after Taha & Daidié (2012)

2.4 Surface Treatments

As already indicated in Figure 2-21, blasted surfaces without further coating have the highest slip factor μ in EN 1090-2. Literature shows that the slip factor μ is mostly influenced by the contact surface roughness (Ivkovic, Djurdjanovic, & Stamenkovic, 2000). Based on this consideration, there is no initial reason for coatings to be applied. However, the reason to apply coatings is that there is a general consensus that coatings provide additional corrosion protection and have a higher slip factor μ . The latter occurs due to weathering of the zinc layer, which increases the surface roughness of the coating (Porter, 1991). However, coatings have proven to creep under sustained loading, causing failure based on the slip-requirement of 0,15 mm. Therefore, EN 1090-2 limits the value μ to 0,4 for coated plates. If higher values for μ want to be used, EN 1090-2 prescribes a test (Annex G of EN 1090-2) in order to determine μ , taking into account the creep sensitivity of the coating over a lifetime of 50 years. Generally, three different coating systems can be distinguished (Hendy & Iles, 2015):

- Hot dip galvanizing
- Thermally sprayed metal coatings
- High performance paint coatings

Attention will also be given to the blasting of surfaces. It should be noted that there are multiple definitions of surface roughness and that in this thesis the surface roughness R_z is used, which refers to the average surface roughness over a specified sampling length.

2.4.1 Hot dip galvanizing

Hot dip galvanizing is one of the most basic surface treatments. The main step in the process is to cover the steel member in zinc using a molten zinc bath at a temperature of around 450 °C. Prior to the zinc bath, the surface of the member is prepared. The steps taken in the hot dip galvanizing process are shown in Figure 2-49.

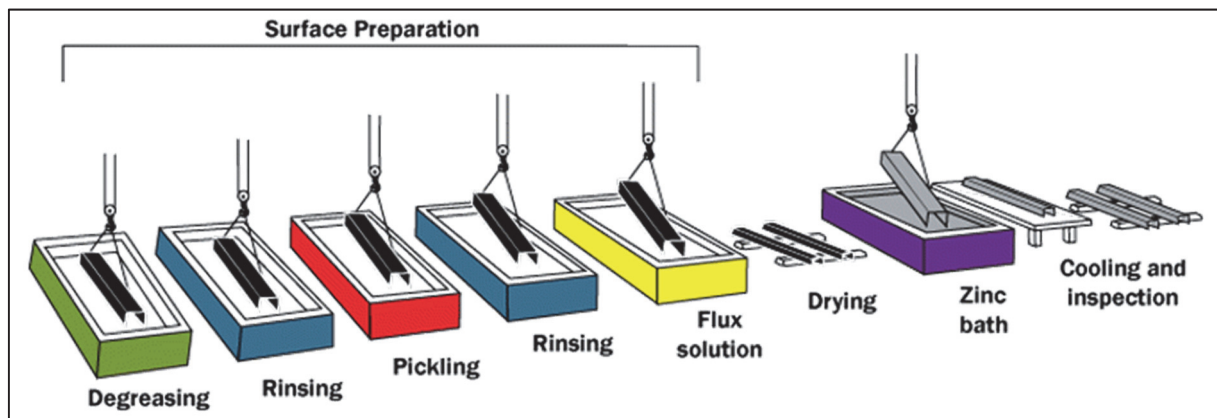


Figure 2-49 - Hot dip galvanizing process (American Galvanizers Association)

The requirements for hot dip galvanizing are laid down in EN ISO 1461. The minimum thickness of the zinc layer is dependent on the thickness of the member. The speed at which hot dip galvanizing can take place is rather high at 180 m/s (SMS Siemag AG). However, the width of the member is limited to the size of the zinc pool.

The steel and zinc undergo a metallurgical reaction (MetalPlate Galvanizing L.P.). The surface layer of the member is pure zinc, which can be attributed to the withdrawal of the member from the zinc bath. This zinc surface is rather soft and causes a low slip factor (it can be as low as

0,2) because it acts as a lubricant (Fisher, Struik, & Kulak, 1974). The cross section of a member that has been hot dip galvanized is shown in Figure 2-50.

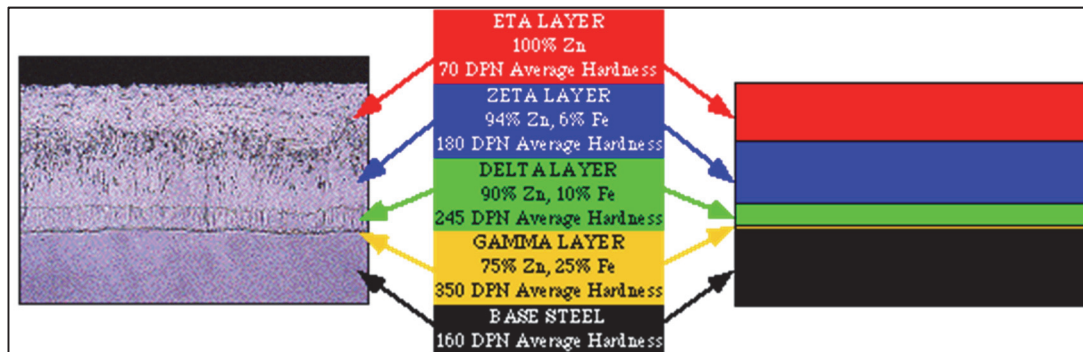


Figure 2-50 - Cross section of hot dip galvanized member (MetalPlate Galvanizing L.P.)

2.4.2 Thermally Sprayed Metal Coatings

Thermally sprayed metal coatings are applied using a material, in powder or wire form, and a heat source (de Vries, Rauhorst, Plasse, & Kerneling, 1999). The material is molten and sprayed onto the surface of a member. The process is regulated in EN ISO 2063. The material that is applied is mostly zinc, aluminium or an alloy of both (see 2.1.4). The process is shown in Figure 2-51.



Figure 2-51 – Thermally Sprayed Metal Coating process, using a wire-source and a hand sprayer (Avant Guards Coatings)

Avant-Guards Coatings lists a number of benefits of thermally sprayed metal coatings over hot dip galvanizing on their website, which include:

- Total control of coating thickness
- Can be done in the field (no factory environment necessary)
- Only the material that comes in contact with steel is to be melted (energy efficient)

Spray metallizing leads to a coating with voids. If the voids would be removed (or squeezed out), the coating thickness would be about 20% thinner. The void problem decreases with time, since zinc corrosion products fill the voids with time. (Lindsley, 2016). A cross section of a member that has undergone thermal spray metallizing is shown in Figure 2-52.



Figure 2-52 - Cross section of a thermally metal sprayed coating (Lindsley, 2016)

2.4.3 High Performance Paint Coatings

The most frequently used high performance paint coatings are alkali and ethyl zinc silicates. The zinc provides galvanic protection, whereas the alkali and ethyl silicates are the binders and are responsible for curing. The main difference between alkali and ethyl silicates is that the first is inorganic and must dispose of water to cure, whereas the latter is organic and needs moisture to cure (Undrum, 2016). This puts a demand on the curing environment: in case of alkali silicates a relatively low ambient moisture content of 50-60% of the surrounding air is required (AkzoNobel, 2015). Generally, the curing of ethyl silicates is a faster and easier process. However, a drawback of ethyl silicates is that they are more prone to shrinkage (Undrum, 2016), but both the organic and inorganic zinc silicates have the problem of mud cracking in case of too thick coating layers. The coating is applied directly to the steel substrate (e.g. by air spray, see Figure 2-54), after surface preparation in accordance with ISO 8504 in order to achieve a good bond. Research confirms that (especially alkaline) zinc silicate coatings are very sensitive to surface impurities of the underlying steel but, if applied correctly, leads to a very good adhesion to the steel substrate due to the primary valence bonding (Undrum, 2016).

A typical cross section of a alkaline zinc silicate coating is shown in Figure 2-53. The grey dots in Figure 2-53 are zinc oxides, whereas the black parts represent the binder(s) (MetalPlate Galvanizing L.P.).

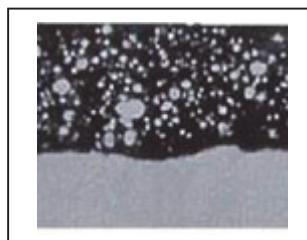


Figure 2-53 - Cross section of an alkaline zinc silicate coating (Lindsley, 2016)



Figure 2-54 - Application of alkali zinc silicate coating (Ashok Paint Agencies)

2.4.4 Blasting of Surfaces

Abrasive blast cleaning is the most important technique for the cleaning and roughening of steel surfaces. During blast cleaning, sharp particles are fed through the nozzle of a spray gun at high speeds. The impact of the particles on the steel causes the removal of rust/dirt and an increased surface roughness. EN ISO 8501 contains the regulations regarding abrasive blast cleaning and differentiates between light, thorough and very thorough blast cleaning. The ultimate result in EN ISO 8501 is blast cleaning to visually clean steel.

Principally, all particles with abrasive properties are suitable for blast cleaning. However, most often metals are used in the form of shot (Figure 2-55, right) or grit (Figure 2-55, left). After impact, the abrasive particles can be recycled by separating them from the fine particles originating from the cleaning/roughening process.



Figure 2-55 - Grit (left) and shot (right) particles used for abrasive blast cleaning (Mogilev Metallurgical Works)

The rougher the steel surface, the more potential arises for embedment and thus for bolt relaxation.

2.5 Actual Pretension Measurement

It is vital to know the pretension present in the bolt, especially after tightening, to ensure a well-performing slip-resistant connection. Also, in lab conditions, the pretension at every point in time may want to be recorded. The pretension in HSFG bolts can be measured in various ways. (Bickford & Nassar, 1998) names the following options:

- Strain-gauged fasteners
- Strain-gauged washers
- Ultrasonic
- Digital Micrometres

The two most common options (strain-gauged fasteners and ultrasonic) are discussed in more detail.

2.5.1 Strain-gauged fasteners

Bolts can easily be equipped with strain-gauges by drilling a hole in the bolt and fixing the strain-gauge with adhesive to the interior of the bolt (Figure 2-56). The bolt strain can be converted to bolt force using the stress-strain relationship. However, equipping all bolts with strain-gauges is rather expensive and complicated but the results are very accurate (Lifetime Reliability Solutions). For experiments where accurate results are paramount, strain-gauged fasteners are a good choice (Bickford, 1990).

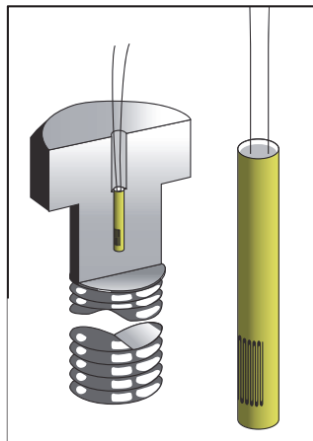


Figure 2-56 - Strain-gauged bolt (Techno Test Instruments)

2.5.2 Ultrasonic

The bolt force can be measured using the Time of Flight (TOF) principle on which ultrasonic measurements are based. The TOF is the time needed for a pulse to travel back to the original location, thus the time for the echo to reach the transmission station. First, the TOF of an unloaded bolt is measured. During tightening, the TOF increases due to bolt elongation and the accompanying bolt strain can be calculated. The principle of ultrasonic bolt measurement is shown in Figure 2-57.

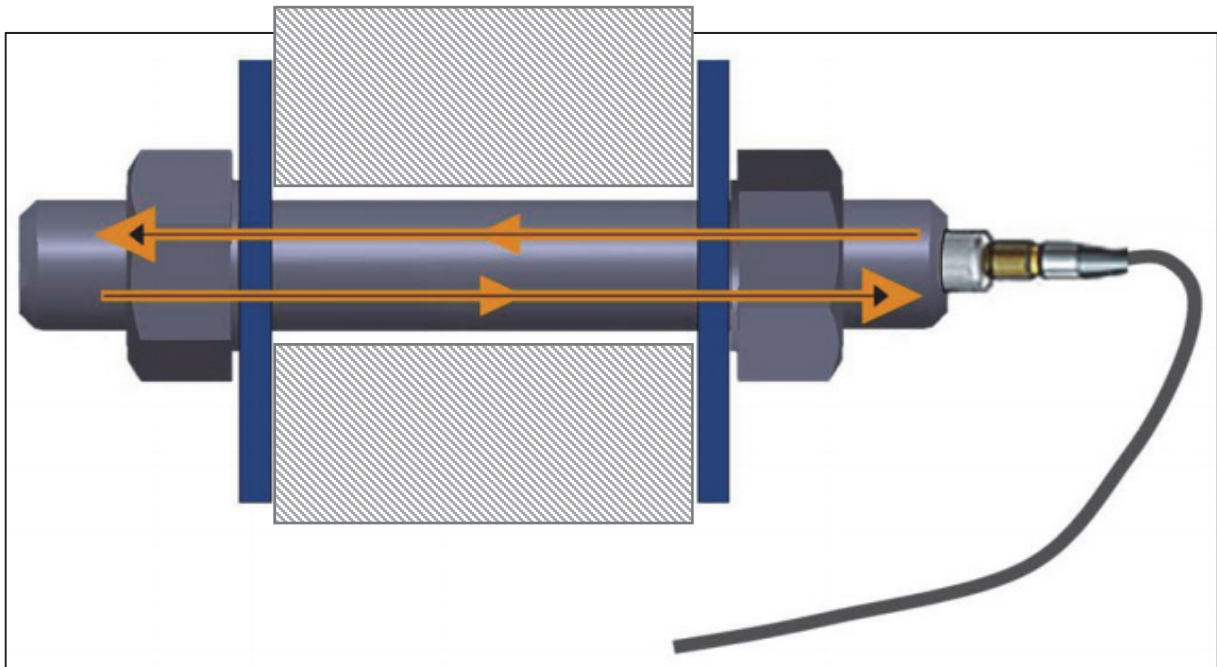


Figure 2-57 - Ultrasonic determination of bolt elongation (Boltight)

Ultrasonic measurements are rather accurate and allow for easy measurements of existing constructions. An advantage in this case is that no investment per bolt is necessary, since the equipment can be used bolt-after-bolt.

3 Test Results

In order to investigate the loss of preload in pretension bolts, test results of past research have been made available. The test results originate from extended creep tests (according to EN 1090-2) which have been carried out for the SIROCO research project at TU Delft, which focuses on the investigation of creep sensitivity of different coatings.

3.1 Test Set-up

Since the test results originate from extended creep tests, the test set-up is identical to the test set-up prescribed in Annex G of EN 1090-2 (Figure 3-1). The test set-up consists of a double lap joint with M20 HSFG bolts of bolt property classes 8.8 and 10.9 and, dependent on the bolt length, of HR and HV bolt systems.

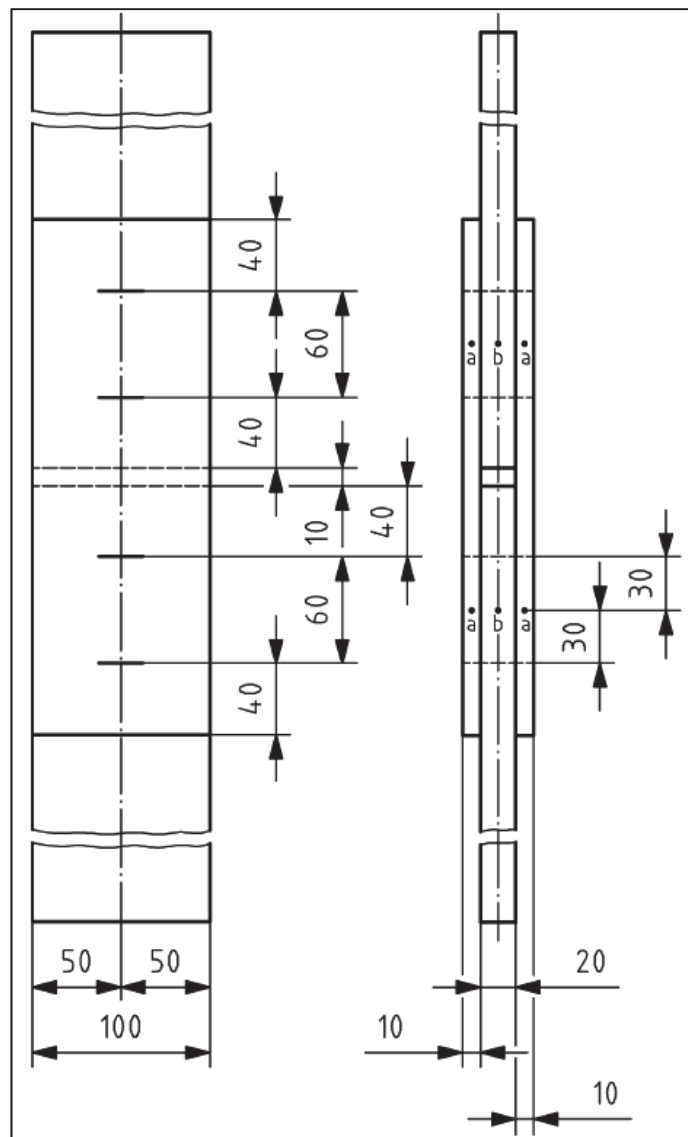


Figure 3-1 - Extended Creep Test Set-up using M20 bolts according to EN 1090-2 (European Committee for Standardization, 2011)

The actual test-setup is shown in Figure 3-2 and is according to the dimensions of Figure 3-1. The LVDTs (linear variable differential transformers) are used to measure the slip and are not of direct particular interest to the research of bolt pretension loss.

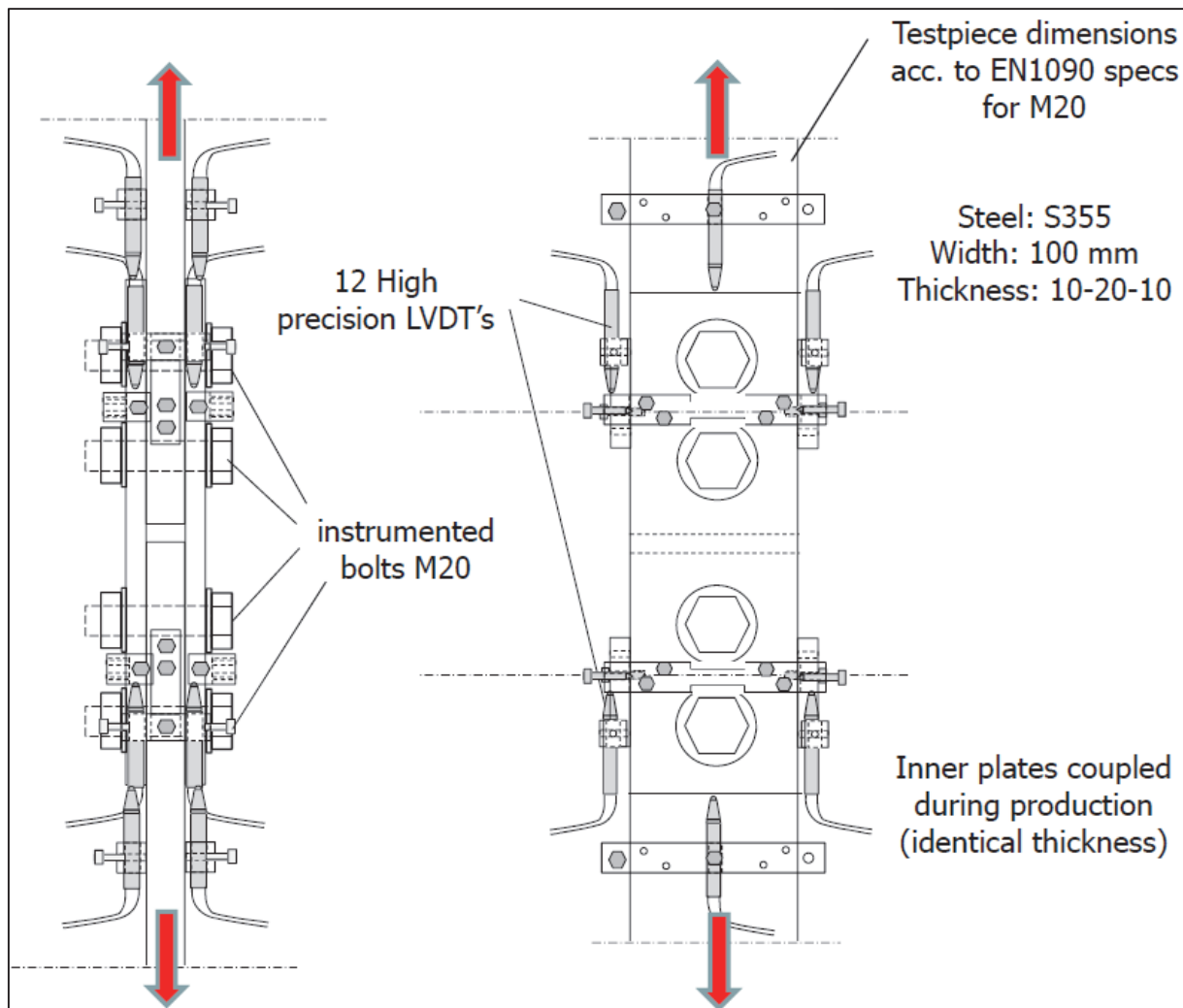


Figure 3-2 - Set-up used to obtain test results, fulfilling EN 1090-2 demands (Vries, P.A. de, 2016)

The bolts are instrumented with glued-in strain gauges (2.5.1) in order to measure the preload in the bolt. Material certificates are available for both the centre and cover plates which are of nominal strength grade S355. The centre plates have a yield stress of $f_{y,ctr} = 409 \text{ MPa}$ and an ultimate tensile strength of $f_{UTS,ctr} = 538 \text{ MPa}$. The values for the (thinner) cover plates are $f_{y,cvr} = 458 \text{ MPa}$ and $f_{UTS,cvr} = 597 \text{ MPa}$. The centre and cover plates have been shot abrasive blast cleaned before the application of the alkali zinc silicate paint with a film thickness of around $80 \mu\text{m}$ and a surface roughness $R_z \approx 80 \mu\text{m}$. The surface preparation of the spray metallized specimen has been carried out using pure zinc. These specimen have a film thickness of $160 \mu\text{m}$ and a surface roughness $R_z \approx 100 \mu\text{m}$. In Appendix A an overview of the precise film thickness and surface roughness per specimen is included.

The dimensions of the bolts are according to EN 14399. The length of the threaded part can be calculated based on the package thickness and bolt shank length, which is shown in Figure 3-3 for the property class 8.8 and 10.9 bolts. Two washers with $h = 4 \text{ mm}$ have been used for both property class 8.8 and 10.9 bolts: one under the head and one under the nut (however, 1 washer is enough for class 8.8 bolts according to EN 1090-2).

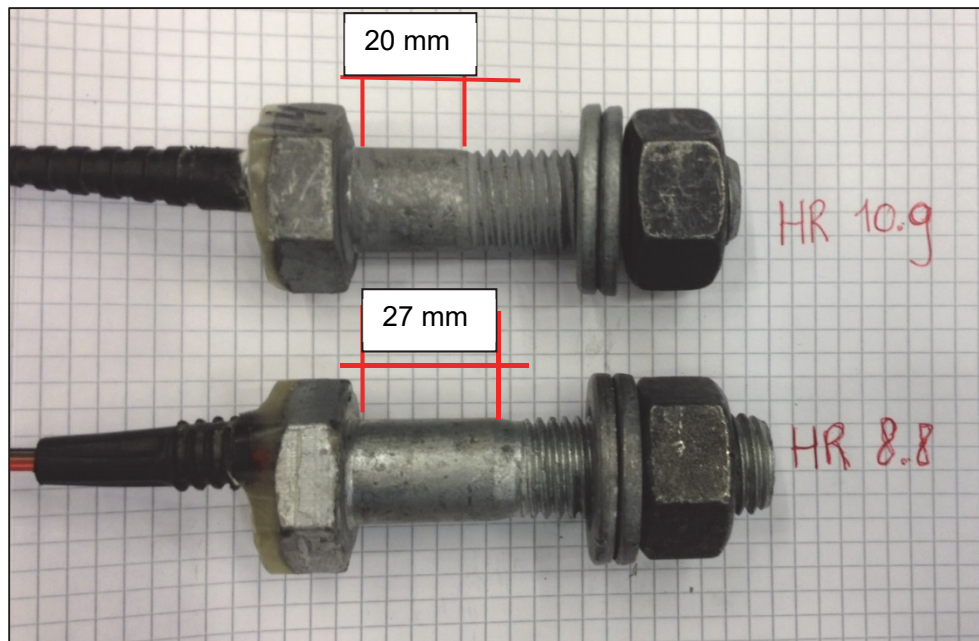


Figure 3-3 - Shank lengths for HR8.8 and HR10.9 bolts (courtesy of P.A. de Vries)

The applied external load leads to stresses in the plates that are between 39% and 56% of the nominal yield stress. The external load is up to 181% of the characteristic slip load defined in EN 1993-1-8.

3.2 Test Matrix

The test results have been obtained using the combination of parameters shown in Table 6. Most of the tests have been carried out with short bolts of 48 mm, whereas only a limited number of tests with longer bolt lengths are available.

Table 6 - Text Matrix

Specimen Code	Surface Treatment of centre and cover plates	Bolt Property Class	Re-Tightening?	Clamping length (mm)	External Force (kN)		
					F_1	F_2	F_3
ASiZN_37	Alkali Zinc Silicate	HR8.8	Yes	48	344	363	397
ASiZN_38	Alkali Zinc Silicate	HR8.8	Yes	48	365	385	398
ASiZN_39	Alkali Zinc Silicate	HR10.9	Yes	48	353	380	400
ASiZN_40	Alkali Zinc Silicate	HR10.9	Unknown	48	376	405	-
ASiZN_43	Alkali Zinc Silicate	HR10.9	No	48	385	-	-
ASiZN_44	Alkali Zinc Silicate	HR10.9*	Yes	48	375	-	-
SM_19	Spray Metallized	HV10.9	No	48	275	336	351
SM_20	Spray Metallized	HV10.9	No	148	275	336	352
SM_30	Spray Metallized	HR8.8	Yes	48	329**	-	-
SM_31	Spray Metallized	HR8.8	Yes	48	329	-	-
SM_37	Spray Metallized	HR10.9	Yes	48	376**	-	-
SM_40	Spray Metallized	HR10.9	Yes	48	340**	-	-
SM_41	Spray Metallized	HR10.9	Yes	48	340**	-	-
SM_42	Spray Metallized	HR8.8	Yes	48	329**	-	-
SM_43	Spray Metallized	HR8.8	Yes	48	312**	-	-
SM_44	Spray Metallized	HR8.8	Yes	48	290**	-	-
SM_45	Spray Metallized	HR8.8	Yes	48	280**	-	-
SM_46	Spray Metallized	HR8.8	Yes	48	280**	-	-
SB_05	Grid Blasted	HV10.9	No	148	524***		
SB_06	Grid Blasted	HV10.9	No	148	518***		
SB_24	Grid Blasted	HR10.9	No	48	488***		
SB_25	Grid Blasted	HR10.9	No	48	450***		

*: The bolts have been pre-tensioned to the level of property class 8.8 according to EN 1090-2

** : The external force gradually decreases with time (up to 12% loss)

***: Short-term test, the mentioned load is the slip load.

The external forces F_2 and F_3 are applied after respectively 7 and 30 days after application of F_1 (if applicable). In the experimental programme, the instrumented bolts have been re-used. Earlier investigation of de Vries (2016) has indicated that there is no significant difference in pretension loss whether the bolts have been used the first time or have been used numerous times already.

3.3 Test Procedure

The test have been carried out according to the schematic shown in Figure 3-4.

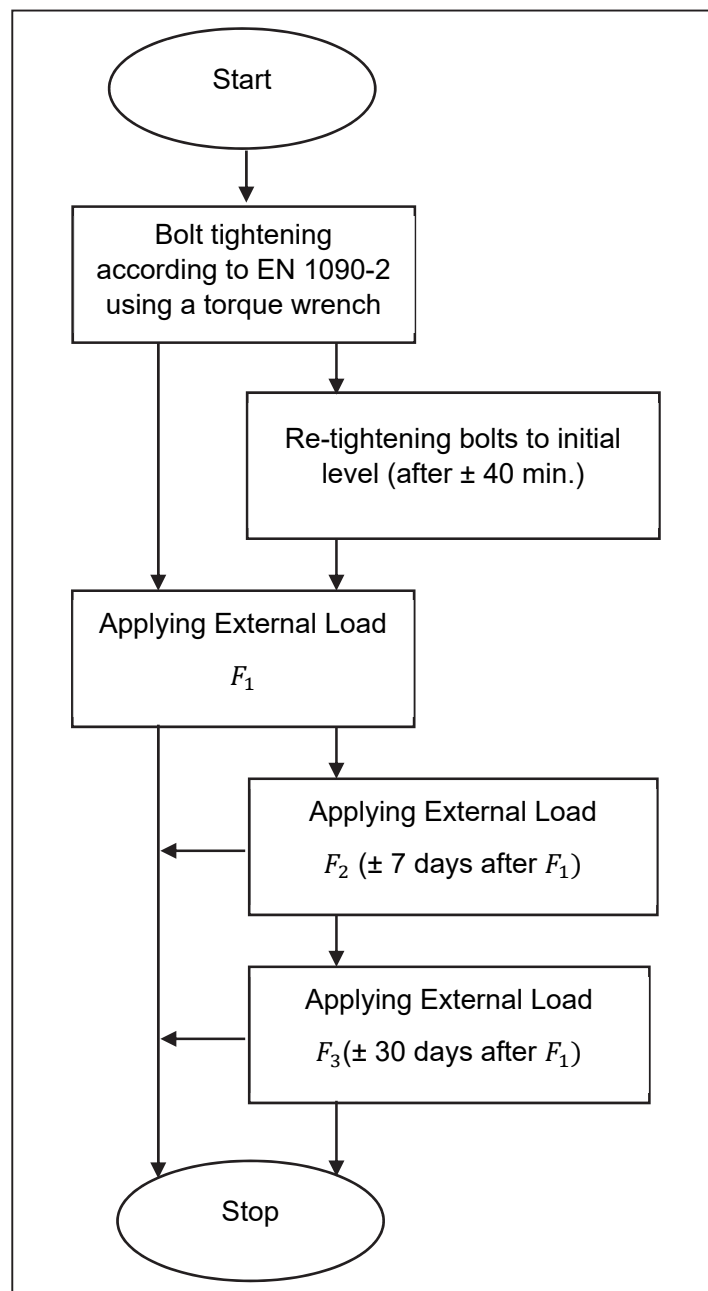


Figure 3-4 - Test Procedure of the SIROCO test programme at TU Delft containing relevant steps for determination of preload loss

3.4 Relaxation directly after tightening

Directly after tightening of the bolts, an immediate drop in preload is observed as can be seen from Figure 3-5. The results from Figure 3-5 clearly show that - generally speaking - spray metallized plates cause a larger reduction in bolt preload than alkali zinc silicate painted specimen. The lowest losses are obtained when using only grid blasted specimen. A difference between property class 8.8 and 10.9 bolts is clearly visible for spray metallized specimen, whereas the effect is unnoticeable for alkali zinc silicate painted specimen. The bolts with a clamping length of 148 mm used in combination with spray metallized specimen have a significantly smaller loss than other spray metallized specimen, most likely due to the lower bolt stiffness compared to the bolts with a clamping length of 48 mm. This effect is less pronounced for sand blasted specimen. The observed preload losses after 30 minutes lay between 1% and 20% of the initial preload force.

The relative preload loss in Figure 3-5 has been computed using (3.1).

$$\text{Rel. P. L.} = \left| \frac{P(t) - P(t = t_{F_{p,c}})}{P(t = t_{F_{p,c}})} \right| \quad (3.1)$$

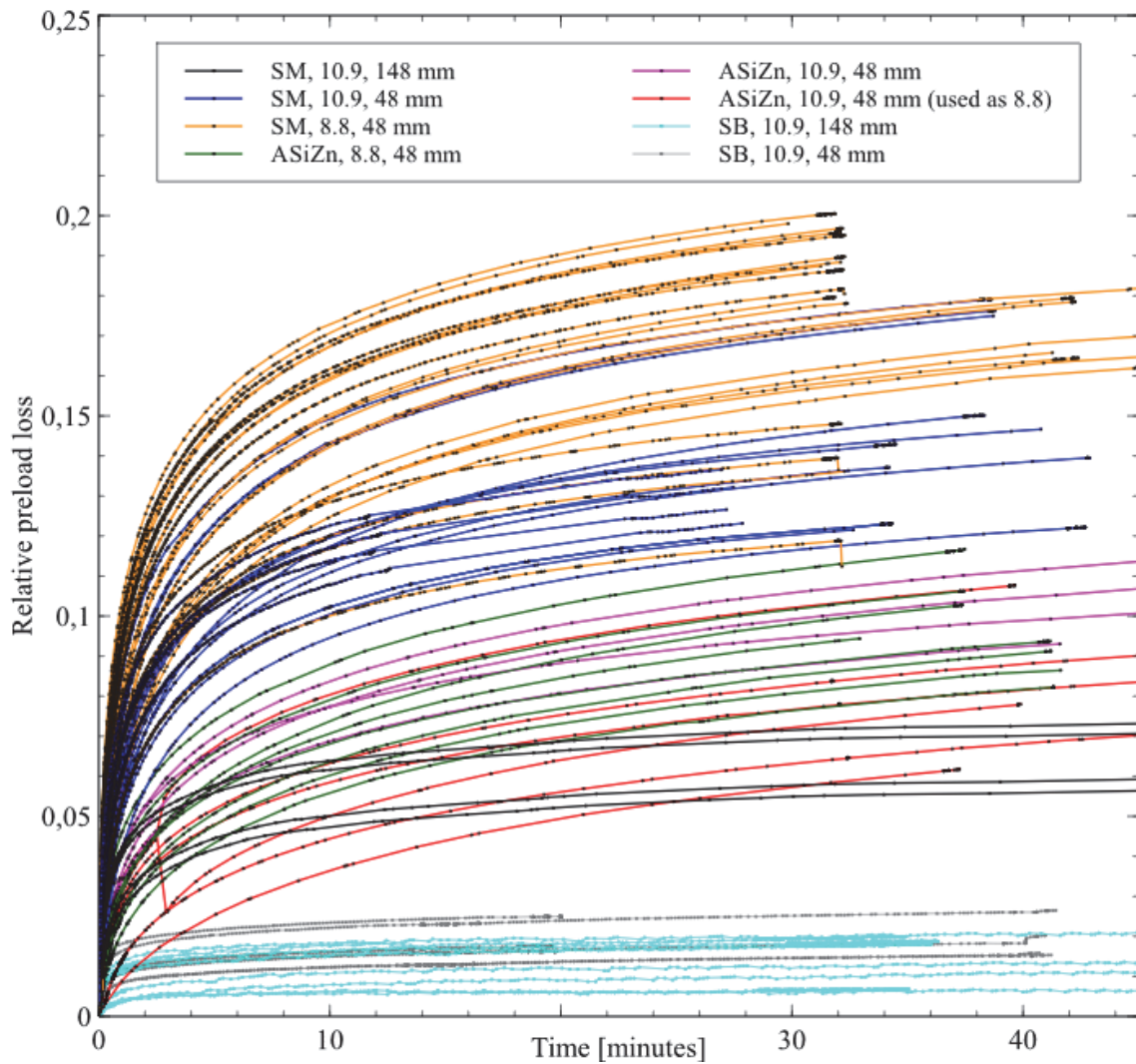


Figure 3-5 - Relative preload loss directly after tightening the bolts for the first time

When plotting the relative preload loss after 30 minutes against the total coating thickness present on the specimen, Figure 3-6 is obtained. This figure clearly suggests that the preload loss is dependent on the total coating thickness.

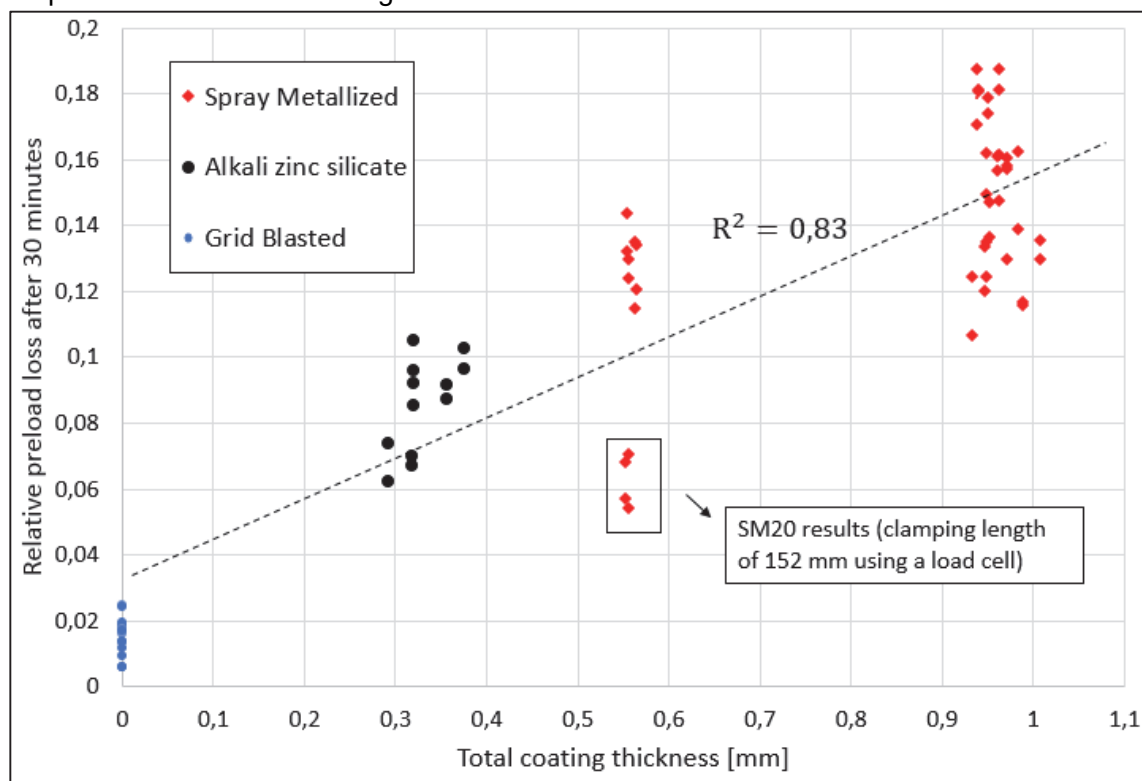


Figure 3-6 - Relative preload loss after 30 minutes versus the total coating thickness of the specimen

The effect of coating thickness on the bolt preload loss has also been confirmed in the research of Satoh et al. (1997). Thick coating films allow for more bolt relaxation, both rotational and non-rotational, than thinner layers (Satoh, Nagatomo, Machida, Endoh, & Enari, 1997).

The results from Figure 3-7 suggest that the relative preload loss after 30 minutes is not dependent on the total surface roughness of the specimen, given the large spread and low correlation coefficient of $R^2 = 0,25$. Rather the relative preload loss is more or less constant per surface treatment group for equal clamping lengths. Since it is generally acknowledged that the surface roughness has a direct effect on bolt relaxation, the hypothesis is adopted that the influence of surface roughness is masked by the coating thickness. It should be noted that all subgroups of specimen have more or less the same coating thickness and surface roughness, and thus it is suggested to carry out more research with a greater diversity in coating thickness and surface roughness per surface treatment.

The lower relative preload loss in longer bolts can be attributed to the lower bolt stiffness and the smaller term $1 - C_b$ or $k_m/(k_b + k_m)$ in (2.12). Also, an influence may be expected from the load cell that has been used to increase the clamping length. The load cell introduces the preload more evenly into the washer and the underlying member. Since the coating is relatively soft and thus easily deformable, the effect is more pronounced for coated than uncoated specimen. The abovementioned effect has been sketched in Figure 3-8. It is however not possible to confirm or quantify the effect with the available experimental data.

In section 4.1 the results directly after tightening are discussed in more detail and a calculation model is suggested.

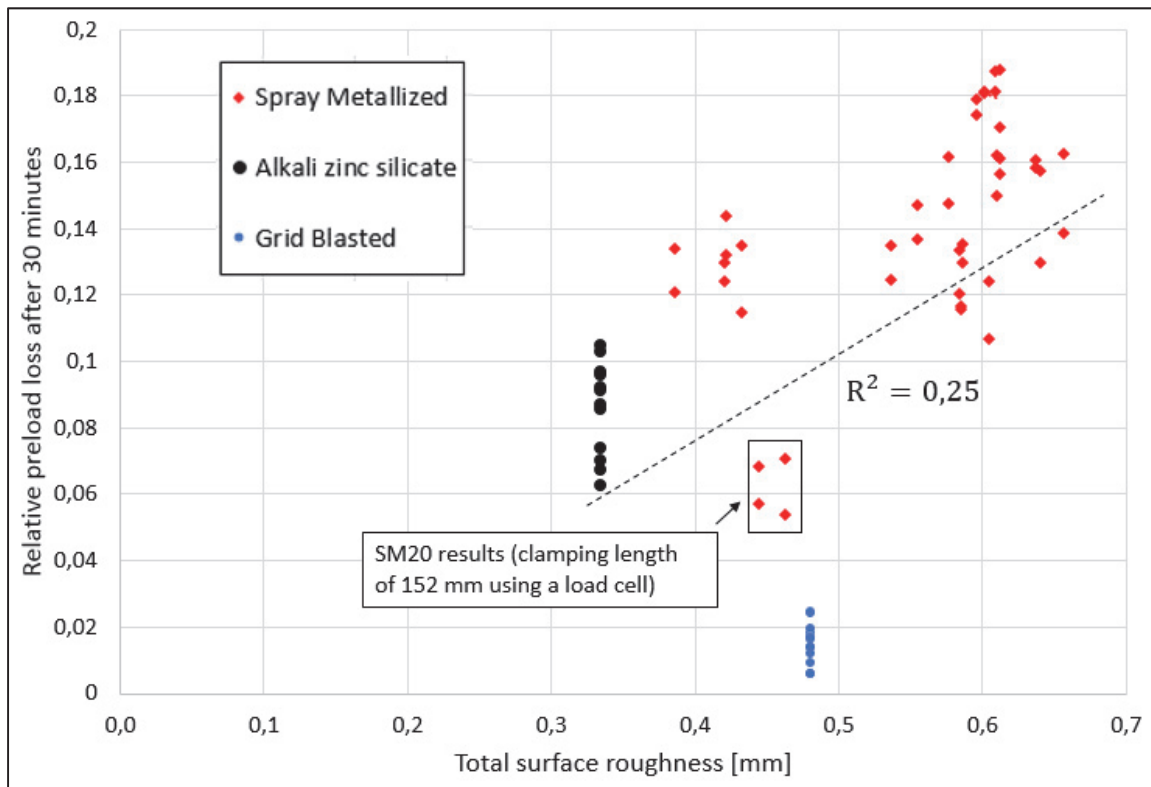


Figure 3-7 - Relative preload loss after 30 minutes versus the total surface roughness of the specimen

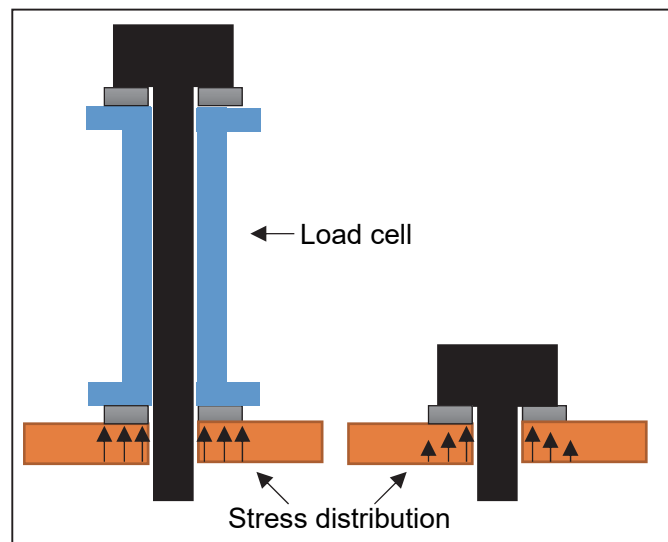


Figure 3-8 – Possible effect of load cell on the introduction of the preload into the underlying plate (not to scale)

3.5 Relaxation directly after re-tightening

Some of the bolts have been re-tightened ± 40 minutes after the initial tightening, whereas other bolts have only been tightened once. The relative preload loss after re-tightening is shown in Figure 3-9. From the test results, it can be observed that the preload losses after re-tightening lay between 2% and 7% of the maximum preload force obtained during re-tightening. The relative preload loss has been calculated using (3.2).

$$\text{Rel. P. L.} = \left| \frac{P(t) - P(t = t_{\text{retight}})}{P(t = t_{\text{retight}})} \right| \quad (3.2)$$

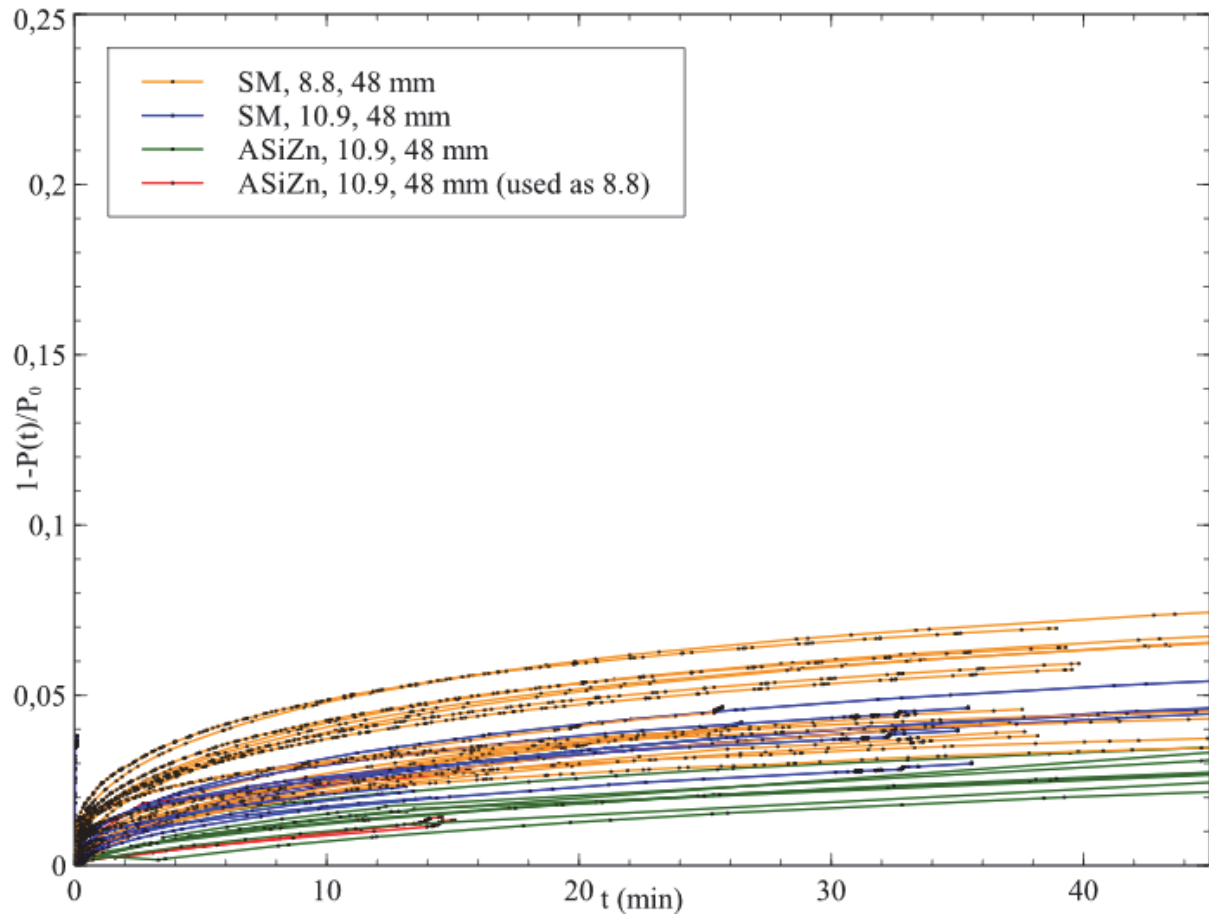


Figure 3-9 - Relative preload loss directly after re-tightening of the bolts

The effect of re-tightening, and its relation with preload loss after the first tightening instance, has been investigated per bolt. The relative preload losses at certain time intervals (10, 20 and 30 minutes) after re- and preloading are compared in Figure 3-10.

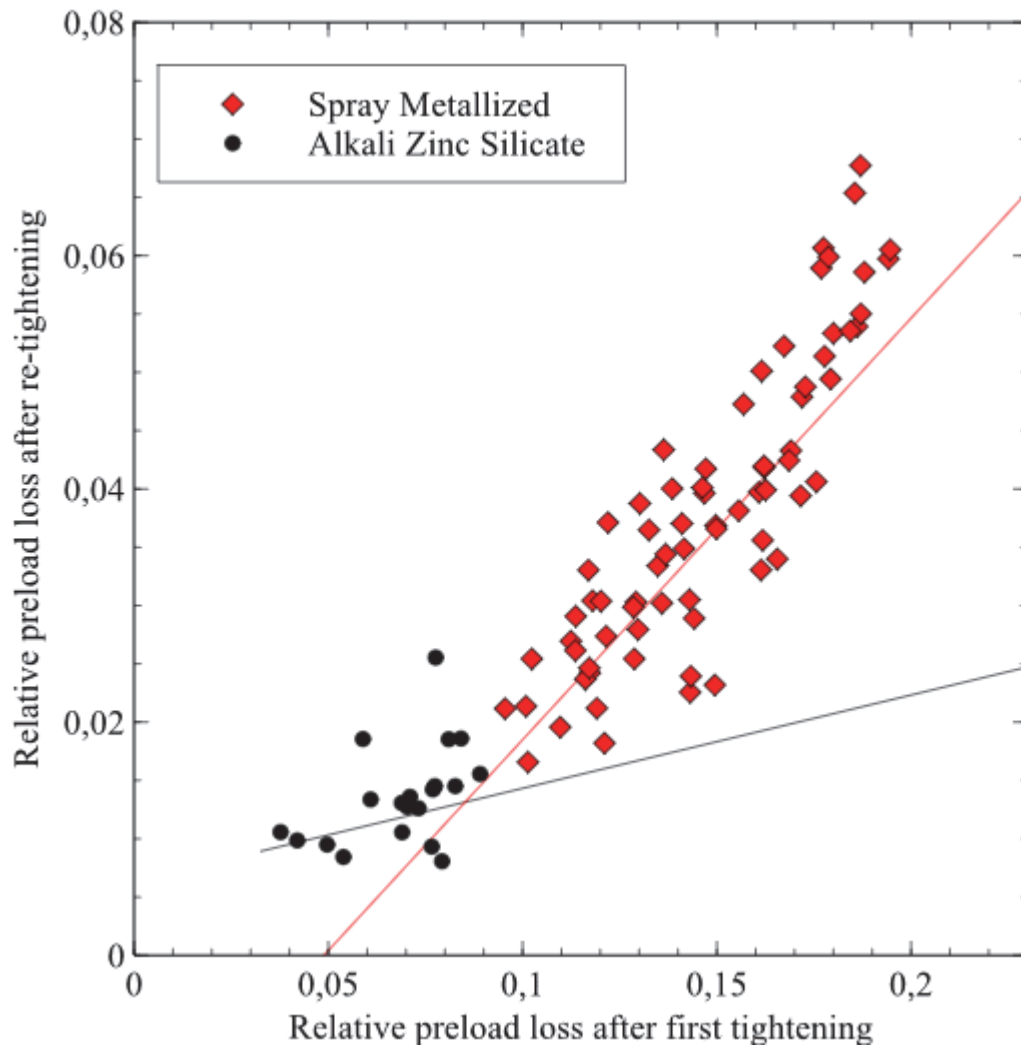


Figure 3-10 - Relative preload loss after re-tightening compared to relative preload loss after first tightening instance (at equal time intervals from (re)tightening)

From Figure 3-10, it can be seen that the relative preload loss after re-tightening is linearly dependent on the preload loss after the first tightening instance in case of spray metallized specimen. The higher the relative preload loss after the first tightening instance, the higher is the relative preload loss after re-tightening, considering equal time intervals after finishing the (re)-tightening procedure.

For alkali zinc silicate specimen, more scatter than dependence is found due to the limited amount of data points – but the general trend is that the preload loss after re-tightening is lower than in case of spray metallized specimen. Also, from Figure 3-10, it can be derived that the relative preload loss after the first tightening instance is always lower for alkali zinc silicate specimen lower than for spray metallized specimen. Apparently, alkali zinc silicate specimen are less susceptible to short term losses than spray metallized specimen. This effect can be attributed to the sensitivity to embedment in the coated plates (highest for spray metallized plates).

Based on the above, it can be concluded that re-tightening the bolts, after allowing for relaxation during a 40 minute time window, reduces the short term losses significantly.

3.6 Relaxation during the application of an external load

During the application on an external shear load, a significant drop in preload level is observed. The preload in the bolts drops due to contraction of the clamped members, which results from the external (tensile) force in these members. The preload loss versus the external load is plotted in Figure 3-11 for $0.25F_1$, $0.5F_1$, $0.75F_1$ and F_1 . The preload loss is calculated using (3.3).

$$P.L. = |P(t) - P(t = t_{\text{startloading}})| \quad (3.3)$$

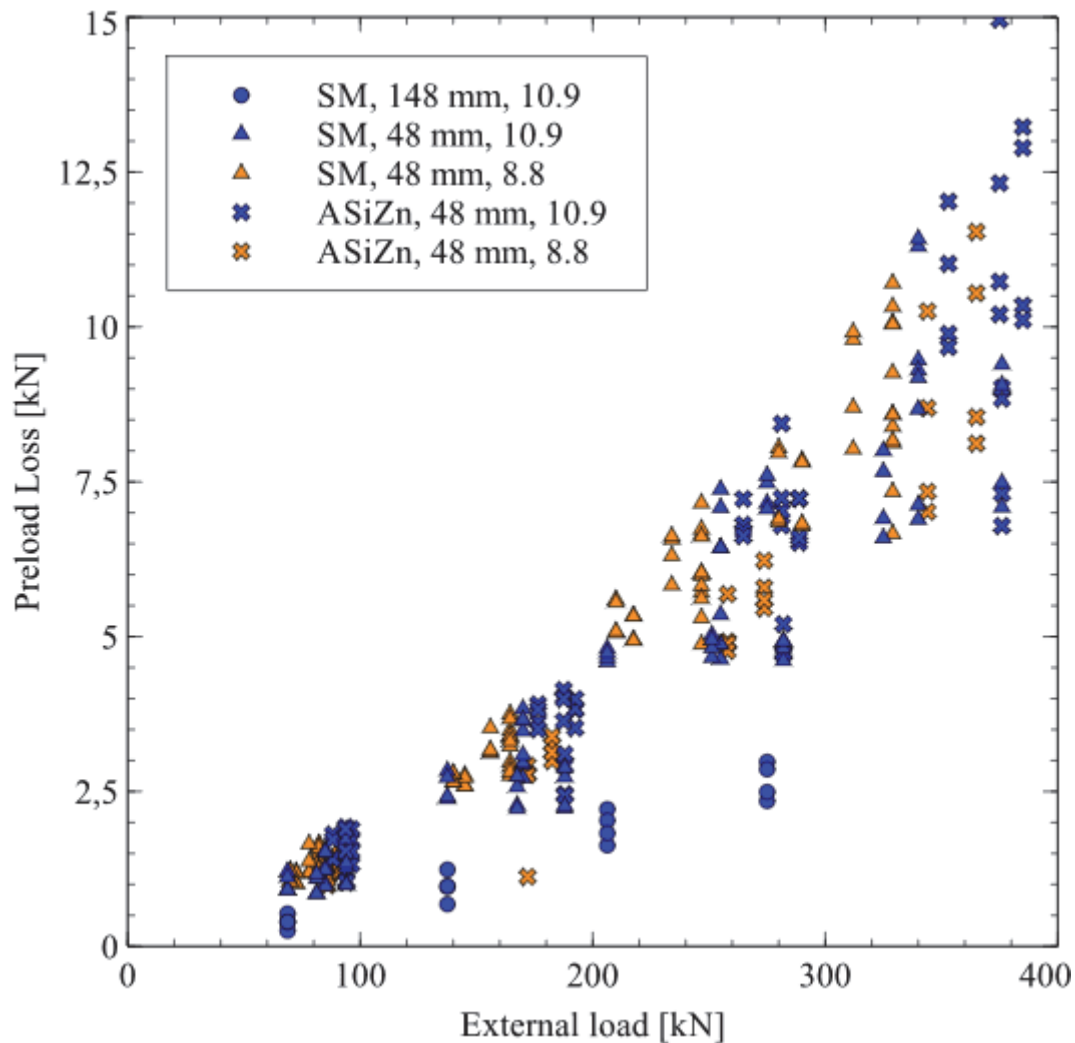


Figure 3-11 - Preload loss due to (static) external load

From Figure 3-11 it can be derived that the preload loss in the bolt is linear with the externally applied (static) load. For higher clamping lengths $\sum t$, the preload loss reduces, in accordance with what was argued in Section 2.1.4, equation (2.11). The test results do not show a clear distinction for the behaviour of property class 8.8 and 10.9 bolts. Similarly, there is no distinct difference between spray metallized and alkali zinc silicate specimen. The latter follows the intuition that lateral plate contraction is indifferent with the coating of the plate.

3.7 Long-term relaxation under static external loading

The long term relative preload loss under the external force F_1 has been investigated for the entire load duration. The effects of the load introduction of F_1 has not been taken into account. The results are plotted using a logarithmic time scale in Figure 3-12. The expression shown in (3.4) is used to calculate the relative preload in the bolt.

$$\text{Relative Preload} = 1 - \frac{|P(t) - P(t = t_{\text{endintro}F_1})|}{P(t = t_{\text{endintro}F_1})} \quad (3.4)$$

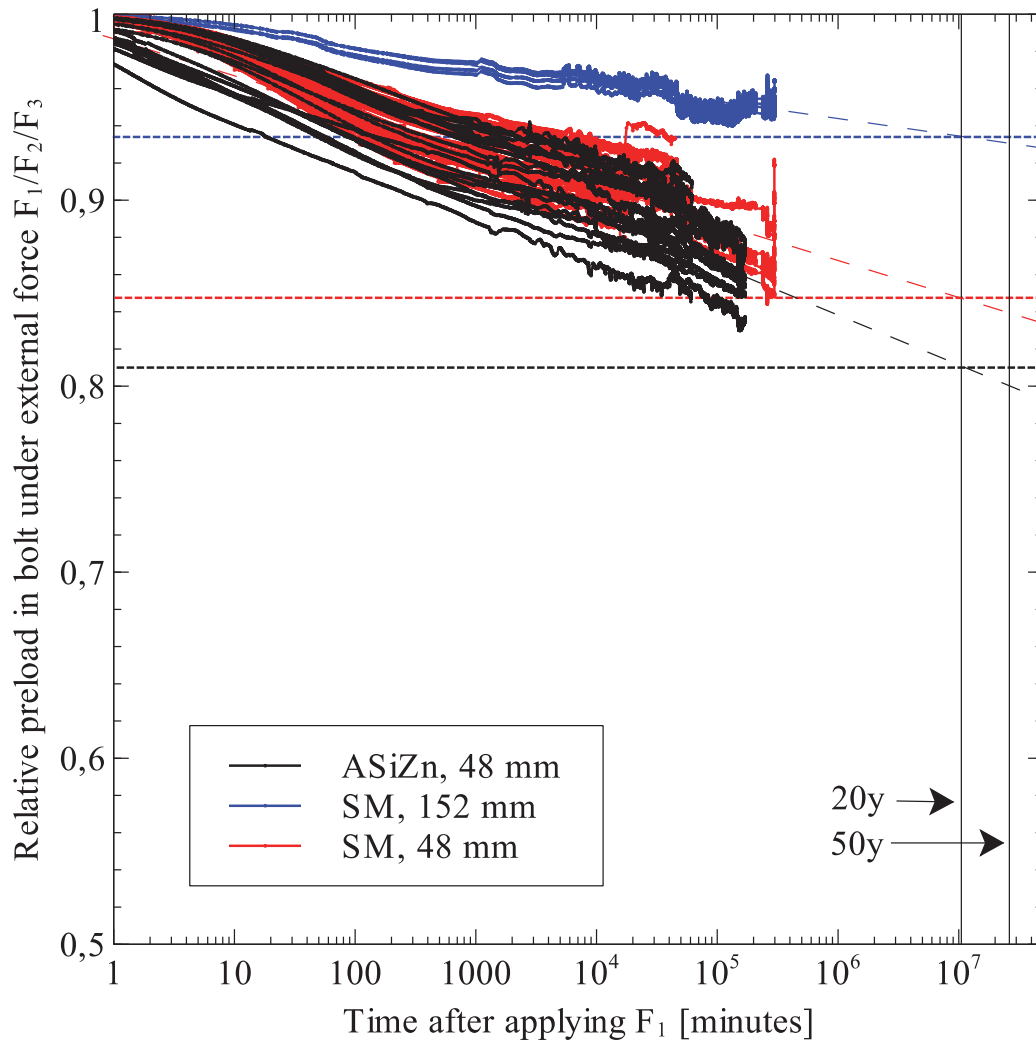


Figure 3-12 – Extrapolated average relative preload in bolt versus log(time)

As can be seen from Figure 3-12, the relative average long-term preload loss after 20 years is 19% for alkali zinc silicate coated specimen and 15% for spray metallized specimen with equal clamping lengths of 48 mm. The effect of the clamping length can be seen through the result of the spray metallized specimen with a clamping length of 152 mm: here the extrapolated relative preload loss after 20 years is (only) 6%.

The research of Heistermann (2011) reports relative pretension losses of 16,8% for ethyl zinc silicate coated plates with 4 coated surfaces in a single lap joint (LT), as shown in Figure 3-13 and Table 7. The number after the symbol R in Table 7 denotes the amount of coated surfaces. These test results have been obtained without external loading, in contrast to the long term lap joint test (LT). All coated surfaces have a film thickness of 80 micron, which is comparable to the alkali

zinc silicate film thickness in the TU Delft research. The results of Heistermann (2011) cannot be directly compared to the results of Figure 3-12, since the results of Heistermann take into account all bolt relaxation effects since tightening and no re-tightening has been carried out. Also, in Heistermann's research, the external load is only 80% of the characteristic slip resistance according to EN 1993-1-8. In the current research, up to 182% of the characteristic slip load is applied to the joint. However, Heistermann concludes that the external load does not significantly change the preload losses. In order to compare results between the current research and Heistermann, only the test result for specimen ASiZn-43 is available (including all other effects, such as external load application), which is shown in Figure 3-14 together with the data of Heistermann. In Figure 3-14 Heistermann's result for an uncoated specimen + three times the result of the relative influence of two sided coating has been plotted. This brings the number of total surfaces to 8, of which 6 are coated (similar as ASiZn-43). However, Heistermann's research is regarding a property class 10.9 M30 bolt with a clamp length of 63 mm, thus $l/d = 2,1$. The TU Delft research has a ratio $l/d = 2,4$ (also property class 10.9). Therefore, Heistermann's prediction is scaled using the theory of Section 5 (e.g. Figure 5-3) with a factor 1,37.

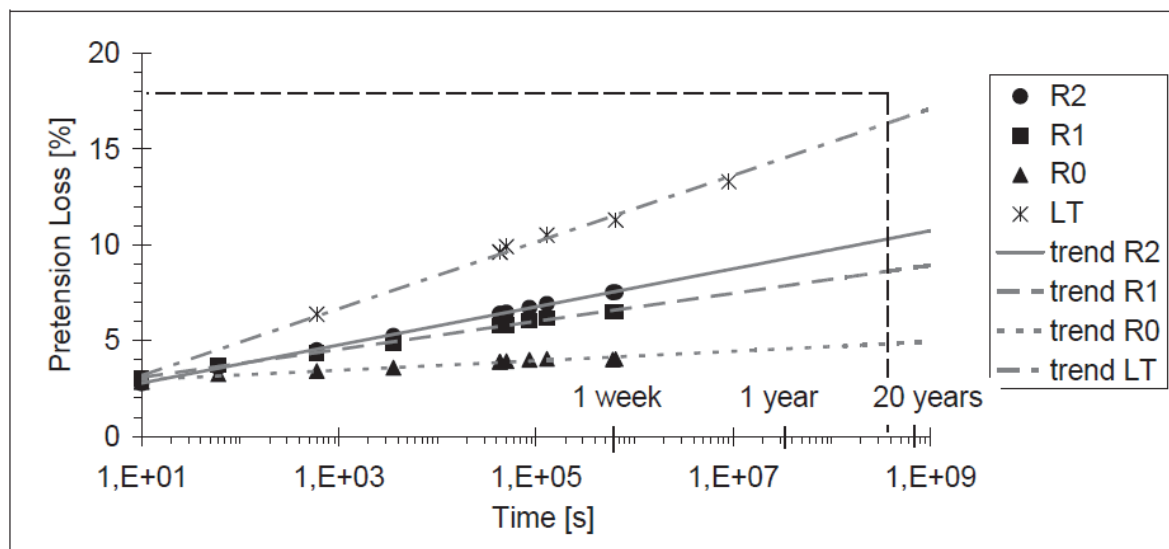


Figure 3-13 Extrapolated average losses of pretension (Heistermann, 2011)

Table 7 - Predicted average loss of pretension [%] depending on the no. of coated surfaces (Heistermann, 2011)

	R0	R1	R2	LT
20 years	4,8	8,8	10,5	16,8

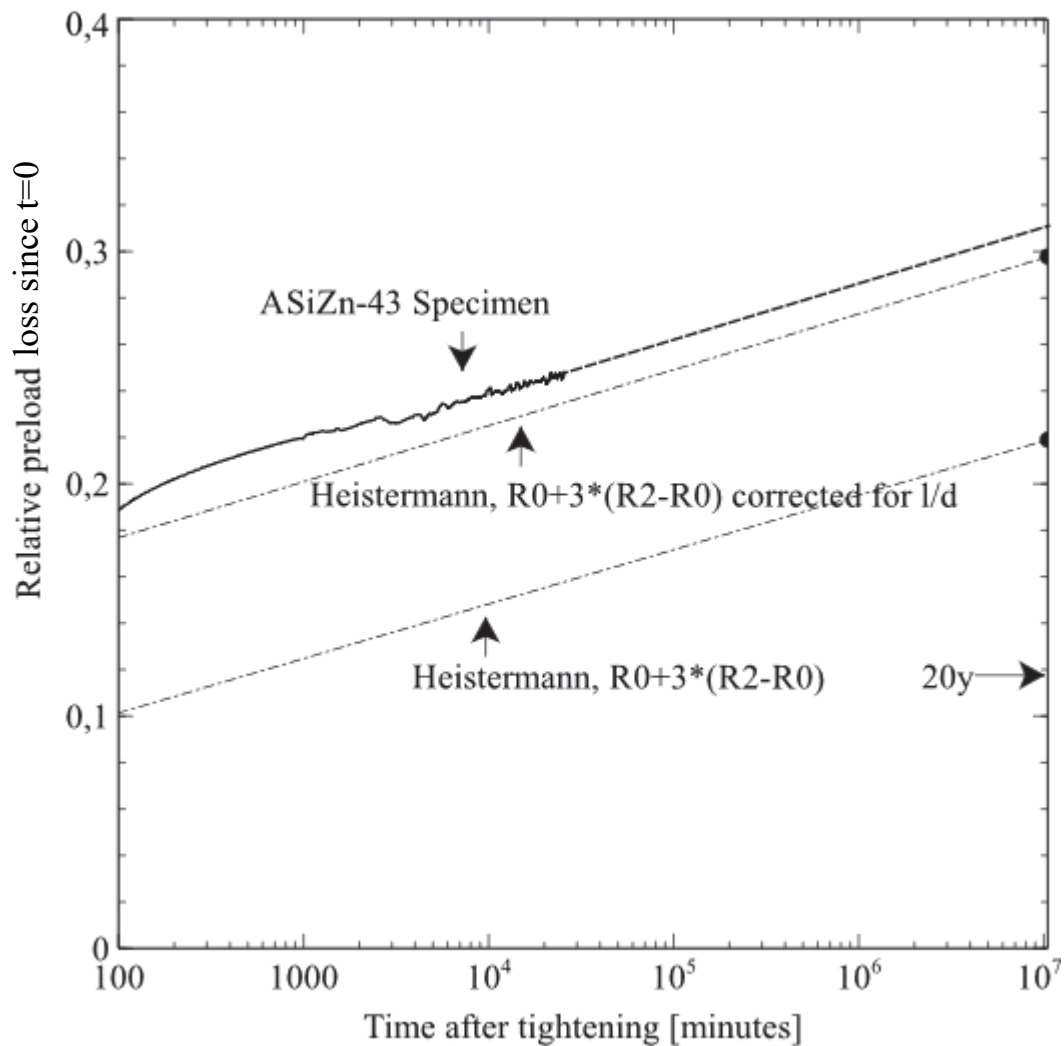


Figure 3-14 – Extrapolated relative preload loss vs time for ASiZn-43 and results from Heistermann (2011)

As can be seen from Figure 3-14, the corrected Heistermann result is very close to the TU Delft test result. The corrected Heistermann model without external loading expects 30% of preload loss after 20 years. The TU Delft model with external loading expect 31% of preload loss in the same period of time. This suggest that the external loading does not significantly influence the long-time preload loss, as was already suggested by Heistermann (2011). This hypothesis is supported by the results shown in Figure 3-16, which shows that there is no significant correlation between the relative preload loss 10000 minutes (approximately 1 week) after re-tightening of the bolts and the magnitude of the external load. Thus, external loading is only influencing bolt relaxation on the short term as has been discussed in Section 3.6.

For the sake of completeness, a similar figure as Figure 3-14 has been plotted for all specimen in Figure 3-15. As can be seen from Figure 3-15, the preload loss after 20 years including all bolt relaxation effects lays between 20% and 31%. No distinction can be made between bolt property class and surface treatment for the available test results. However, it can be noticed that the result for the re-tightened bolts are better (lower loss) than for the ASiZn-43 bolts that have only been tightened once.

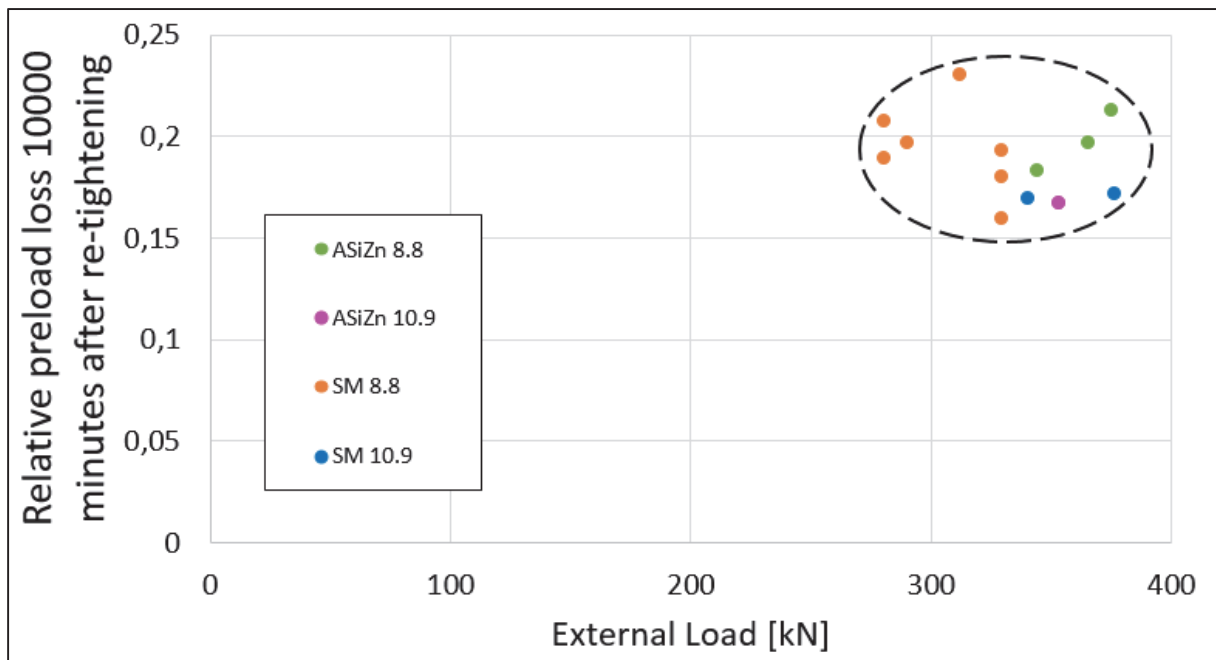


Figure 3-16 - Relative preload loss after 10000 minutes vs external load

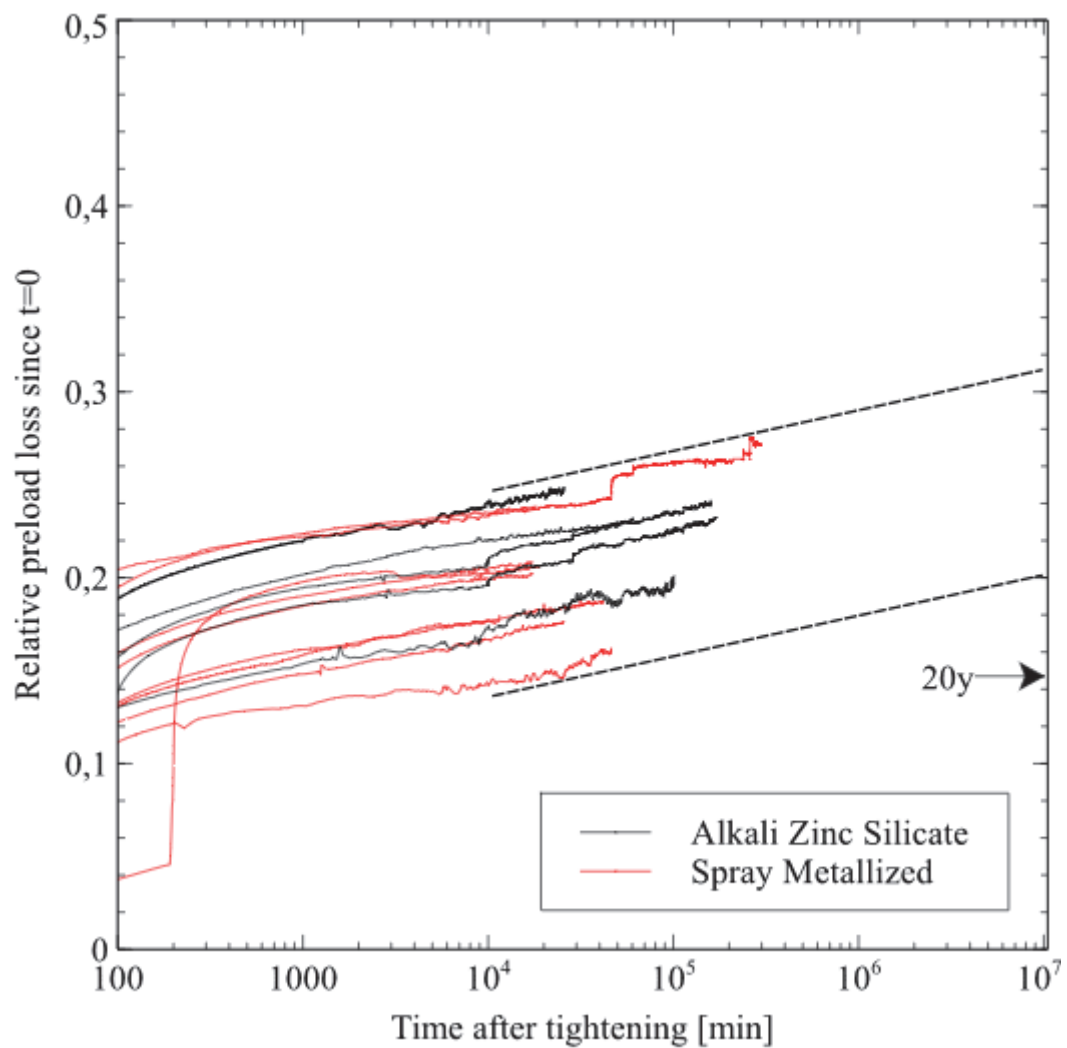


Figure 3-15 - Extrapolated relative preload loss since (re)-tightening vs time

When only looking at the first 10000 minutes (7 days) after the external loading on a conventional horizontal time axis, it becomes evident that the relative preload loss curve is not smooth, but rather rough. This is illustrated in Figure 3-17. However, not all curves have such distortions. In case such rough distortions are present, the interval between repetition is about 1300-1500 minutes (22-25 hours). Assuming an average interval of 24 hours, the distortions in the curve may well be caused by temperature differences over the course of the day.

During this experiment, the relative preload loss after 7 days lay between 6,5% and 11,5% for bolts with a clamping length of 48 mm. The relative preload loss in Figure 3-17 has been computed using (3.5).

$$\text{Rel. P. L.} = \left| \frac{P(t) - P(t = t_{\text{endintro}F_1})}{P(t = t_{\text{endintro}F_1})} \right| \quad (3.5)$$

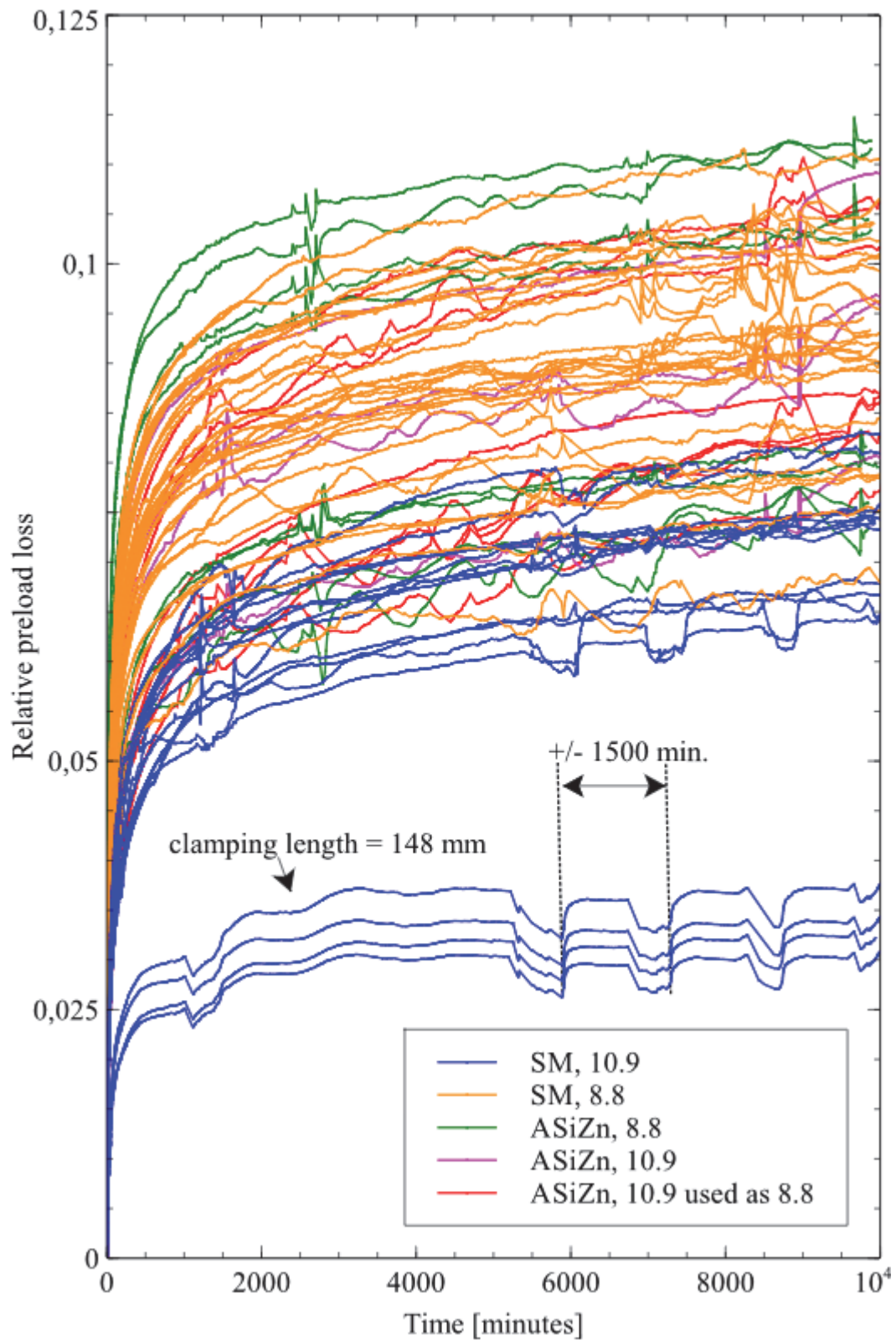


Figure 3-17 - Long-term preload loss, while sustaining external force F_1

4 Discussion & Modelling

4.1 Relaxation directly after tightening

4.1.1 Analytical Model based on experimental results

As can be seen from Figure 3-5 (Section 3.4), most of the short-term preload loss occurs within 30 minutes after tightening of the bolt. The relationship between the relative preload loss and the total coating thickness and surface roughness has already been shown in Figure 3-6 and Figure 3-7. In order to allow for modelling of the relaxation directly after tightening, it is suggested to convert the preload loss to a joint deformation and compare it with the total coating thickness. This can be done using the theory of Section 2.1.4, via (4.1). The results are shown in Figure 4-1.

$$f_z = \frac{\Delta F_{p,c}}{k_b \cdot \left[\frac{k_m}{k_b + k_m} \right]} \quad (4.1)$$

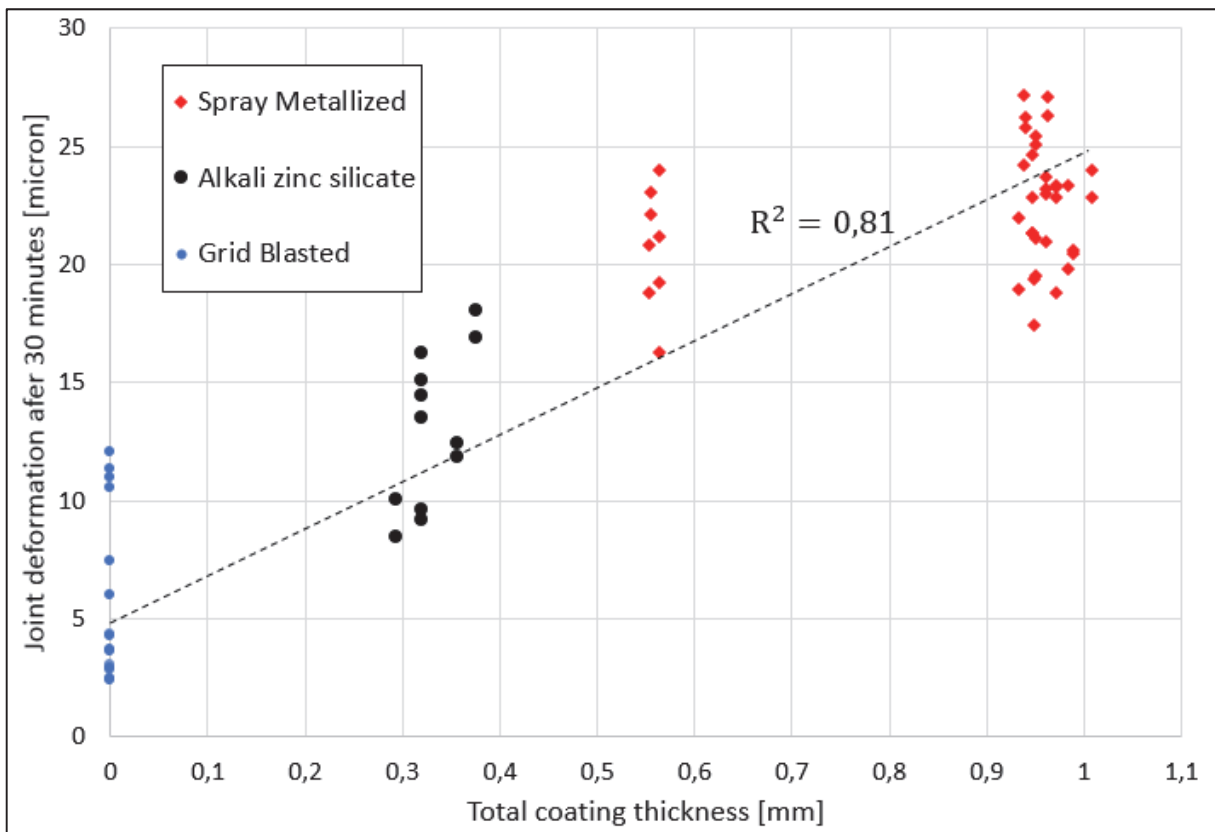


Figure 4-1 - Joint deformation 30 minutes after preloading versus total coating thickness for clamping length of 48 mm

As already mentioned in Section 3.4, not enough diversity is present within the data to draw a conclusion based on coating thickness. However, the hypothesis is backed up by the research of Yang & DeWolf (2000). Yang & DeWolf have investigated the bolt relaxation after 21 days. In order to compare results, the TU Delft data corresponding to a 21 day period has been plotted against the results of Yang & DeWolf in Figure 4-2. As can be seen from the plot, the joint deformation increases linearly with the total coating thickness. The results that have been obtained using a load cell have been left out.

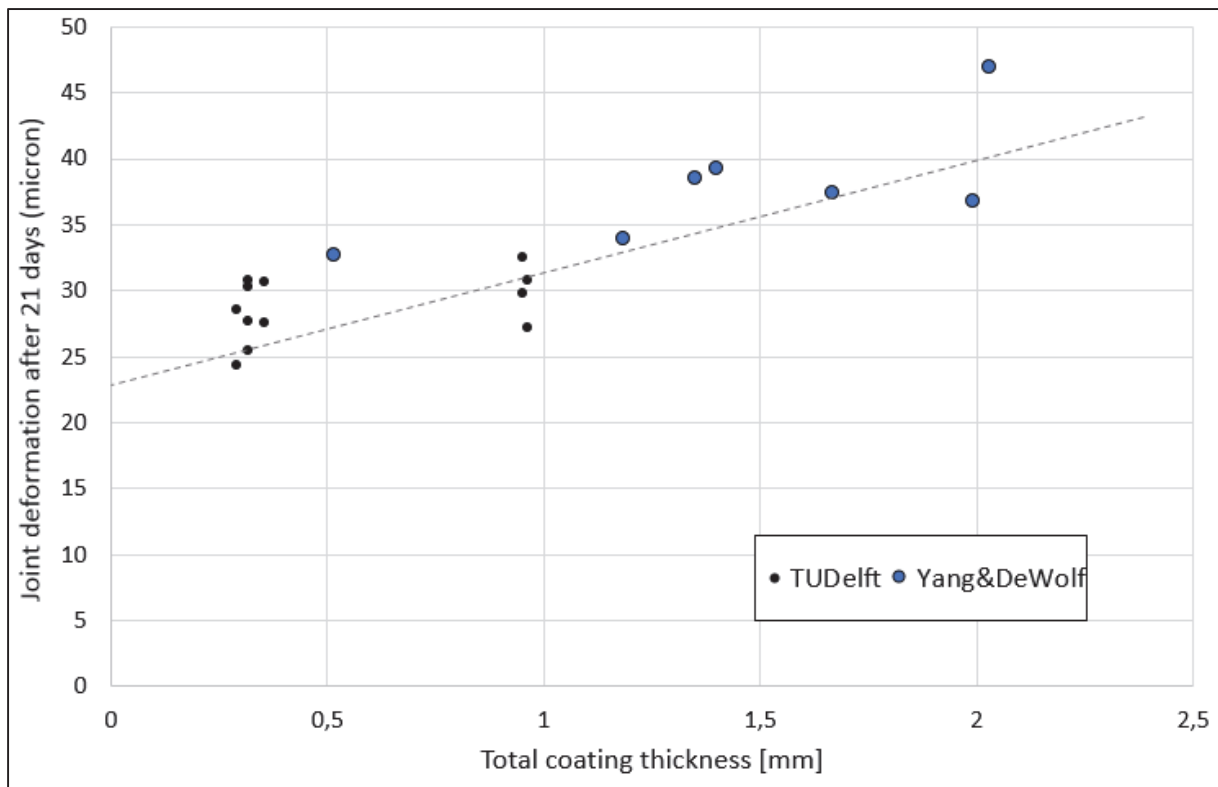


Figure 4-2 - Joint deformation 21 days after preloading versus total coating thickness for results of TU Delft and Yang & DeWolf (2000)

When plotting the joint deformation versus time as in Figure 4-3, it becomes evident that all subgroups have a distinct position with respect to each other in terms of bolt/joint contraction. From highest joint deformation to lowest bolt deformation:

1. Spray Metallized, property class 8.8 bolts
2. Spray Metallized, property class 10.9 bolts
3. Alkali Zinc Silicate, property class 10.9 bolts
4. Alkali Zinc Silicate, property class 8.8 bolts
5. Grid Blasted, property class 10.9 bolts

In case of grid blasting, the joint deformation is already constant after a very short period in comparison to other surface treatments.

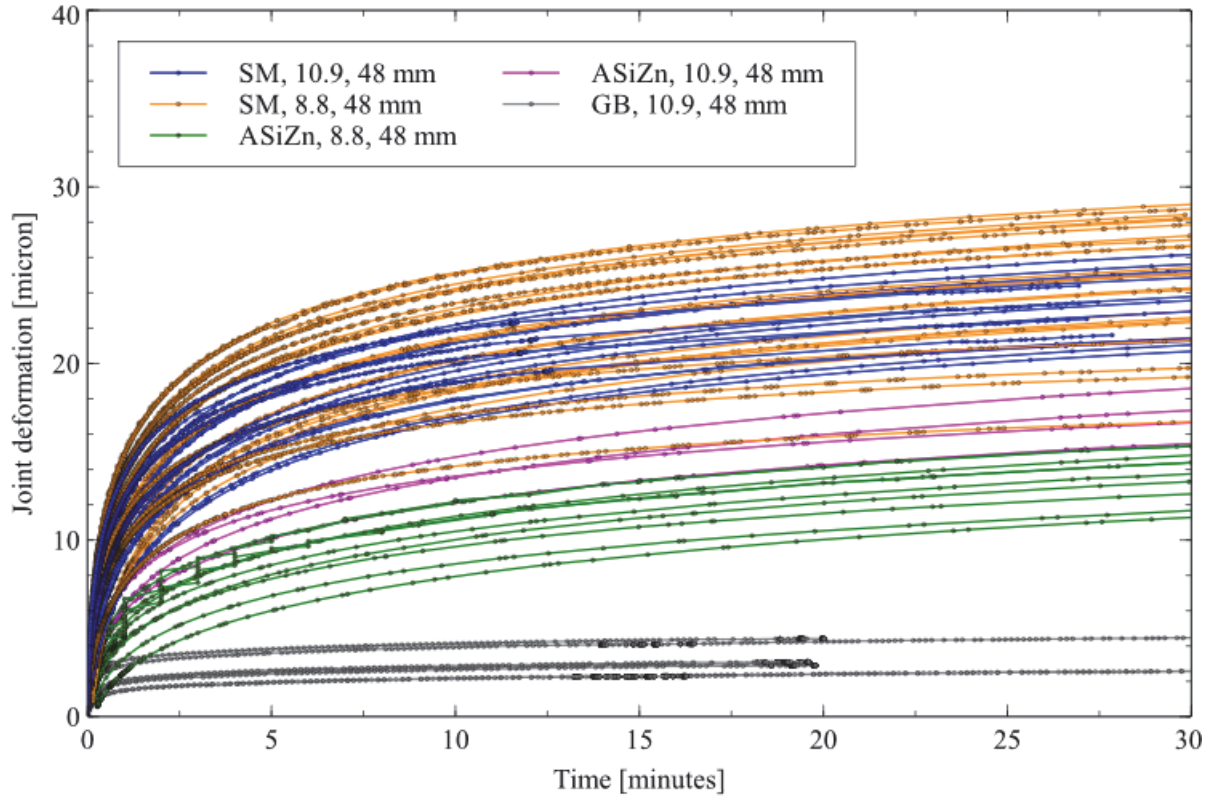


Figure 4-3 - Joint deformation versus time

Based on Figure 4-1 and under the assumption that after 30 minutes the relative values of joint deformation will not change (which is supported by Figure 4-3), the tentative estimation of the joint deformation 30 minutes after tightening as a function of total coating thickness is given by (4.2), in which f_z is the joint deformation (micron) and $\sum t_c$ is the sum of all coating thicknesses for $\sum t_c > 0$ (micron).

$$f_z = 17 \cdot 10^{-3} \cdot \sum t_c + 7,03 \quad (4.2)$$

The effect of the higher relative preload loss for property class 8.8 bolts with respect to class 10.9 bolts for spray metallized specimen can be explained by the combination of Figure 4-4 and the bolt properties per property class. The ratio of the bolt tensile strength over the yield strength is expressed by (4.3) and (4.4).

$$8.8: \quad \frac{f_{ub}}{f_{yb}} = \frac{800}{640} = 1,25 \quad (4.3)$$

$$10.9: \quad \frac{f_{ub}}{f_y} = \frac{1000}{900} = 1,11 \quad (4.4)$$

The pretension level according to the Eurocode is depicted in (4.5). Substituting f_{ub} in terms of f_y using (4.3) and (4.4) in (4.5) yields (4.6) and (4.7).

$$F_{p,C} = 0,7 \cdot f_{ub} \cdot A_s \quad (4.5)$$

$$8.8: \quad F_{p,C} = 0,7 \cdot 1,25 \cdot f_y \cdot A_s = 0,875 \cdot f_y \cdot A_s \quad (4.6)$$

$$10.9: \quad F_{p,C} = 0,7 \cdot 1,11 \cdot f_y \cdot A_s = 0,778 \cdot f_y \cdot A_s \quad (4.7)$$

In both the case of property class 8.8 and 10.9, the yield stress is not attained and the non-linear branch of the stress-strain diagram is not yet reached (see Figure 2-7). During preloading, both the class 8.8 and 10.9 bolts have been overloaded. The percentage overshoot per specimen is shown in Figure 4-4.

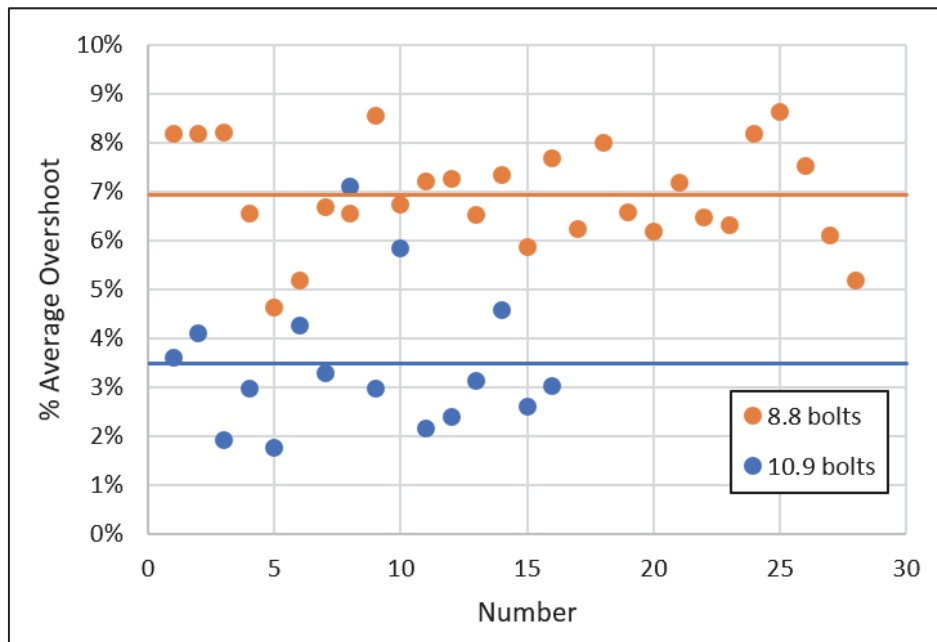


Figure 4-4 - Percentage overshoot per SM specimen

The average overload for 8.8 bolts was 7% and for 10.9 bolts 3,5%. Substituting the average overload in (4.6) and (4.7) gives bolt stresses as indicated in (4.8) and (4.9).

$$8.8: \sigma_b = 1,07 \cdot 0,875 \cdot f_y = 0,94 \cdot f_y \quad (4.8)$$

$$10.9: \sigma_b = 1,035 \cdot 0,778 \cdot f_y = 0,81 \cdot f_y \quad (4.9)$$

On average, the class 8.8 bolts are almost on the non-linear branch of the stress-strain diagram. For the class 8.8 bolts with the highest overshoot or a lower yield strength than is to be expected, the non-linear branch has been reached (bolt stress is larger than the proof stress S_p). The class 10.9 bolts have not yet reached the non-linear branch of the stress-strain diagram. The class 8.8 bolts that are on the non-linear branch of the stress-strain diagram, deform plastically. The plastic deformation is non-recoverable and thus does not play a role in the bolt contraction. So to say, the bolt is slightly too long for the depth of the hole. This leads to a relative preload-loss directly after tightening that is larger than in case of class 10.9 bolts. It should be noted that during this experiment the preload was obtained rather accurately, but that in practice often higher preloads are obtained. It is suggested to carry out more investigation into the effect of the tightening method, the resulting preload and the subsequent preload loss.

For alkali zinc silicate specimen, the relative loss of class 10.9 bolts is higher than for class 8.8 bolts. The plasticity mentioned above does apply to this case, since the overshoot for alkali zinc specimen was only marginal (on average 2%) for all bolts. However, the alkali zinc silicate is a rather dense and stiff primer compared to the soft / air void-containing spray metallized primer. Thus, in contrast to spray metallized primers, the magnitude of deformation of the alkali zinc silicate coating is dependent on the preload. It is expected that spray metallized primers will deform due to their softness and air inclusions, largely independent of the preload level.

4.2 Bolt relaxation due to load application

4.2.1 Derivation of Analytical Model

The application of the tensile axial load in the centre plates causes a reduction of preload in the bolts, as indicated by the test results. In this chapter, an analytical model is derived and validated against the available test results.

In order to predict the preload loss due to loading of the joint by means of introducing a tensile force in the centre plates, it is vital to recapitulate on the essential knowledge regarding the relationship between stresses and corresponding strains. The externally applied load always leads to stresses smaller than the yield stress of the centre and lap plates, this means – in the case of steel – that there is a linear relationship between stress and strain. More abstractly, it means that Hooke's Law (4.10) is valid.

$$\sigma = E\varepsilon \quad (4.10)$$

The Poisson effect, named after Siméon Poisson, causes strains to occur perpendicular to the direction of loading. Since steel is an isotropic material, the combination of Hooke's Law and the Poisson effect leads to the three dimensional stress-strain relationship of (4.11).

$$\begin{aligned} \varepsilon_{xx} &= \frac{1}{E_p} [\sigma_{xx} - \nu(\sigma_{yy} + \sigma_{zz})] \\ \varepsilon_{yy} &= \frac{1}{E_p} [\sigma_{yy} - \nu(\sigma_{xx} + \sigma_{zz})] \\ \varepsilon_{zz} &= \frac{1}{E_p} [\sigma_{zz} - \nu(\sigma_{yy} + \sigma_{xx})] \end{aligned} \quad (4.11)$$

The sign convention is chosen in such a way that the x-axis runs parallel to the specimen, the y-axis runs in the width-direction and the z-axis runs in the thickness direction. This is shown in Figure 4-5.

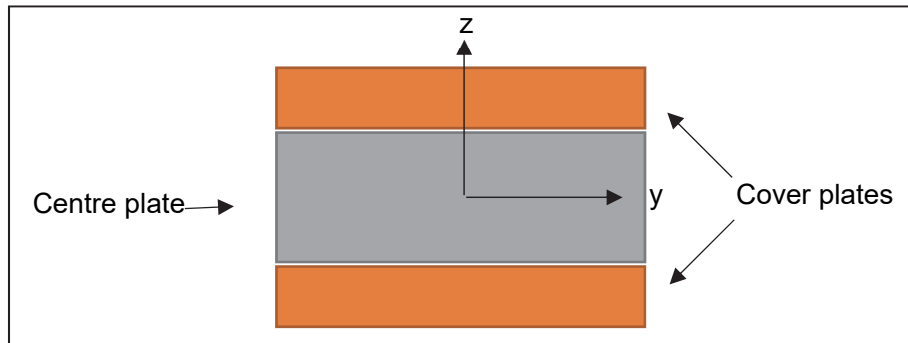


Figure 4-5 - y-z axis convention

In the undisturbed region of the connection, i.e. where no load transfer between the centre plate and the cover plates occurs, the centre plate is free to contract in both y- and z-directions. However, in the 'disturbed' region, i.e. the zone in which load transfer by friction takes place, the contraction in y-direction is constrained. This results from the fact that the centre plate wants to expand with respect to the undisturbed region (since part of its force is taken over by the cover plates) and simultaneously the cover plates want to contract in y-direction due to the load taken over from the centre plate. Since the two cover plates carry the same stress as the centre plate, the expansion/contraction in y-direction is of equal magnitude and thus the constraint is a full restraint. Figure 4-6 shows a top view of the abovementioned phenomenon.

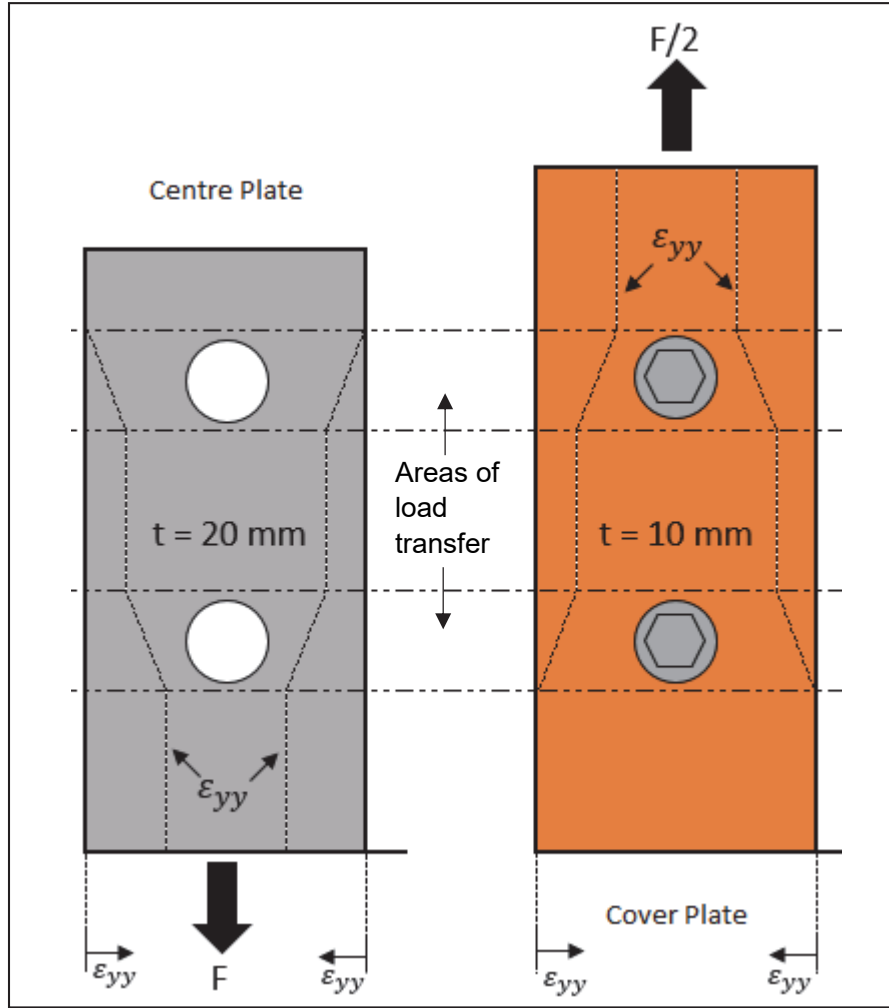


Figure 4-6 - Restrained lateral contraction in y-direction (only 1 cover plate shown) (not to scale)

The restrained lateral contraction (4.12) of the centre and cover plates introduces an additional stress σ_{yy} (4.13), in addition to the already present σ_{xx} originating from the load F .

$$\varepsilon_{yy} = 0 \quad (4.12)$$

$$\sigma_{yy} = \nu(\sigma_{xx} + \sigma_{zz}) \quad (4.13)$$

The preload has already been applied before and thus does not influence the current mechanism, hence (4.14) can be substituted in (4.13) and (4.11), which yields (4.15).

$$\sigma_{zz} = 0 \quad (4.14)$$

$$\varepsilon_{zz} = \frac{1}{E_p}(-\nu^2 - \nu)\sigma_{xx} \quad (4.15)$$

The transversal strain in the thickness-direction (4.15) causes the clamped members to contract (minus sign) and the bolt will follow the thickness reduction and shorten. With respect to σ_{xx} it must be noted that this stress is the average stress of all members in the clamped package (within the grip length) in the respective disturbed zone (4.16).

$$\sigma_{xx} = \frac{F}{bt_{s2}} \quad (4.16)$$

The shortening of the bolt happens due to the contraction of the centre and cover plates. Also, each washer is assumed to contract in thickness-direction due to the slenderness of the washer. Load introduction is assumed to happen under a 45° angle. Since the cross sectional area of the washer is rather small compared to the clamped package, its contribution is still ignored in the calculation of the mean longitudinal stress σ_{xx} (4.16). The stress σ_{xx} is present over a large part of the washer and generates a negative strain (contraction) in the thickness direction. The boundary conditions are the same as that for the clamping package (4.12). The abovementioned principle and the dimensions of the washers used are shown in Figure 4-7.

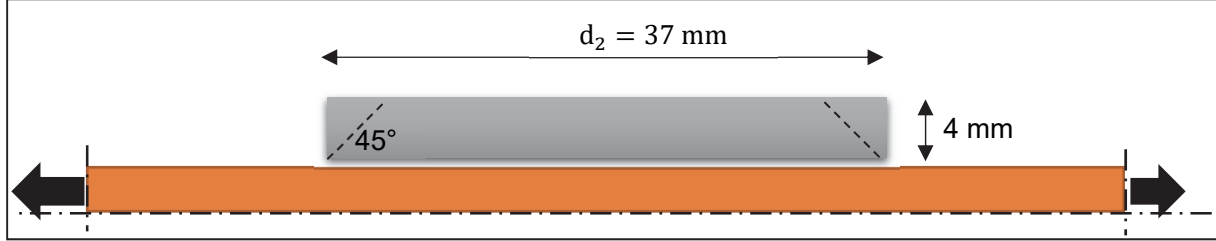


Figure 4-7 – Washer of an M20 bolt on cover plate. Load spreading under 45° angle (only a small part of the cover plate is shown).

Based on the above, for specimen with no collar and only washers, the total height of the clamped package effected by the transversal load application is equal to the sum of the grip length t_{s2} and the height h of the washers (4.17).

$$\sum t = t_{s2} + \sum h \quad (4.17)$$

The total shortening of the bolt (4.18) due to the negative strain (contraction) of the clamped package can be calculated using (4.15) and (4.17)

$$\Delta l_b = f_z = \varepsilon_{zz} \sum t \quad (4.18)$$

Using the theory of Section 2.1.4, the preload loss can be determined using (4.19).

$$\Delta F_{p,C,load} = f_z \cdot k_b \cdot \left[\frac{k_m}{k_b + k_m} \right] \quad (4.19)$$

Combining (4.15), (4.16), (4.18) and (4.19), the loss of preload due to external tensile loading can be written as (4.20).

$$\Delta F_{p,C,load} = \left[\frac{1}{E_p} (-v^2 - v) \frac{F}{b t_{s2}} \cdot \sum t \right] \cdot \left[\frac{k_b k_m}{k_b + k_m} \right] \quad (4.20)$$

The plate stiffness k_m and the bolt stiffness k_b are to be determined according to Section 2.1.4.

4.2.2 Comparison between model and experimental results

The bolt force loss according to the analytical model is plotted against the actual bolt force loss obtained from the long-term experiments in Figure 4-8, for external loads of magnitude $0.25F_1$, $0.5F_1$, $0.75F_1$ and F_1 (the groups are still distinguishable in the graph in ascending order).

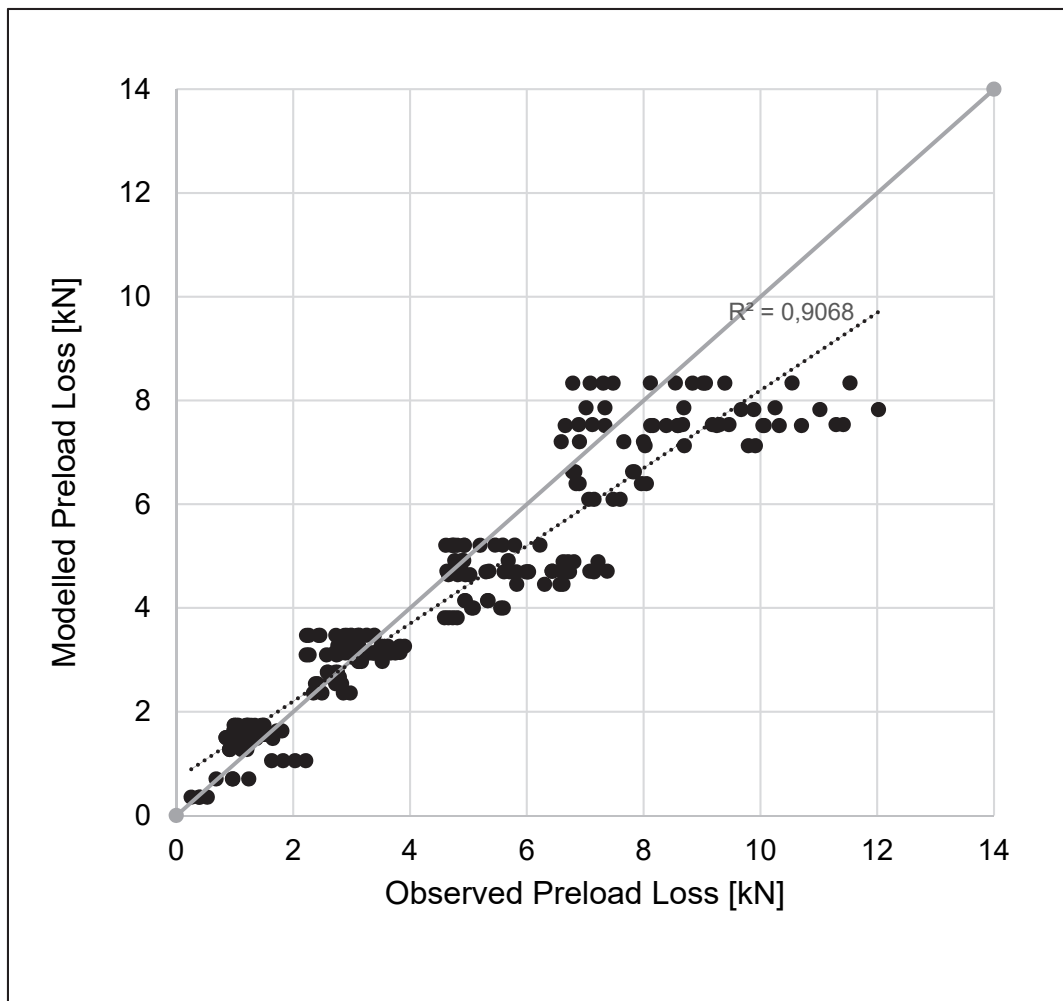


Figure 4-8 - Modelled preload loss versus observed preload loss

As can be seen from Figure 4-8, the model is rather accurate with $R^2 = 0.91$. Only for higher preload losses due to higher external loads, more scatter occurs. Generally more preload loss occurs than that is to be expected from the model. There is no significant difference in the magnitude of the deviation for different surface treatments. When averaging the results per bolt group (two bolts), the scatter reduces and $R^2 = 0.94$ is obtained. The fact that more scatter occurs for higher external forces can partly be understood through Figure 4-9, which shows that for higher external loads the preload loss in the outer bolt (bolt 1) is smaller compared to the preload loss in the inner bolt (bolt 2). A possible explanation is that the outer bolt, which has been tightened last and caused bolt relaxation in the inner bolt due to elastic interaction, transfers most of the load at low external loading levels, which causes surface flattening and consequently bolt relaxation mainly in the outer bolt. At higher external loads, the inner bolt starts to transfer more load since at this location the plate's surface is undamaged compared to the outer bolt. Until the surfaces are equally flattened, the inner bolt will continue to transfer more load than the outer bolt. After this has happened, it is expected for both bolts to transfer equal amounts of load and thus experience equal reductions in preload level. Unfortunately, this final step has not been reached in the experiments and hence it is not possible to confirm this hypothesis.

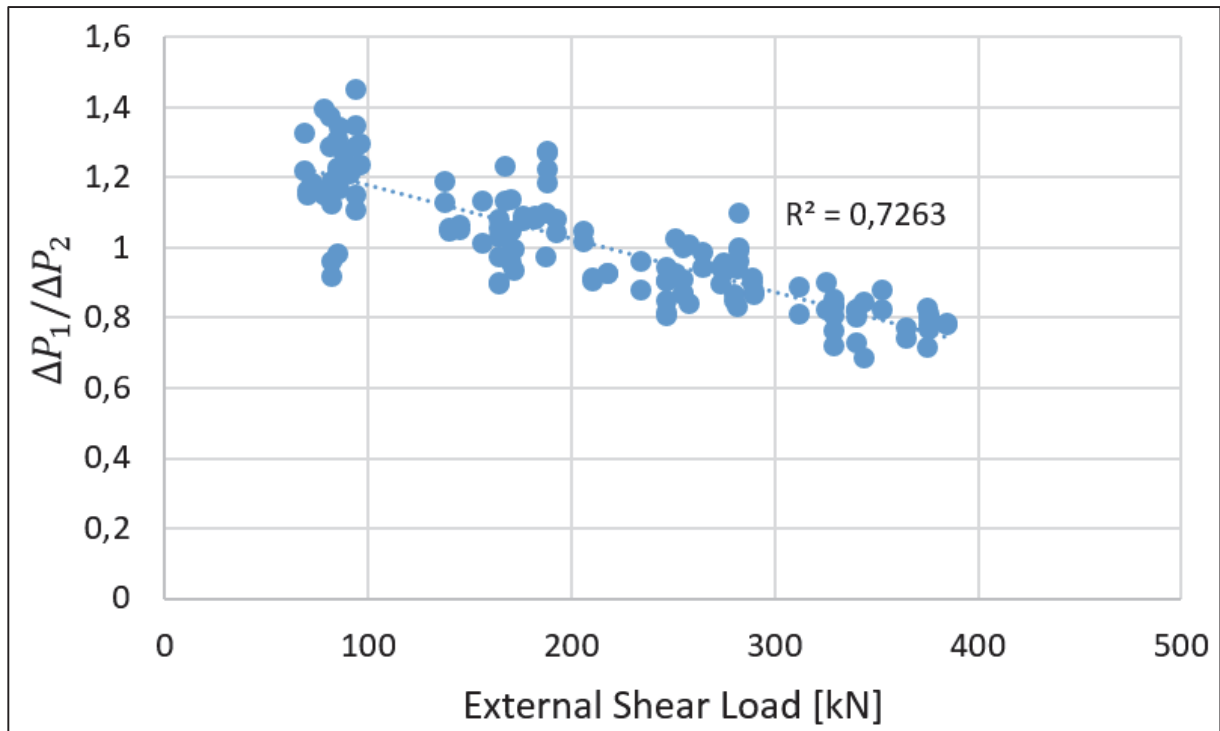


Figure 4-9 - Preload loss in bolt 1 over preload loss in bolt 2 vs. external shear load

The concept of additional bolt relaxation through wear at increasing external load levels is supported by research showing that micro-slip first occurs further away from the bolt hole at low load levels, where it does not influence the bolt significantly (Ibrahim & Pettit, 2005). At increasing external loads, the micro-slip develops closer to the bolt hole and bolt relaxation starts as a result of surface wearing. This is the same effect that has been described by Husson (2008) as already discussed in Section 2.2.4. Hence, it can be explained why the model is increasingly diverging from reality for increasing external loads. Since the current calculation model can only predict one value per specimen, unequal (re)distribution of forces cannot be taken into account.

5 Successful Strategies

The aim of this chapter to provide an overview of connection detailing that leads to a relatively low preload loss over time. The central question in this chapter is “*what connection detailing leads to less than 10% of preload force loss after 24 hours*”

The following assumptions are made:

- The bolts are tightened to the pre-defined level of EN 1090-2 for class 8.8 bolts without an overshoot, using 2 washers;
- The bolts are re-tightened after the initial tightening;
- The external load is static and is larger than the slip resistance according to EN 1993-1-8 (so that the experimental results can be used directly).
- The surface coating is an alkali zinc silicate or spray metallized primer with a respective film thickness of respectively 80 and 160 micron per surface;
- No use of collars / load cells.

This Section is regarding the set-up shown in Figure 5-1. The main variable in this study is the ratio l/d . An increase of l means an increase in bolt length and total plate thickness, thus no collars or load cells are used.

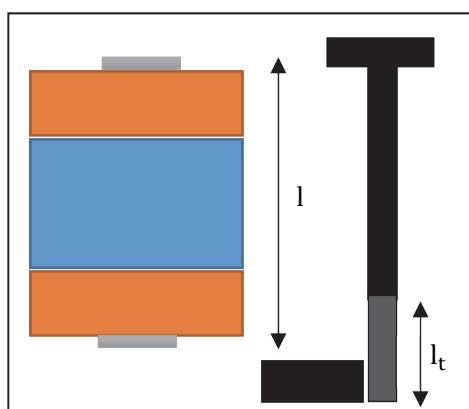


Figure 5-1 - Set-up of test study

The thread length is assumed to be according to Figure 5-2 and it is assumed that 5 mm of the thread length sticking through the nut. The washer and nut dimensions have been obtained from Figure 5-2 as well. Figure 5-3 shows the relative preload loss per 10 micron of joint deformation as a function of the ratio l/d for various bolt sizes. This graph has been obtained using the theory of Section 2.1.4.

Basic dimensions and lengths l_s and l_g of HR Assemblies ac. to PN EN 14399-3:2007										
Nominal dimension/Thread d	M12	(M14) ^a	M16	(M18) ^a	M20	M22	M24	M27	M30	M36
Thread length (inf.) b	L1	30	34	38	42	46	50	54	60	78
	L2	-	40	44	48	52	56	60	66	84
	L3	-	-	-	-	65	69	73	79	97
Shank	\approx thread diameter d									
Bolt head height k	7,5	8,8	10	11,5	12,5	14	15	17	18,7	22,5
Nom. max Nut Height m	10,8	12,8	14,8	15,8	18	19,4	21,5	23,8	25,6	31
Width across flats S	22	24	27	30	32	36	41	46	50	60
Washer diameter	24	28	30	34	37	39	44	50	56	66
Washer height	3	3	4	4	4	4	4	5	5	6

- L1 - for $L_{nom} \leq 125$ mm length
 L2 - for $125 \text{ mm} < L_{nom} \leq 200$ mm length
 L3 - for $L_{nom} > 200$ mm length

Figure 5-2 - Basic Dimensions of HR Assemblies (European Committee for Standardization, 2015)

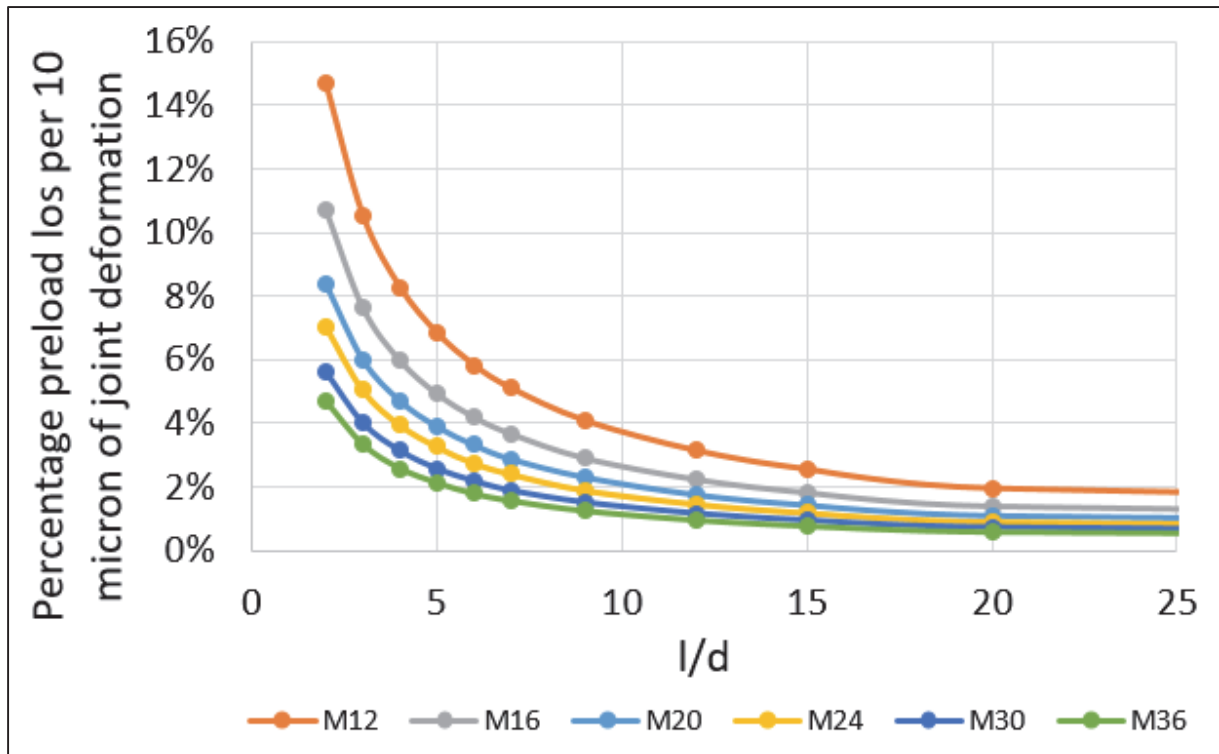


Figure 5-3 - Percentage of preload loss per 10 micron of joint deformation as a function of l/d

However, in absolute sense, larger bolt dimensions lead to higher preload losses, as can be seen from Figure 5-4. Also, larger bolt dimensions are pretensioned to a higher preload level, increasing the potential amount of embedment and thus of total preload loss.

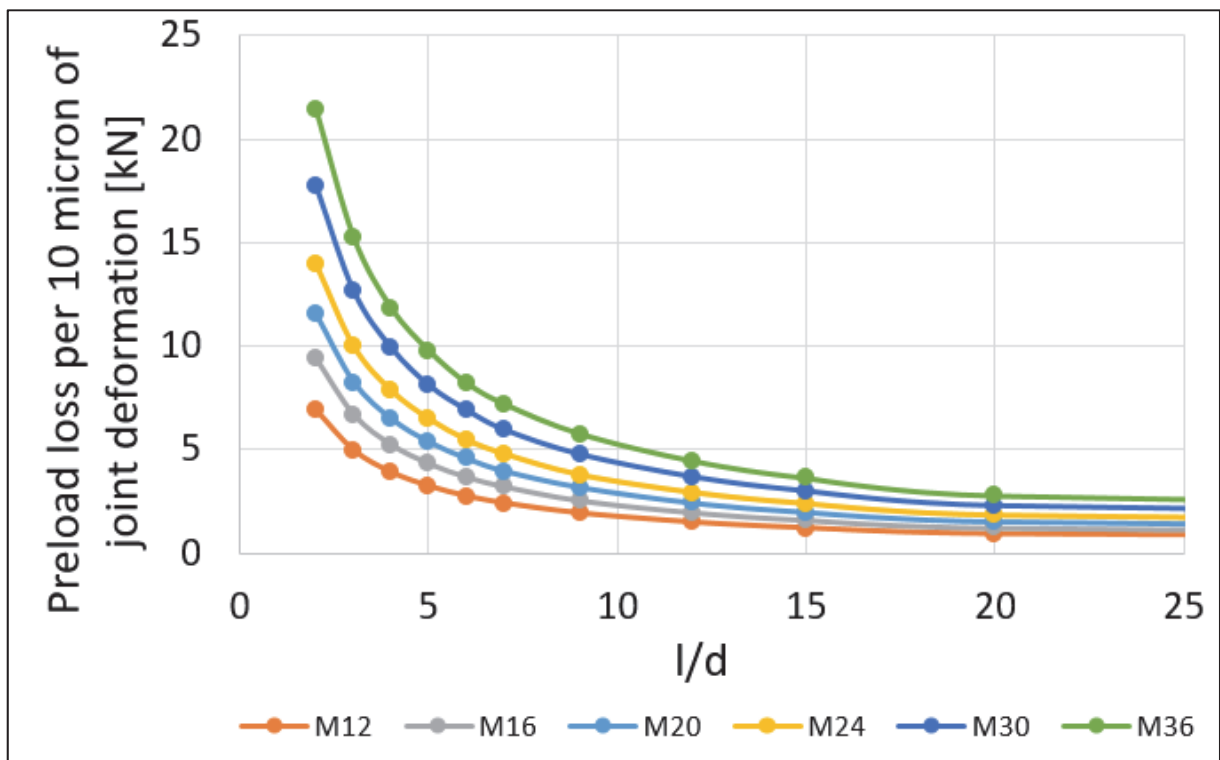


Figure 5-4 - Absolute preload loss per 10 micron of joint deformation as a function of l/d

The preload loss decreases with increasing values of l/d due to the reduction in bolt stiffness. As a result, the compensation factor $1 - C_b$ of Eq. (2.12) (see also Eq. (5.1)) increases (also due to a reduction in k_m) but this does not have a significant effect on the final joint stiffness for pretension losses. It is therefore recommended to choose for bolts with a longer length in order to reduce the (relative) preload loss.

The average joint deformation 24 hours after (re)tightening for the test data has been calculated using (5.1).

$$f_z = \frac{\Delta F_{p,c}(t = 24h)}{k_b \cdot \left[\frac{k_m}{k_b + k_m} \right]} \quad (5.1)$$

The average joint deformation after 24 hours is shown in Table 8.

Table 8 - Average joint deformation after 24 hours

Surface Treatment	Average joint deformation 24 hours after re-tightening [micron]
Alkali Zinc Silicate	25,9
Spray Metallized	27,8

Combining Table 8 and the M20 results from Figure 5-3, the expected minimum ratio l/d for which the preload losses are less than 10% 24 hours after re-tightening of the bolts can be found. This is illustrated in Figure 5-5, which indicates that the minimum ratio $l/d \geq 5$ for both surface treatments in case of an M20 bolt. If the bolts are only tightened once, the average joint deformation is 40 micron for both surface treatments and a minimum ratio l/d necessary for less than 10% of preload loss is $l/d \geq 8$. This once again underlines the advantage of re-tightening the bolts.

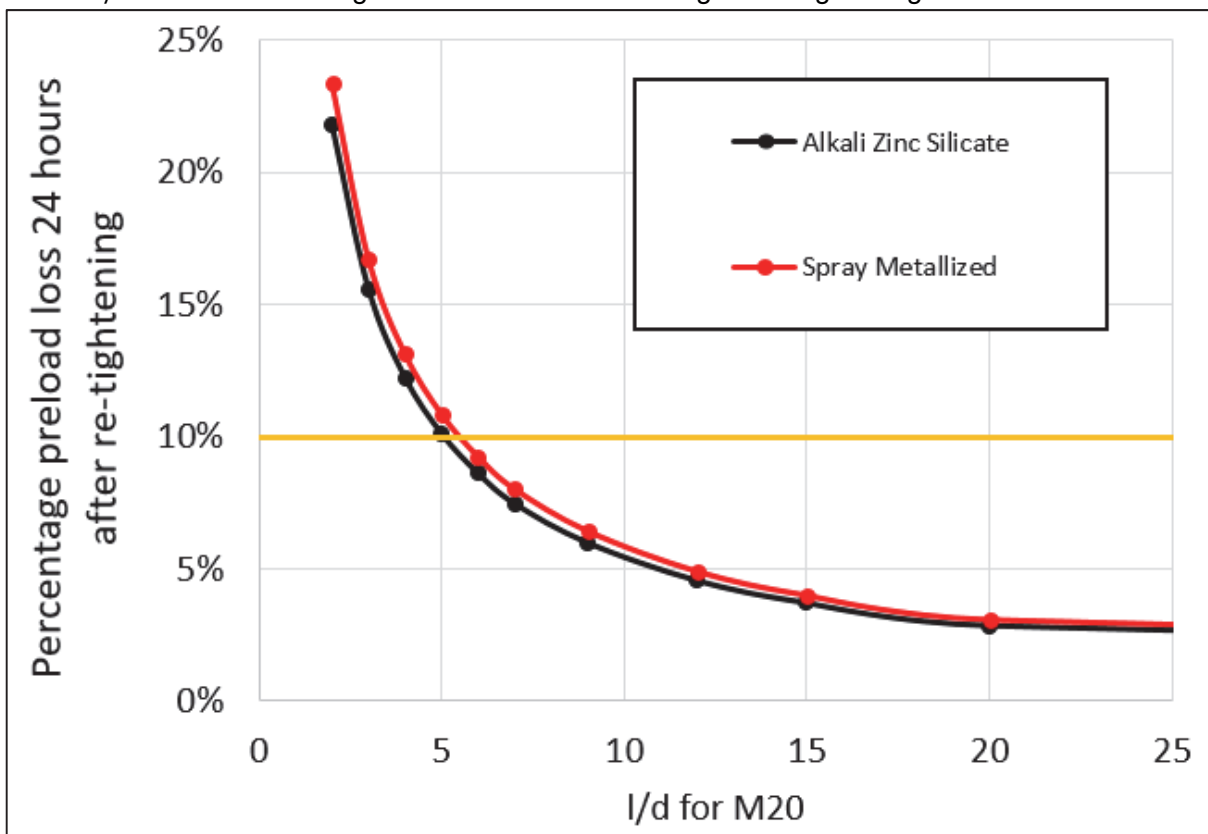


Figure 5-5 - Percentage preload loss 24 hours after re-tightening as a function of l/d

If a joint with relatively thin plates (small l/d) is foreseen, an option is to install a collar around the bolt to increase the bolt length. In this case, care should be taken in choosing the dimensions (length, cross section) of the collar. A flexible collar will lead to a small value of k_m/k_b (see Figure 5-6), which helps reducing preload losses, but will also lead to large value of $C_b = k_b/(k_m + k_b)$ and thus a potentially large bolt force increase. A stiff collar will lead to a larger value of k_m/k_b and will thus not significantly help in reducing preload losses, but will perform better under in-service conditions due to a lower C_b . It should be noted that k_m in this case is calculated as a spring in series, consisting of a plate spring and a collar spring. Since the stiffness of long bolts is generally low, the absolute effect of the factor $1 - C_b$ is limited. The best strategy is to choose for a stiff collar and to reduce the potential joint deformation. The dimensions of the collar can be calculated based on the bolt stiffness and plate stiffness, assuming a target value for C_b .

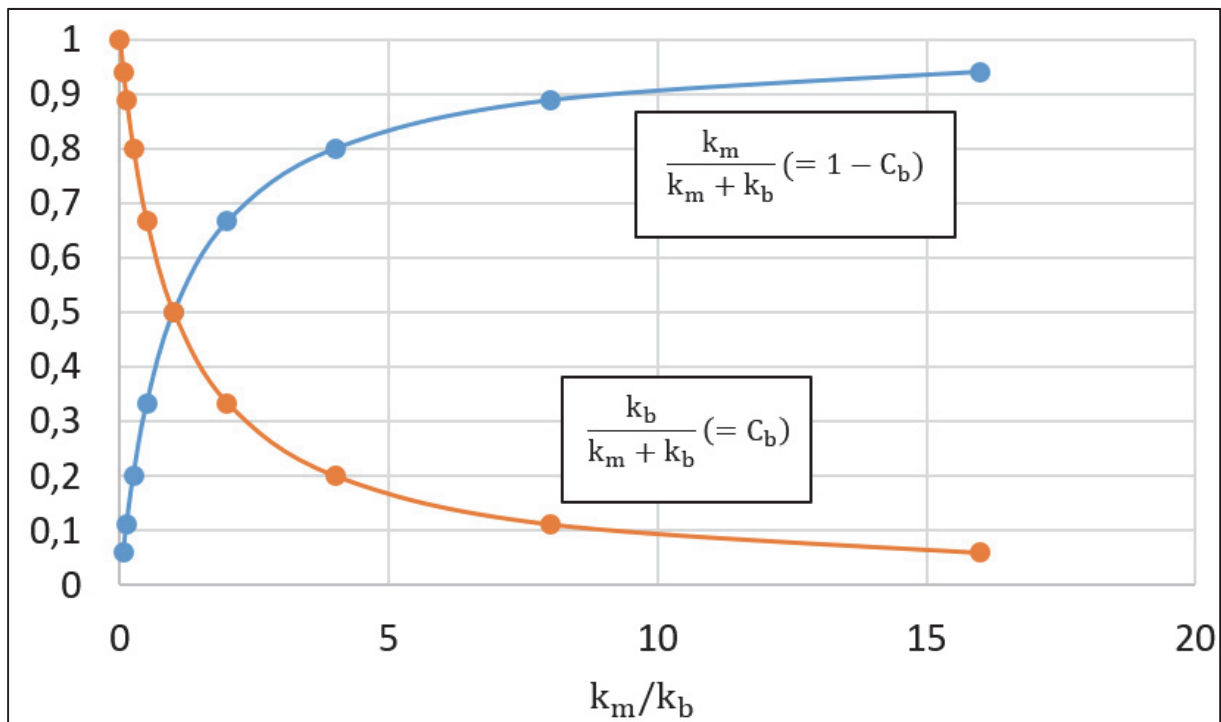


Figure 5-6 - C_b and $1-C_b$ as a function of the stiffness ratio k_m/k_b

In order to improve the in-service performance of the joint, i.e. to reduce the increase of the bolt force, it is not per se necessary to increase the clamp length of the bolt. Another way of increasing C_b is to reduce the axial stiffness EA of the shank of the bolt. The easiest way of reducing the axial stiffness is to reduce the shank cross section (e.g. by milling), as shown in Figure 5-7. A more complicated way would be to use a material for the shank with a lower Young's Modulus.

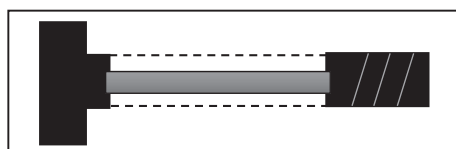


Figure 5-7 - Bolt with reduced shank area

One of the most important strategies to reduce preload loss is to choose for a coating system that is not sensitive to embedment. As shown in Chapter 3, the preload loss in uncoated connections is significantly lower than in coated connections. Using the hypothesis that the coating has a larger influence than the surface roughness on bolt relaxation, it is suggested to use a rougher surface to increase the slip resistance rather than a coating system. However, the corrosion protection of the connection must in this case still be provided in another way.

Conclusion

Pretension loss occurs in all preloaded bolts, regardless of their size, length or the surface treatment of the plate assembly. Numerous causes for bolt relaxation exist, although for joints in civil engineering structures, the main reasons for bolt relaxation are elastic interactions, embedment, static and cyclic loading and long-term relaxation or creep. Only elastic interactions and cyclic loading (vibration loosening) may cause complete bolt loosening, whereas the other causes may only be responsible for bolt relaxation to a certain magnitude. Several systems are on the market which limit the amount of bolt relaxation due to vibration loosening.

Bolt relaxation starts directly after preloading due to embedding of the joint elements. Re-tightening the bolts after 30-40 minutes reduced the preload losses significantly in the experimental programme, and thus may be a good strategy to maintain a high bolt preload. Bolt relaxation due to introduction of a static external shear load can be predicted quite accurately with a simple linear-elastic calculation model. The model accuracy reduces with increasing external force due to flattening of the surface asperities and the subsequent joint deformation. However some authors suggest that, on the long-term, bolt relaxation is mostly unaffected by static external loading. This hypothesis cannot be confirmed or rejected based on the current research.

The experiments carried out at TU Delft show a clear distinction in bolt preload loss between coated and uncoated plates within the clamping package. Uncoated plates lead to significantly lower preload losses directly after tightening of the bolts than in case of coated plates. The total coating thickness is a good predictor of bolt relaxation. The influence of surface roughness of the plates cannot be quantified in the current research, since it is masked by the influence of the coating. However, guide values for joint deformation due to flattening of surface roughness are available in VDI 2230.

Bolt relaxation is not only governed by joint deformation (e.g. due to embedding), but also by the joint design itself. Theoretically and experimentally it is proven that a higher ratio of bolt (clamping) length over bolt diameter l/d leads to relatively lower preload losses. In order to achieve high ratios of l/d either l may be increased by installing a collar, or d may be decreased by installing a bolt with a smaller diameter. The latter option requires more bolts for the same slip resistance.

References

- Abid, M., Khalil, M. S., & Wajid, H. A. (2015). An Experimental Study on the Relaxation of Bolts. *IJUM Engineering Journal*, 16(1), 43-52.
- AkzoNobel. (2015, October 6). *Interzinc 697 - Protective Coatings*. Retrieved from International-PC: <http://www.international-pc.com/PDS/2567-P-eng-A4.pdf>
- Alcoa Fastening Systems & Rings. (n.d.). *HuckBolt (R) Installation Sequence*. Retrieved from Alcoa Fastening Systems & Rings: <http://www.afsrhuck.net/us/en/Products/Fasteners/HuckBolts.html>
- American Galvanizers Association. (n.d.). *Hot-Dip Galvanized Steel vs. Zinc Spray Metallizing*. Retrieved from Galvanizeit: http://www.galvanizeit.org/uploads/publications/Galvanized_Steel_vs_Zinc_Spray.pdf
- Andrews Fasteners Ltd. (n.d.). *Basic Bolt Dimensions HR Bolts*. Retrieved from Andrews Fasteners Ltd.: <https://www.andrewsfasteners.uk/standards/en-14399-3-basic-bolt-dimensions-hr-bolts/>
- AppliedBolting. (n.d.). *Standard DTI*. Applied Bolting Technology, Vermont.
- Ashok Paint Agencies. (n.d.). *Zinc Silicate Primer*. Retrieved from Ashok Paint Agencies: <http://www.ashokpaints.com/berger-paints.html>
- Avant Guards Coatings. (n.d.). *About Zinc Metallizing*. Retrieved from Avant Guards Coatings: <http://www.avantguardscoatings.com/zinc.html>
- Beardmore, R. (2012). *Useful tables - Joint Stiffness*. Retrieved from Roymech: http://www.roymech.co.uk/Useful_Tables/Screws/Joint_Stiffness.html
- Berenbak, J. (2012). *Evaluation Tightening Preloaded Bolt Assemblies According to EN 1090-2*. Delft: Bouwen met Staal.
- Bickford, J. H. (1990). *An Introduction to the Design and Behaviour of Bolted Joints*. New York: M. Dekker.
- Bickford, J. H. (2008). *Introduction to the Design and Behaviour of Bolted Joints*. New York: CRC Press.
- Bickford, J. H., & Nassar, S. (1998). *Handbook of Bolts and Bolted Joints*. New York: M. Dekker.
- Blake, A. (1985). *Design of Mechanical Joints*. New York: Taylor & Francis Inc.
- Blendulf, B. (2009). *Pushing the Limits*. Retrieved from Global Fastener News: <http://globalfastenernews.com/ftp/Blendulf-Fall%2009.pdf>
- Blume, D. (1969). Wann müssen Schrauben gesichert werden? *Verbindungstechnik*, 25-30.
- Blume, D., & Illgner, K. (1988). *Schrauben Vademecum*. Neuss: Bauer & Schaurte Karcher.
- Boltight. (n.d.). Ultrasonic Bolt Measurement. *Introduction to Ultrasonic Bolt Load Measurement*. Boltight - Hydraulic Bolt Tensioning, Walsall.
- BoltScience. (n.d.). *Joint Diagrams with External Forces Applied*.
- Chakherlou, T. N., Oskouei, R. H., & Vogwell, J. (2008). Experimental and numerical investigation of the effect of clamping force on the fatigue behaviour of bolted plates. *Engineering Failure Analysis*, 15(5), 563-574.
- Chambers, W. (1875). *Chamber's Encyclopaedia*. Philadelphia: J.B. Lippincott Company.

- Culpepper, M. (2009). *MIT OpenCourseWare 2.72*. Retrieved from MIT:
http://ocw.mit.edu/courses/mechanical-engineering/2-72-elements-of-mechanical-design-spring-2009/lecture-notes/MIT2_72s09_lec12.pdf
- Davet, G. (2007). *Why do Gasketed Joints Leak?* Retrieved from Solon Manufacturing Co.:
<http://www.solonmfg.com/springs/pdfs/JointLeaksLoRez.pdf>
- de Vries, S., Rauhorst, J., Plasse, B., & Kerneling, F. (1999). What to do? Electroplating or Metal Spraying? In *IDE442 Materialiseren* (pp. 1-5). Delft.
- Eccles, B. (2011). *Bolt Science*. Retrieved from Self-Loosening of Threaded Fasteners:
<http://www.boltscience.com/pages/self-loosening-of-threaded-fasteners.pdf>
- ESDEP. (n.d.). *ESDEP 11.3.2: Connections with Preloaded Bolts*. Retrieved from ESDEP.
- European Committee for Standardization. (2011). *NEN-EN 1090-2: Execution of Steel Structures and Aluminium Structures - Part 2: Technical Requirements for Steel Structures*. Delft: Nederlands Normalisatie Instituut.
- European Committee for Standardization. (2011). *NEN-EN 1993-1-8: Design of Steel Structures- Part 1-8: Design of Joints*. Delft: Nederlands Normalisatie Instituut.
- European Committee for Standardization. (2015). *NEN-EN 14399: High Strength Structural Bolting Assemblies for Preloading*. Delft: Nederlands Normalisatie Instituut.
- Fisher, J. W., & Beedle, L. S. (1964). Bibliography on Bolted and Riveted Structural Joints, ASCE Manual No. 48 (67-15). *Fritz Laboratory Reports*.
- Fisher, J. W., Struik, J. H., & Kulak, G. L. (1974). *Guide to Design Criteria for Bolted and Riveted Joints*. New York: Wiley.
- Friede, R., & Lange, J. (2009). Self Loosening of Prestressed Bolts. *Nordic Steel Construction Conference 2009*, (pp. 272-279). Malmö.
- Graves, F. (1984). Nuts and Bolts. *Scientific American*, 136-144.
- Heistermann, C. (2011). *Behaviour of Pretensioned Bolts in Friction Connections*. Licentiate Thesis, Luleå University of Technology, Luleå.
- Hendy, C., & Iles, D. (2015). *Steel Bridge Group: Guidance Notes on Best Practice in Steel Bridge Construction*. Berkshire: Steel Construction Institute.
- Husson, W. (2008). *Friction Connections with Slotted Holes for Wind Towers*. Licentiate Thesis, Luleå University of Technology, Luleå.
- Ibrahim, R. A., & Pettit, C. L. (2005). Uncertainties and Dynamic Problems of Bolted Joints and Other Fasteners. *Journal of Sound and Vibration*, 857-936.
- International Organization for Standardization. (2009). *ISO 898-1: Mechanical Properties of Fasteners Made of Carbon Steel and Alloy Steel - Part 1: Bolts, Screws and Studs with Specified Property Classes - Coarse Thread and Fine Pitch Thread*. Geneva: International Organization for Standardization.
- Ivkovic, B., Djurdjanovic, M., & Stamenkovic, D. (2000). The Influence of the Contact Surface Roughness on the Static Friction Coefficient. *Tribology in Industry*, 22(3&4), 41-44.
- Jha, N. K. (2015). *Green Design and Manufacturing for Sustainability*. Boca Raton: CRC Press.
- Jiang, Y., Zhang, M., & Lee, C. H. (2003). A Study of Early Stage Self-Loosening of Bolted Joints. *Journal of Mechanical Design*.
- Kulak, G. L. (2005). *High Strength Bolting for Canadian Engineers*. Toronto: Quadratone Graphics Ltd.

- Lifetime Reliability Solutions. (n.d.). *Bolt Tensioning*. Retrieved from Lifetime Reliability Solutions: http://www.lifetime-reliability.com/free-articles/precision-maintenance/Summary_of_Bolt_Tensioning.pdf
- Lindsley, M. (2016, March). Are all zinc coatings created equal? *The Construction Specifier*.
- Mahmoud, H. N., Lopez, S. R., & Riveros, G. A. (2016). *Causes of Pretension Loss in High-Strength Bolts*. Washington D.C.: US Army Corps of Engineers.
- Mann, A. P., & Morris, L. J. (1984). Lack of Fit in High Strenght Bolted Connections. *Journal of structural engineering*, 110(6), 1235-1252.
- Maryland Metrics. (n.d.). *Junker Test Principle*. Retrieved from MDMetric: <https://mdmetric.com/nordlock/Nord-Lock%20-%20Junker%20test%20principle.htm>
- Messler, R. W. (2004). *Joining of Materials and Structures: From Pragmatic Process to Enabling Technology*. Burlington: Elsevier Butterworth-Heinemann.
- MetalPlate Galvanizing L.P. (n.d.). *Coating Comparison*. Retrieved from Metalplate Galvanizing L.P.: <http://www.metalplate.com/techdept/coatingcomp.php>
- Mogilev Metallurgical Works. (n.d.). *Chilled Iron Shot and Grit*. Retrieved from Mogilev Metallurgical Works: <http://www.mmz.by/en/production/technical-cast-iron/>
- Nord-Lock Bolt Securing Systems. (n.d.). *Nord-Lock SC-washers*. Retrieved from Nord-Lock: <http://www.nord-lock.com/nl/nord-lock/wedge-locking/sc-washers/steel-construction-washers/>
- Oskouei, R., & Chakherlou, T. (2009). Reduction in Clamping Force due to Applied Longitudinal Load to Aerospace Structural Bolted Plates. *Aerospace Science and Technology*(13), 325-330.
- Park Tool. (2015). *Basic Thread Concepts*. Retrieved from Park Tool: <http://www.parktool.com/blog/repair-help/basic-thread-concepts>
- Patil, M. J., Shilwant, S., & Kadam, S. S. (2006). Self-Loosening of Bolted Joints: A Parametric Study. *NCRTM 2006*, (pp. 350-354).
- Pencom. (n.d.). *Pitch, Major and Minor Bolt Diameter*. Pencom, San Carlos.
- Porter, F. C. (1991). *Zinc Handbook: Properties, Processing and Use in Design*. Boca Raton: CRC Press.
- Ramey, G. D., & Jenkins, R. C. (1995). *Experimental Analysis of Thread Movement in Bolted Connections Due to Vibrations*. Auburn: Auburn University.
- Raynor-Keck, L. (2013, 7). Torque vs. Tension: Is There a Clear Winner? *Wind Systems Magazine*, pp. 32-36.
- Reuther, D., Baker, I., Yetka, A., Cleary, D. B., & Riddell, W. (2014). Relaxation of ASTM A325 Bolted Assemblies. *Journal of Structural Engineering*, 140(9), 01014060-1 - 04014060-7.
- Sase, N., & Fujii, H. (2001). Optimizing Study of SLBs for Higher Anti-Loosening Performance. *Journal of Materials Processing Technology*, 174-179.
- Satoh, Y., Nagatomo, T., Machida, H., Endoh, S., & Enari, T. (1997). An Evaluation Test for the Influences of the Paint-Film upon Self-Loosening of Fasteners. *Railway Technical Research Institute, Quarterly Reports*, 61-65.
- Shoji, Y., & Sawa, T. (2005). Analytical Research on Mechanism of Bolt Loosening due to Lateral Loads. *Pressure Vessels and Piping Division Conference 2005*, (pp. 1-7). Denver.

- SKF. (2001). *Bolt Tightening Handbook*. Retrieved from SKF - Linear Motion & Precision Technologies:
http://www.brammer.com.pl/DOWNLOAD/SKF_napinacz_srub_Hydrocam_podrecznik.pdf?download=172
- SMS Siemag AG. (n.d.). *Hot-Dip Galvanizing Line for Top Quality Demands*. Retrieved from SMS-Siemag: http://www.sms-siemag.com/download/W7_309E_Hot-dip_galvanizing_line_Kosice.pdf
- Steel Industry Guidance Notes. (2008). *European Standard for Preloadable Bolts*. Retrieved from SteelConstruction.org: <https://www.steelconstruction.org/custom/uploads/2016/04/SIGNS-SN26.pdf>
- Taha, B., & Daidié, A. (2012). Effect of Axial Preload on Double-Lap Bolted Joints: Numerical Study. *2012 11th Biennial Conference on Engineering Systems Design and Analysis*, (pp. 1-8). Nantes.
- Techno Test Instruments. (n.d.). *Our Products: Strain Gages for Bolts*. Retrieved from Techno Test Instruments: http://catalogue.techno-test.com/products/4-Sens_r_System_S_luti_ns/138-Strain_Gages/879-KYOWA_KFG_Bolts-Strain_Gage_for_Stress_Measurement_on_Bolts_KFG_C20_.html
- Tentec. (2006). *Tips on Bolt Tensioning*. Retrieved from Tentec:
<http://cdn.pes.eu.com/assets/articles/tips-on-tensioningpdf-64.pdf>
- Undrum, H. (2016). *Silicate- or Epoxy Zinc Primers - The Superior Protection*. Sandefjord: Jotun AS.
- VDI. (2003). *VDI 2230: Systematic Calculation of High Duty Bolted Joints - Joints with One Cylindrical Bolt*.
- Vries, P.A. de. (2016, May 20). *Siroco - Bouwen met Staal*. Retrieved from Bouwen met Staal: http://www.bouwenmetstaal.nl/uploads/evenementen/techniekdag2016/05_Slip_resistant_connections_preload_in_bolts_pdv_May_2016.pdf
- Washington, B. (2013). Torque vs Tension: Is There a Clear Winner? (L. Raynor-Keck, Interviewer)
- Wikimedia Commons. (2010). Diagram of an isotropic linear elastic material with Poisson ratio of 0.5 subject to axial forces.
- Wilbur, W. (1905). *History of the Bolt and Nut Industry of America*. Ward & Shaw.
- WindTechTv.org. (n.d.). *Hydraulic Torque Wrench*. Retrieved from WindTechTv.org.
- Yang, J., & DeWolf, J. T. (1999). Mathematical Model for Relaxation in High Strength Bolted Connections. *Journal of Structural Engineering*, 125(8), 803-809.
- Yang, J., & DeWolf, J. T. (2000). Relaxation in High-Strength Bolted Connections Using Galvanized Steel. *Journal of Bridge Engineering*, 5(2), 99-106.

Appendix A: Surface Treatment per Specimen

Specimen	Rz (micron)								Film Thickness (micron)							
	Top CP		Low CP		LP1		LP2		Top CP		Low CP		LP1		LP2	
ASiZn-37	83	83	83	83	84		84		80	79	65	68	72		87	
ASiZn-38	83	83	83	83	84		84		107	92	87	75	85		73	
ASiZn-39	83	83	83	83	84		84		80	68	101	104	72		98	
ASiZn-40	83	83	83	83	84		84		66	78	69	69	72		68	
SM-19	84	102	100	121	107		93		145	145	140	140	140		134	
SM-20	118	108	99	108	123		114		138	138	136	136	149		131	
SM-30	104	95	100	109	90		133		141	141	146	146	142		130	
SM-31	94	106	86	102	89	90	121	109	162	170	155	165	165	154	153	158
SM-37	100	99	101	99	95	91	108	92	161	169	190	160	175	159	168	156
SM-40	103	83	89	93	117	103	110	121	155	171	160	202	138	159	150	153
SM-41	91	101	93	120	83	106	94	108	153	180	156	163	149	165	150	149
SM-42	90	94	98	96	116	119	101	81	165	162	160	164	159	144	155	154
SM-43	89	110	96	84	90	98	97	173	170	173	163	168	162	151	170	157
SM-44	95	101	96	118	94	74	93	80	165	166	177	157	157	149	154	158
SM-45	106	135	89	118	108	77	92	92	164	149	169	158	162	150	168	155
SM-46	91	92	103	108	94	113	135	87	148	162	159	162	163	163	161	164
SB-05	80	80	80	80	80		80									
SB-06	80	80	80	80	80		80									
SB-24	80	80	80	80	80		80									
SB-25	80	80	80	80	80		80									

CP: Center plate

LP: Lap plate (cover plate)

The surface roughness of the grid blasted plates has been determined by sampling rather than by individual measurements per plate. The sample report is presented on the next page.

Werkstattauftrag

<u>Auftrag an:</u>	Abt. 500 <input checked="" type="checkbox"/> Herr Genz	LA3/240/14/143001
<u>Material/Probenmaß/ Walzrichtung:</u>	56 Zugstäbe (400 x 100 x 20) mm 56 Laschen (290 x 100 x 10) mm	
<u>Probenanzahl:</u>	112	
<u>Arbeitsschritt:</u>		
<u>Arbeitsschritt:</u>	Entfetten mit Lösungsmittel	
<u>Arbeitsschritt:</u>	Strahlen	
<u>Sollwerte</u>		
<u>Rauheit Rz:</u>	ca. 80 µm, mittel (G), mind. Sa 2 ½	
<u>Strahlmittel:</u>	Hartgussgranulat	
<u>Druck:</u>		

Datum:

Auftraggeber:

Fr. Berger

<u>Istwerte</u>			
<u>Strahlmittel/Charge:</u>	Beb. Genz's 9 IKS		
<u>Druck:</u>	5 bar		
<u>Rauheit Rz:</u>	77,56 µm		
<u>Mittenrauheit Ra:</u>	11,53 µm		
<u>Spitzenzahl RPC:</u>	00029/cm		
<u>Rillenbreite RSm:</u>	337,3 µm		
<u>Proben weitergeben an:</u>	Abt. 200 <input type="checkbox"/>	Abt. 300 <input type="checkbox"/>	Abt. 400 <input type="checkbox"/>

Datum:

Bearbeiter:

22.10.2014

R. Genz

Ra	N=05
Xq	11,53 µm
S	88,76 µm
Max	12,39 µm
Min	10,58 µm
R	81,81 µm
RzD	N=05
Xq	77,56 µm
S	88,31 µm
Max	88,67 µm
Min	71,80 µm
R	14,82 µm
Ra	N=05
Xq	00029/cm
S	00002/cm
Max	00032/cm
Min	00026/cm
R	00006/cm
Rm	N=05
Xq	337,3 µm
S	24,87 µm
Max	378,7 µm
Min	312,5 µm
R	65,28 µm